

Copyright

by

Yue Li

2007

**The Dissertation Committee for Yue Li Certifies that this is the approved version of  
the following dissertation:**

**THE ROLE OF POSTSYNAPTIC MUSCLE FIBERS IN  
MAINTENANCE AND REPAIR OF MAMMALIAN  
NEUROMUSCULAR JUNCTIONS**

**Committee:**

---

Wesley J. Thompson, Supervisor

---

Harold Zakon

---

Karen Artzt

---

Mendell Rimer

---

Bing Zhang

**THE ROLE OF POSTSYNAPTIC MUSCLE FIBERS IN  
MAINTENANCE AND REPAIR OF MAMMALIAN  
NEUROMUSCULAR JUNCTIONS**

**by**

**Yue Li, B.S.**

**DISSERTATION**

Presented to the Faculty of the Graduate School of  
The University of Texas at Austin  
in Partial Fulfillment  
of the Requirements  
for the Degree of

**DOCTOR OF PHILOSOPHY**

The University of Texas at Austin  
May, 2007

## **Dedication**

*I dedicate this dissertation to my parents and my husband for their unconditional love  
and support.*



## **Acknowledgements**

I am grateful to the members of my dissertation committee, Drs. Wesley J. Thompson, Harold Zakon, Karen Artzt, Mendell Rimer and Bing Zhang; especially my PI, Wes, who showed me the way to become a true scientist.

I acknowledge and thank all current and former members of the Thompson Lab: Michelle Fiedler-Mikesh, Chris Hayworth, Le Tian, Hyuno Kang, Jane Lubischer and Ian Morrison for their help, shoulders, patience and insightful discussions.

I would like to thank Angela Bardo and John Mendenhall for all their help with the confocal microscopy work.

I also want to thank my dear friends back in China and here in the States for brightening my days with their genuine friendships.

# **The Role of Postsynaptic Muscle Fibers in Maintenance and Repair of Mammalian Neuromuscular Junctions**

Publication No. \_\_\_\_\_

Yue Li, PhD

The University of Texas at Austin, 2007

Supervisor: Wesley J. Thompson

Previous studies from our lab showed that terminal Schwann cells (TSCs) are actively involved in the restoration of functional synapses during reinnervation at mammalian neuromuscular junctions (NMJs). However, it is unclear what induces TSCs to extend processes that guide the nerve growth (Son and Thompson, 1995a,b). Is it the loss of the axon or instead, some signal arising from denervated muscle fibers? The main objective of my dissertation was to examine whether muscle fibers can be the source of signals affecting TSC growth.

In Chapter 2, I report that both TSCs and nerve terminals are maintained at the former junction even after their underlying muscle fiber degenerates. Some of the original AChRs are surprisingly sustained at the synaptic sites for a long time with the preserved pretzel pattern. These results show that the postsynaptic target is not necessary for the maintenance of presynaptic structures.

In Chapter 3, I report that following fiber regeneration, newly formed AChRs are clearly separated from the persisting receptors at most locations and they are apposed by

the nerves. Moreover, as the fiber regenerates, TSCs begin to grow processes. Nerve sprouts then follow these processes to form new synaptic sites beyond the old receptor territory. My observations therefore show that signals for nerve growth arise from regenerating fibers and they appear to act by first affecting TSCs. Such signals seem diffusible because I saw that TSCs on surrounding fibers also began to grow during regeneration.

In Chapter 4, I report that new junctions on the regenerated fibers are very dynamic. They undergo continual remodeling and eventually take on an ‘en grappe’ pattern. Since the synapses on undamaged fibers are normally very stable, these observations suggest that regeneration has set in place a process whereby the synapses are unable to stabilize. Interestingly, this appears to be the case in muscles that degenerate as a consequence of muscular dystrophy.

My findings are important because they suggest an active role of the postsynaptic muscle fiber not in synapse maintenance but rather in generating signals that attract innervation after injury.

## Table of Contents

List of Tables.....	xii
List of Figures.....	xiii
CHAPTER 1 Introduction.....	1
Degeneration and regeneration of muscle fibers following muscle injury .....	2
The response of nerve terminals to the loss of postsynaptic cells following muscle fiber damage .....	7
The factors contributing to reestablishing synaptic connection.....	8
The importance of Schwann cells at the NMJs.....	10
Terminal Schwann cells extend processes beyond the endplate area after denervation and guide regenerating axons to follow their path .....	12
Terminal Schwann cells guide the growth of axon sprouts between two synaptic sites.....	12
What induces terminal Schwann cells to grow processes?.....	15
CHAPTER 2 Terminal Schwann cells and Nerve Terminals Are Maintained at The Neuromuscular Junction after Removal of Postsynaptic Muscle Fibers .....	17
Abstract.....	17
Methods .....	18
Animals .....	18
<i>In Vivo</i> Procedure .....	19
Laser Ablation.....	20
<i>In Vivo Image</i> Capture and Analysis .....	20

Other live staining .....	21
Histochemistry.....	21
<i>In Vitro</i> Image Capture and Analysis .....	22
Physiology.....	23
Results .....	23
Individual muscle fibers can be ablated with a laser microbeam.....	23
Despite the damage to the underlying muscle fiber, the nerve terminal and its SCs remain initially intact.....	33
Repeated imaging does not induce any changes to the NMJs .....	35
Some AChRs present at the time of muscle fiber ablation persist for months.....	37
Despite degeneration of the muscle fiber, nerve terminals and Schwann cells retain their original configurations at former synaptic sites.....	47
Discussion.....	59
The maintenance of some AChR sites at the original NMJ following muscle degeneration.....	60
The maintenance of TSCs and nerve terminals following muscle fiber degeneration .....	61
CHAPTER 3 Terminal Schwann Cell Processes Are Induced by Regenerating	
Muscle Fibers During The Formation of New NMJs.....	65
Abstract.....	65
Methods .....	66
Results .....	67
As ablated muscle fibers regenerate, newly synthesized receptors can	

be detected by applying a second color of fluorophore-tagged BTX.....	67
New AChRs on regenerating muscle fibers are added gradually to the synaptic sites and take the general pattern of the original one .....	71
New AChRs commonly do not overlap with the original AChRs viewed en face and they are situated at a different plane in the Z axis .....	74
Nerve terminals are associated with all the sites of new receptor deposition .....	82
Terminal Schwann cells extend processes along the regenerating fibers and guide terminal sprouts that establish new synaptic sites.....	85
Terminal Schwann cells also extend processes from nearby intact fibers during muscle fiber regeneration .....	91
Discussion .....	95
Accumulation of new AChR sites by nerve terminals on the regenerating muscle fibers.....	96
Induction of terminal sprouts by regenerating muscle fibers.....	98
Induction of Schwann cell processes by regenerating muscle fibers and their leading role in synapse formation .....	100
The absence of terminal sprouts from surrounding intact fibers.....	102
 CHAPTER 4 New NMJs on Regenerated Muscle Fibers Undergo Constant,	
Long Term Remodeling.....	105
Abstract.....	105
Methods .....	106

Results .....	106
Newly formed NMJs on regenerated fibers start to change around 2 weeks after fiber damage.....	106
Continuous remodeling is common for the NMJs on regenerated fibers.....	111
Nerve terminals extend many fine processes and take on an ‘en grappe’ appearance on long-term regenerated fibers.....	114
The distribution of AChR sites and their alignment with the nerve terminals are changed in the 3-D space on long term regenerated fibers.....	117
NMJs on the intact muscle fibers in the same muscle as the ablated fibers change little.....	120
Discussion .....	123
The dynamism of the newly formed NMJs on regenerated muscle fibers.....	123
The implications of ‘en grappe’ endplates on the regenerated muscle fibers.....	125
CHAPTER 5 Conclusion .....	127
The relationship between the muscle fiber and the maintenance of the neuromuscular junction.....	128
The relationship between Schwann cell processes and muscle fibers ....	133
The abnormal morphology of the NMJs on the regenerated fibers and its implications in muscle disease and aging.....	135
Concluding remarks .....	137
Bibliography .....	139
Vita .....	148

## LIST OF TABLES

Table 2.1	Summary of data: Comparison of the properties of AChR, TSCs and nerve terminal (NT) of the former junction 2 or 3-4 days after fiber damage.....	53
-----------	--	----



## LIST OF FIGURES

Figure 1.1	Schematic representation of the major events in fiber degeneration after focal injury of tibialis anterior (TA) muscle in mice.....	5
Figure 1.2	Schematic representation of the major events in muscle fiber regeneration.....	6
Figure 1.3	The proposed role of Schwann cells in inducing and guiding nerve sprouting in partially denervated muscle.....	14
Figure 2.1	Single muscle fiber can be ablated by laser microbeams .....	25
Figure 2.2	All the sole plate nuclei in the muscle fiber are labeled by propidium iodide (PI) 1 hour after laser ablation .....	27
Figure 2.3	1 day after laser ablation, injected dye quickly leaks from the damaged fiber but not from an intact fiber .....	29
Figure 2.4	Injected dye also can not stay in the damaged fiber if the electrode is placed on the former junction.....	30
Figure 2.5	Macrophages invade the entire damaged fiber, including underneath the junction.....	32
Figure 2.6	Laser ablation itself does not disrupt the layout of AChR, terminal Schwann cells (TSCs) and nerve terminal (NT).....	34
Figure 2.7	Vital repeated imaging does not induce any changes to NMJs on intact muscle fibers .....	36
Figure 2.8	The intensity of rho-BTX labeled AChRs is much fainter 3 days following fiber damage, but its pattern is maintained .....	38
Figure 2.9	The remaining original AChR can be revealed by rho-BTX staining 3 days after fiber damage.....	39
Figure 2.10	The presence of persistent AChR at synaptic sites on ablated fibers can be verified using an antibody against another receptor subunit ( $\beta$ ) .....	41
Figure 2.11	The intensity of AChR labeling gets continuously dimmer on the intact muscle fibers because of receptor turnover .....	44
Figure 2.12	Some of the original AChRs persist at the former synaptic sites for a long time after fiber degeneration .....	45
Figure 2.13	Comparison of the intensity drop of the AChR labeling on the damaged and the intact fibers within one month.....	46
Figure 2.14	In many cases the original junction collapses dramatically following fiber degeneration.....	49

Figure 2.15	The arborization of both TSCs and the nerve terminal is fully preserved despite the degeneration of its underlying fiber .....	50
Figure 2.16	Short TSC processes and terminal sprouts are sometimes detected 4 days after fiber damage.....	52
Figure 2.17	TSC processes and nerve terminal (NT) are seen apposing the AChR at all levels 3 days after fiber damage by confocal microscopy .....	55
Figure 2.18	The order of the apposition of the junctional components is changed on the damaged fiber in Z axis after fiber degeneration ....	57
Figure 2.19	4-Di-2-Asp staining does not reflect the position of the nerve terminals as faithfully as CFP transgene expression .....	64
Figure 3.1	AChR can not be saturated with bungarotoxin using conventional methods.....	70
Figure 3.2	New AChR sites appear gradually at the junction on a regenerating fiber.....	73
Figure 3.3	New AChR sites are added to the original AChR area at some places but not at others.....	75
Figure 3.4	In one case, new AChRs appeared to occupy all of the original AChR sites .....	76
Figure 3.5	Higher magnification shows that the structure of the junctional folds of the new NMJ is different from those of the intact NMJ .....	77
Figure 3.6	New and old AChR sites are present at the same position in an en face view but are not at the same location when viewed 3 dimensionally .....	79
Figure 3.7	New AChR sites can sometimes be found to be situated beneath the original AChR sites.....	80
Figure 3.8	New AChRs and old AChRs always overlap with each other in all dimensions on fibers that were not ablated.....	81
Figure 3.9	Nerve terminals are associated with new AChR sites as well as old AChR sites during early fiber regeneration .....	83
Figure 3.10	New receptor sites located far beneath the original sites are apposed by nerve terminals during early fiber regeneration.....	84
Figure 3.11	Short TSC processes are present with terminal sprouts on regenerating fibers .....	86
Figure 3.12	TSC processes accompany terminal sprouts that are underneath the original basal lamina sheath .....	88

Figure 3.13	TSC processes induce and guide terminal sprouts that then recruit new AChR clusters during muscle fiber regeneration.....	90
Figure 3.14	TSCs also extend processes on the nearby intact muscle fibers during fiber regeneration.....	93
Figure 3.15	4-Di-2-Asp staining is sometimes seen present in unknown cell processes around the junctional area.....	104
Figure 4.1	Newly formed NMJs on the regenerated muscle fibers show some morphological abnormalities around 1 month after fiber damage .....	108
Figure 4.2	Sometimes the morphological abnormalities appear early in the NMJs on regenerated fibers and progressively get more distinct over time .....	110
Figure 4.3	NMJs on the regenerated fibers undergo slow but continuous remodeling .....	112
Figure 4.4	NMJs on the regenerated muscle fibers are transformed into an ‘en grappe’ pattern in months.....	115
Figure 4.5	Each nerve terminal bulb is aligned with each receptor island.....	116
Figure 4.6	Endplates on the intact fibers have smooth outlines in their 3-dimensional views .....	118
Figure 4.7	The relative position of the AChR and NT is changed in 3-D space in the junctions on the regenerated fibers .....	119
Figure 4.8	NMJs on intact muscle fibers are usually stable for a long time .....	121
Figure 5.1	Schematic illustration of the model for synaptic elimination in adult NMJs .....	131

## **CHAPTER 1**

### **INTRODUCTION**

Skeletal muscle fibers are multinucleated, tube-like cells with the length varying in humans from a few millimeters to more than 50 cm. Their diameter can range from 15 to 20  $\mu\text{m}$  (extrinsic eye muscles) to more than 100  $\mu\text{m}$  in trained athletes. Skeletal muscle is composed of 2 main components: the myofibers and the connective tissue. The myofibers are innervated by nerves at sites called neuromuscular junctions (NMJs) and are responsible for the contractile function of the muscle. The connective tissue binds the individual muscle fibers together during muscle contraction and keeps the capillaries within the muscle structure. It also creates a supportive skeleton for the myofibers, combining the contraction of individual fibers into a joint effort and an efficient locomotion. Each myofiber is attached at both ends to the connective tissue of a tendon called myotendinous junctions (MTJs). The connective tissue is composed of 3 levels of sheaths called the endomysium, perimysium, and epimysium (Borg and Caulfield, 1980; Takala and Virtanen, 2000). The most inner layer is the endomysium (also called the basement membrane), that surrounds each myofiber. It contains molecules involved in

expression and location of NMJs (details discussed below). The middle layer is the perimysium, which combines anywhere from some tens to a couple hundred individual myofibers together into larger structures called fascicles. The outer layer is the epimysium, which is fairly thick and surrounds the entire muscle.

Muscle fibers are innervated in a central band. On each fiber there is a specialized structure called the neuromuscular junction (NMJ), which is the synapse in the peripheral nervous system (PNS). Since NMJs are bigger, simpler and more accessible than the synapses in the central nervous system (CNS), they are the most studied of all synapses and they provide a basic notion to scientists of how nervous systems work in mammals.

A NMJ is comprised of three components: a single motor axon coming from the neuron located in the spinal cord; the glial cells that are specifically called Schwann cells (SCs) in the periphery; and the muscle fiber. SCs wrap around the axon before it comes to the terminal and form myelin around it, those are called myelinating Schwann cells; or they just extend processes that just cover the branches of axon terminal at the junction, those are called non-myelinating Schwann cells or terminal Schwann cells (TSCs). Axon terminals make synapses with muscle fibers through acetylcholine receptors (AChRs), but are separated from these receptors by the synaptic cleft (range from 20 to 50nm).

### **Degeneration and regeneration of muscle fibers following muscle injury**

Skeletal muscle is comprised of heterogeneous muscle fibers that differ in their physiological and metabolic parameters (Gunning and Hardeman, 1991). It is this diversity that enables different muscle groups to provide a variety of functional properties. Particularly, it plays a central role in the control of whole-body metabolism.

Therefore, it becomes very important to understand how muscles exert their normal functions and how they behave during disease at both cellular and molecular level. Studies have been performed using exercise, electrical stimulation, transgenic animal models, and disease models to address how muscles repair themselves after damage (Schultz, 1989; Lake, 1992; Anderson, 1998). All these studies will help develop therapeutic approaches to ameliorate muscle injuries and diseases in the future.

On the cellular level, each muscle fiber is a multinucleated cell in mammals. This gives it one unique property from singly nucleated cells where injury to the cell is concerned. For a singly nucleated cell, once its plasma membrane is broken, the intracellular components will leak out. Macrophages then migrate to the damaged cell and phagocytose all the debris including the nucleus. The cell is dead eventually. However, it is quite different with muscle fibers. Since the muscle cell is so big and contains so many nuclei along its length, if the membrane is broken at one place, only the segment which includes the damaged area and its vicinity will degrade. The two ends of that fiber will be protected from degradation by a temporary membrane formed following injury, separating the intact part from the damaged segment. The open damaged segment will be invaded by macrophages and other leukocytes from immune system. These cells will phagocytose all the broken debris in the damaged area in about 1 day. This degradation process to the injured muscle fibers is particularly referred to as ‘Segmental Necrosis’ (Carpenter and Karpati, 1989; Papadimitriou et al., 1990) (Figure 1.1).

Regeneration of muscle fibers also happens very quickly. When fibers are injured, not only immune cells are activated to clean up the damaged area, but also satellite cells are activated to proliferate and migrate to the injured site where they differentiate into

myoblasts (Schultz et al., 1985). Satellite cells are the progenitor cells for muscle fibers located underneath the basement membrane surrounding each myofiber (Mauro, 1961; Schultz and McCormick, 1994). They are usually quiescent after the muscle matures, but they can be activated in response to muscle trauma, such as hypertrophy or injury. Muscle is able to efficiently regenerate after repeated damage; therefore, they always maintain a viable pool of satellite cells in the endomysium. Physiologically, the times of muscle fiber regeneration has a limit under the condition that the supply of satellite cells is not exhausted; otherwise, muscle regeneration will be impaired as what happens in Duchenne muscular dystrophy.

Once the myoblasts are committed, they will keep on dividing and later fuse with each other to form a new myotube at the damaged area. Since the rest of the fiber is still intact, separated by a temporary membrane from the necrotic segment, the new myotube will then fuse with the rest of the original fiber at its two ends to form a new fiber (Carpenter, 1990) (Figure 1.2). After that, the new fiber will grow in diameter at the regenerated segment to become as large as the undamaged segments. It takes about two weeks for a damaged muscle fiber to regenerate and regain its growth rate similar to the intact ones (van Mier and Lichtman, 1994). The regenerated fibers also regain their physiological properties as same as the intact fibers (Grubb et al., 1991).

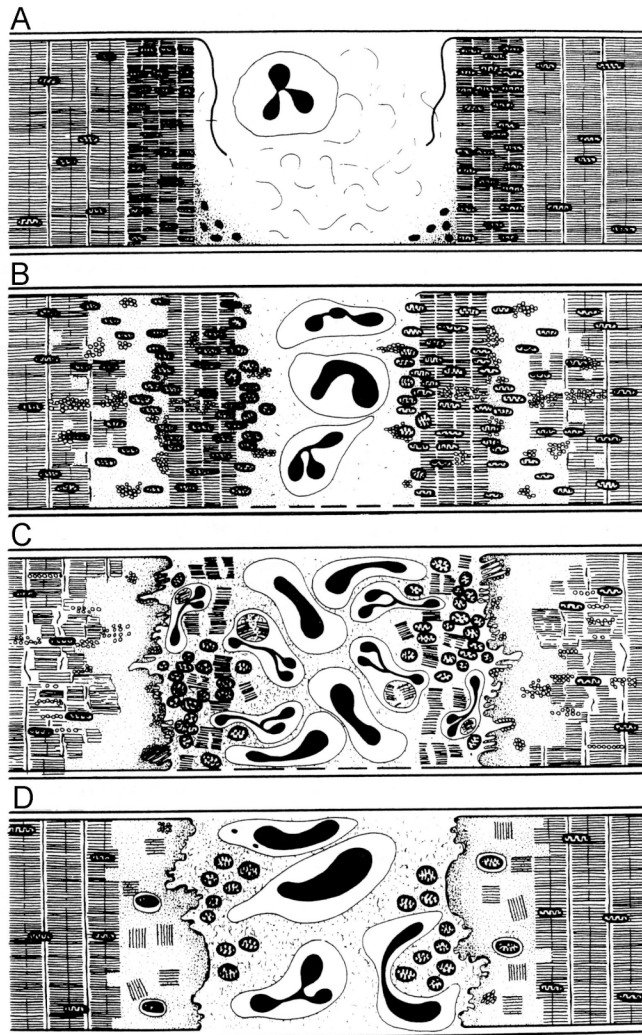


**Figure 1.1 Schematic representation of the major events in fiber degeneration after focal injury of tibialis anterior (TA) muscle in mice.**

A. 3 hrs after injury, a central relatively clear zone bordered by hypercontracted myofibrils marks the site of injury, while the plasmalemma has collapsed onto the face of the supercontracted segment. A few polymorphonuclear leukocytes (PMN) have invaded the injured area. B. at 6 hrs, the injured segment is infiltrated with many PMN and occasional macrophages. The plasmalemma is discontinuous and a myofibrillar-free zone has appeared between the supercontracted myofibrils and the undamaged sarcoplasm. Mitochondria and various vesicles have aggregated at the periphery of the stump. C. at 12 hrs, phagocytosis of the supercontracted myofibrils and associated organelles is well advanced. A tortuous demarcating membrane has formed separating the necrotic area from the structurally intact sarcoplasm. At the junction of the demarcating membrane and the plasmalemma, interdigitations are conspicuous. D. 24 hrs after injury, the necrotic area is now almost devoid of damaged muscle elements and the predominant infiltrating phagocytes are macrophages. The demarcating membrane is much less tortuous and scattered myofilaments and autophagosomes can be seen in this relatively organelle-free myoplasm of the sealed myofiber. (adapted from Papadimitriou et al., 1990)



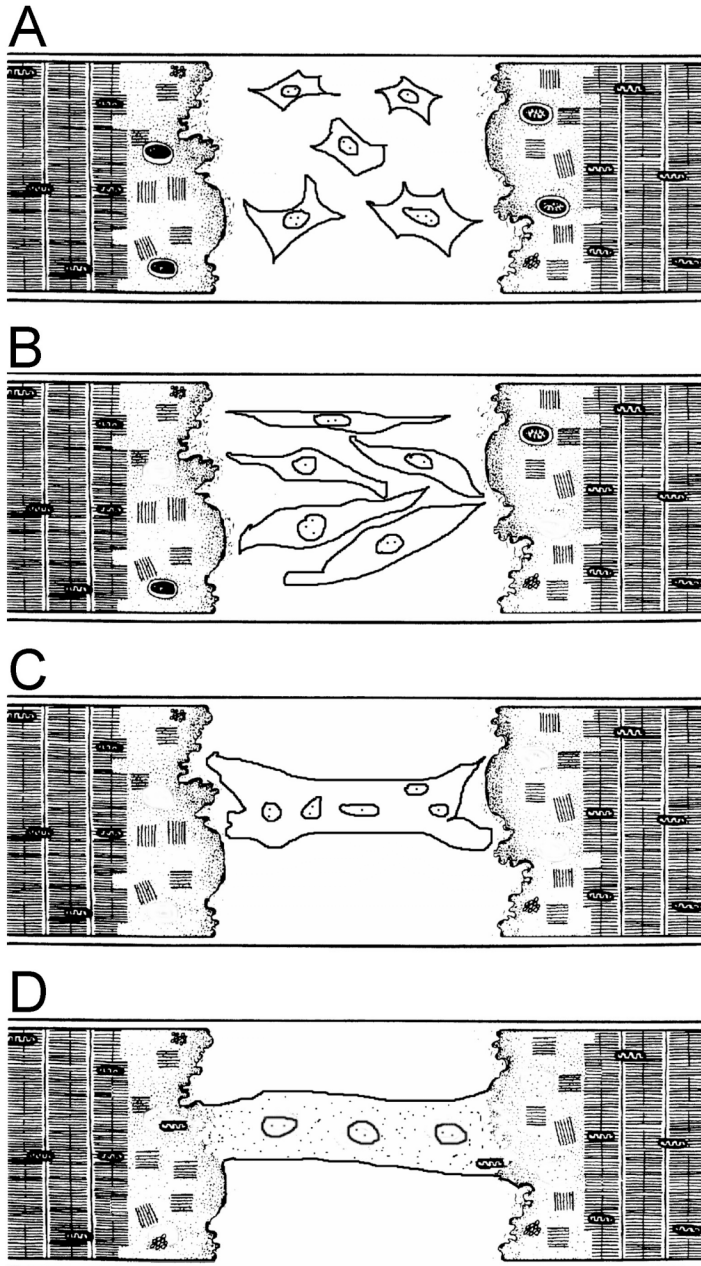


**Figure 1.2: Schematic representation of the major events in muscle fiber regeneration.**

(A) Satellite cells in the connective tissue around the damaged fiber exit their normal quiescent state following the injury of the muscle. The activation leads to their proliferation and migration to the injured site. (B) After they reach the injured site, they will differentiate into myoblasts. (C) Myoblasts fuse with each other and form a thin myotube. (D) In the end, the membrane of the new myotube at both of its end fuses with the membrane that separates the intact segments from the injured site, such that a continuous fiber is re-made. At the regenerated site, muscle nuclei are always aligned in the center.

## **The response of nerve terminals to the loss of postsynaptic cells following muscle fiber damage**

Nerve terminals formed by motoneurons located in the spinal cord make synaptic contact with muscle fibers. If muscle damage occurs far from the junctional area, the regeneration will only include new myotube formation as described above. However, if the muscle fiber damage includes the NMJ area, then the regeneration process not only includes new myotube formation, but also involves new NMJ formation.

It was shown in living mice that when muscle fibers were cut on both sides of the endplates, motor nerve terminals retracted quickly from the junctions following muscle fiber degeneration. AChRs also disappeared within a couple of days. Nerve terminals would stop retraction when fiber regeneration began and instead, regrew to reestablish synapses with the newly expressed AChRs on the new fibers. Some original synaptic sites were reoccupied by new receptors while some new sites were added as well. Eventually the alignment between AChRs and their nerve terminal branches would regain its perfection at the junction, looking the same as a junction on an intact fiber (Rich and Lichtman, 1989b). These results suggested that the maintenance of the nerve terminal at the neuromuscular junction is dependent on the presence of the postsynaptic cell—muscle fiber. On the other hand, the pattern of the new receptor plaque is directed by the organization of nerve terminals.

However, there is controversy as to whether the same events happen in frogs. By using repeated vital imaging, another group showed conflicting results in amphibians. They cut the muscle fibers and left motor innervation intact. In addition, the regeneration of muscle fibers was prevented by X-irradiation. They found that nerve terminals were in

fact well maintained at synaptic sites during the first 1-2 months after removal of postsynaptic cells and on average, 85% of the original number of nerve terminal branches was retained. Even after long periods of target loss, 6-9 months, there were still some nerve terminal branches left at synaptic sites. Therefore, they suggested that the cues for the persistence of nerve terminal branches at synaptic sites in the absence of postsynaptic cells likely lay external to muscle fibers, either associated with the synaptic basal lamina or the terminal Schwann cells (Dunaevsky and Connor, 1998).

Another interesting issue is that when rat soleus muscle was damaged by notexin application (Notexin is a component of the venom of the Australian tiger snake *Notechis scutatus*), some of the original AChR molecules were still detected even when the muscle degeneration was complete and a new fiber had grown. Electron microscopy showed that components of the junctional membrane seemed to stay longer than those of the extrajunctional membrane. However, the fate of this remnant of muscle membrane was not clear since regeneration happened quickly (in 3-4 days) and the membrane of the new myotube soon became closely apposed to the remaining basal lamina at the junction (Slater and Allen, 1985). This result also suggested that some of the AChR molecules are attached to the basal lamina at normal NMJs.

### **The factors contributing to reestablishing synaptic connection**

New myofibers that form inside their original basal lamina mostly become innervated at the original synaptic sites. In order to find out what factor(s) influence the growth of the regenerating axons to the original synapse or the accumulation of new acetylcholine receptors (AChRs) on the original synaptic sites, people damaged and

denervated cutaneous pectoris muscles in frogs in the 1970s. Regenerating axons growing inside the surviving perineurium reached the original synaptic sites within 2 weeks. This happened similarly in damaged fibers either allowed to regenerate or prohibited from regeneration by X-irradiation (Sanes et al., 1978). In addition, if the nerve was prevented from reinnervation for a month, new AChR clusters can still be accumulated at the original synaptic sites on the regenerated fibers. The density of the receptors was the same as that at normal NMJs. Synaptic folds in the fiber surface also resembled those at normal NMJs (Burden et al., 1979). These experiments suggest that whatever the factor(s) causing the precise return of new NMJs to the original site are, they reside in the surviving original basal lamina.

This is the same in mammals. New “ectopic” NMJs were formed by implanting a foreign nerve onto rat soleus muscle. Then the muscle fibers were damaged at different stages of these NMJ formation. Only when muscle fibers and nerve were damaged after “ectopic” NMJs matured (about 8 days or longer) were new AChR clusters found in the region of “ectopic” NMJs, as well as acetylcholinesterase (AChE) activity on regenerated fibers. If muscle and nerve were damaged 4 days or less after “ectopic” NMJ formation, neither receptor nor esterase was detected on the regenerated fibers (Slater and Allen, 1985). These results support the idea that a mature basal lamina is necessary for AChR accumulation at original sites after muscle damage.

Subsequently, investigators have tried to find out the specific molecules in the basal lamina that are responsible for AChR accumulation. There are several molecules residing in the basal lamina: laminin  $\alpha 2$ ,  $\alpha 4$ ,  $\alpha 5$ ,  $\beta 2$ ,  $\gamma 1$ ; agrin; AChE; neuregulin; collagen etc. (Laurie and Leblond, 1983; Patton, 2003). Among all, agrin proved to be the

crucial molecule causing receptor clusters (Reist et al., 1992; Cohen et al., 1997; Gautam et al., 1996).

### **The importance of Schwann cells at NMJs**

When studying NMJs, convention has usually placed interest on the synaptic transmission between axon terminals and AChRs on the muscle fiber, overlooking the importance of Schwann cells, the peripheral glia cells. Schwann cells were first discovered by Theodore Schwann, a German physiologist more than 150 years ago, in 1839. Since then, people have found that these cells don't just generate myelin for axons; they play more roles and perform more functions in PNS. First, they were shown to participate in the buffering of ionic concentration through potassium and sodium channels located on their surface (Kuffler and Nicholls, 1966; Newman, 1984; Barres, 1991). Second, it was found that Schwann cells also have receptors (such as glutamate receptor, GABA receptor) on their surface *in vitro* and *in vivo*. Those receptors are believed to influence Schwann cell proliferation and myelin protein expression or respond to the signals sent by neurons (Chiu and Kriegler, 1994; Dememes et al., 1995; Magnaghi et al., 2006). Third, glia cells can release trophic factors, providing a nourishing environment for neurons (Marchionni et al. 1997). Some of those factors can promote the survival of motor neurons (Henderson et al., 1994) while others are important in promoting either the growth of motor neurons or the process extension of Schwann cells themselves (Anton et al., 1994). On the other hand, neurons also excrete trophic factors to support and modulate Schwann cell growth. The axonal supply of neuregulin during early development is required for the survival of the precursor cells

that give rise to Schwann cells later on (Dong et al., 1995). The presence of neuregulin is also crucial to keep Schwann cells alive in neonatal animals and if muscle is denervated in neonates, Schwann cells will undergo apoptosis but can be rescued by exogenous application of glial growth factor 2 (Trachtenberg et al., 1996). Thus, the trophic interactions between motor neurons and Schwann cells are reciprocal. They depend on each other especially in early development. Similar effects were proposed by Verdi et al. (Verdi et al., 1996) for sympathetic neurons and their glial cells.

As stated above, according to their position and myelination, Schwann cells are subdivided into two groups. The cells that wrap around axons along their length and make myelin are called myelinating Schwann cells, while the others that cover the axon terminal and are located at the NMJ are called terminal Schwann cells (TSCs). In the past decade, terminal Schwann cells have been shown to be of special importance at the junction. They are involved actively in the maintenance and repair of NMJs (details below, Son et al., 1996). In normal muscles, terminal Schwann cells can sense synaptic transmission through receptor binding and ATP released by motor neurons (Robitaille, 1995; Robitaille et al., 1997) and change their gene expression as a consequence (Georgiou et al., 1994). At the same time, terminal Schwann cells can ‘talk’ back to neurons by modulating neurotransmission in intact muscle preparations (Robitaille, 1998). The ability of those cells to undergo immediate morphological changes in response to denervation and paralysis suggests that these cells also play an important role in synaptic restoration during reinnervation (Son and Thompson, 1995a,b).

### **Terminal Schwann cells extend processes beyond the endplate area after denervation and guide regenerating axons to follow their path**

Terminal Schwann cells not only regulate synaptic activities in normal muscles, they also play critical roles in synaptic recovery following nerve injury. In 1992, Reynolds and Woolf reported that terminal Schwann cells grew long processes, which sometimes formed a network away from synapses, in response to denervation (Reynolds and Woolf, 1992). Although they did not believe that this growth could help nerve regeneration because the processes appeared to be random, more recent evidence has shown that they actually do. Besides denervation, blocking neurotransmission with application of botulinum toxin to muscles also causes terminal Schwann cells to grow processes (Son and Thompson, 1995b). Therefore, terminal Schwann cells are able to sense neuronal activities and respond to denervation and paralysis.

However, how are these processes involved in nerve regeneration? During reinnervation, regenerating axons follow old Schwann cell tubes previously associated with axons, leading to individual endplates. Most of the time, they don't stop at the junction but continue to grow beyond the endplate area and form terminal sprouts. These sprouts are always found to be associated with Schwann cell processes (Son and Thompson, 1995a). The *in vivo* images later on revealed that Schwann cell processes always precede terminal sprouts.

### **Terminal Schwann cells guide the growth of axon sprouts between two synaptic sites**

During nerve regeneration, most of the endplates are reinnervated by the regenerated axons following the original Schwann cell tube. However, there are some

endplates that will be innervated by axons from nearby junctions. This is more obvious in partial denervation (Figure 1.3). Under these circumstances, the terminal sprouts growing from the innervated junction were again found to be associated with Schwann cell process extending from the denervated junction and interconnecting the two synaptic sites (“Schwann cell bridges”) (Son and Thompson, 1995a). Furthermore, Schwann cells rarely form bridges between two denervated endplates, but were more inclined to do so between a denervated endplate and an innervated endplate following partial denervation. This result implies that some trophic factors are likely to induce the growth of terminal Schwann cell processes (Love and Thompson, 1999).



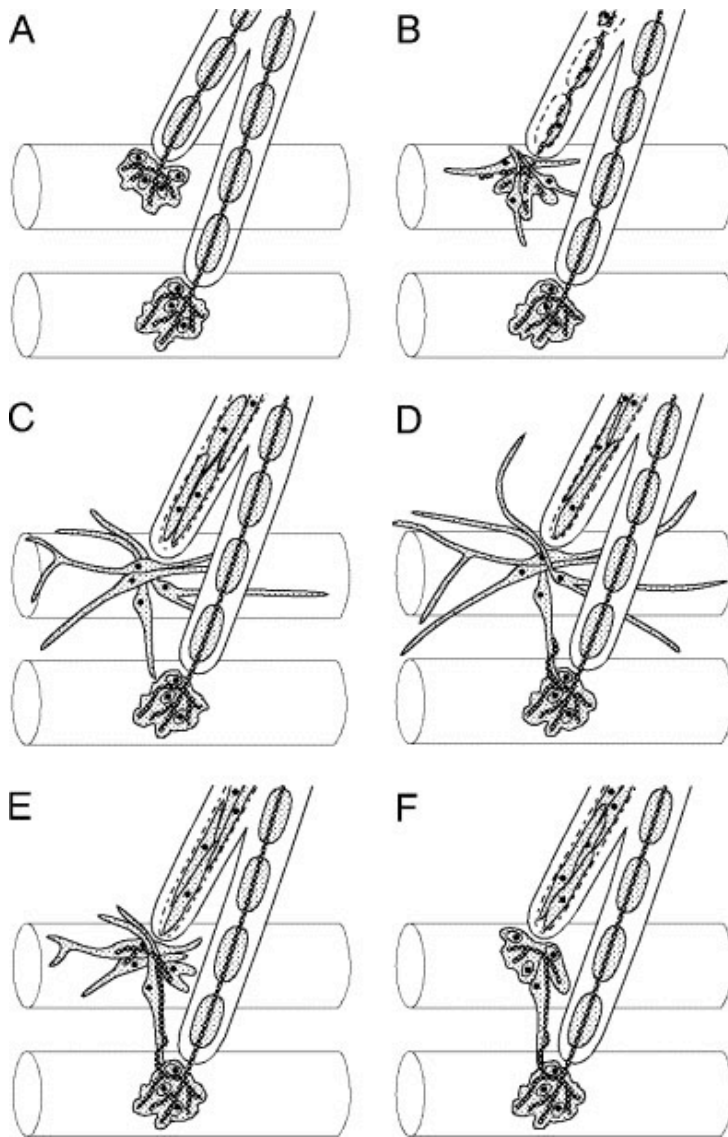


**Figure 1.3 The proposed role of Schwann cells in inducing and guiding nerve sprouting in partially denervated muscle.**

(A) Two myelinated axons innervating two muscle fibers. Terminal Schwann cells cover the nerve terminal processes at each junction. (B) Partial denervation of the muscle injures the axon that innervates the top muscle fiber. This axon begins to degenerate (indicated by dashed line) and the terminal Schwann cells at its endplate begin to extend processes. In (C), one of the processes extended from the Schwann cells at the denervated junction on the top muscle fiber has reached the nerve terminal remaining on the bottom muscle fiber. In (D), contact with the Schwann cell induces the nerve terminal on the bottom muscle fiber to sprout. The sprout is guided in its growth by the Schwann cell process. In (E), the nerve sprout has grown to reinnervate the denervated endplate, and the terminal Schwann cells here have begun to retract their processes. (F) The consequence of these events: the denervated muscle fiber is now innervated by a sprout arising from the fiber that remained innervated following the partial denervation. (From Son et al., 1996)

### **What induces terminal Schwann cells to grow processes?**

Denervation causes terminal Schwann cells to grow processes beyond the junctional area. However, this does not absolutely mean that loss of the axon is the only cause of growth. The growth of Schwann cell processes maybe due to the changes in status of the muscle, as well. Indeed, it was found that direct stimulation of a partially denervated mouse soleus muscle inhibited axon sprouting from the surrounding innervated muscles and it did so by activating the denervated fibers (Brown and Holland, 1979). This suggests that after partial denervation, whatever signals that were released from the paralyzed fibers were able to spread from the denervated muscle fibers to the nerves on the innervated fibers and initiated terminal sprouting. Similar results were also seen when a single muscle fiber was irradiated by laser beams. Degeneration of muscle fibers did not cause nerve sprouting, but regeneration of the fibers did. The regenerating fibers can induce terminal sprouts not only from themselves, but also from nearby intact fibers (van Mier and Lichtman, 1994). This obviously showed that regenerating fibers were able to send out some diffusible signals to induce nerve sprouts from surrounding intact fibers. Since terminal sprouts are believed to follow terminal Schwann cell processes, this result raises the issue of whether terminal Schwann cells are induced to grow by muscle fiber regeneration as well. If this is true, it means that changes to the muscle fibers initiate NMJ remodeling. Terminal Schwann cells serve as a medium for that to occur, and nerve terminals follow their path under any conditions. Such a result would inform and direct future research to focus on looking for the molecules secreted by regenerating muscle fibers. Knowledge of such factors could be used to assist in the repair of NMJs in muscle injuries and diseases. This will be the principal question I want

to address in my thesis.

## **CHAPTER 2**

### **TERMINAL SCHWANN CELLS AND NERVE TERMINALS ARE MAINTAINED AT THE NEUROMUSCULAR JUNCTION AFTER REMOVAL OF POSTSYNAPTIC MUSCLE FIBERS**

#### **ABSTRACT**

In order to examine how terminal Schwann cells and nerve terminals respond to muscle fiber damage, I conducted vital imaging experiments in which I damaged individual muscle fibers with a laser microbeam and examined the response of GFP-expressing Schwann cells and CFP-expressing motor axons during muscle fiber degeneration and regeneration in transgenic mice. In the course of these experiments, I noted an unexpected persistence of the alignment of synaptic components. Two days after muscle fiber damage, the synaptic site was obviously shrunken, presumably due to the loss of the underlying muscle fiber. Acetylcholine receptors labeled with bungarotoxin prior to fiber ablation, although more faintly labeled, persisted afterwards. The arborization of the terminal Schwann cells (TSCs) and the nerve terminals also were shrunken, but not obviously changed in their branching pattern. Even 4 days after fiber

damage, near the time when a newly regenerated fiber is sometimes seen within the sheath of the previous fiber, some of the old (bungarotoxin-labeled) receptors were still visible at the original synaptic sites (they can last for months). Additionally, nerve terminals and Schwann cells had neither retracted nor extended from the synaptic site. All these observations suggest that as a muscle fiber degenerates following extrasynaptic damage, the synaptic components, including some persistent AChR remain in alignment. This implies that this synaptic alignment has structural components that persist following loss of the postsynaptic muscle fiber and the changes in synaptic signaling that must result.

## **METHODS**

### **Animals**

Double transgenic mice were used in the experiments. These animals express two, soluble, cytoplasmic fluorescent proteins: EGFP (enhanced green fluorescent protein) driven by a glial specific promoter (S100) in Schwann cells (generated in the lab), and CFP (cyan fluorescent protein) driven by the Thy1 promoter in motor neurons (Feng et al., 2000). All mice were derived by inbreeding of C57BL6 and DBA strains and no effort was made to breed to minimize differences in genetic background. Genotyping of fluorescent mice was accomplished by observing a piece of ear under a fluorescence dissecting microscope. For experimental convenience, in most cases mice were bred between a wildtype and a homozygosity for both EGFP and CFP transgene, therefore, their progeny used in the experiments would always bear a copy of each transgene insertion.

## ***In Vivo* Procedure**

The *in vivo* surgery was conducted following the methods of Jeff Lichtman et al. (Lichtman et al., 1987). Mice were anesthetized by intraperitoneal injections of ketamine/xylazine (0.10-0.15 ml of a 0.9% NaCl solution containing 17.4 mg/ml ketamine and 2.6 mg/ml xylazine), and placed on the microscope stage in a supine position. The mouse's front limbs were secured with rubber bands. Its breathing was mechanically controlled by a small respirator (model 683; Harvard Apparatus, Holliston, MA). All the hair on the ventral neck was removed with Nair. Using aseptic surgery, the left sternomastoid muscle was exposed by a midline incision in the ventral neck. The postsynaptic acetylcholine receptors (AChRs) were then labeled with rhodamine-conjugated bungarotoxin (rho-BTX, Molecular Probes, 5 min of 2 $\mu$ g/ml in sterile lactated Ringer's, followed by rinsing with the same Ringer's, Baxter Healthcare Corp.). Given the large safety factor of the neuromuscular junction in adults (>70% of AChRs must be blocked to disrupt transmission, Lingle and Steinbach, 1988), this dosage should not block postsynaptic activity. The sternomastoid muscle was slightly elevated by a stainless steel ring attached to a small manipulator. A similar ring was also placed on the ventral surface of the muscle surrounding the central band of neuromuscular junctions to both stabilize the muscle and provide a space filled with sterile lactated Ringers for the immersion objectives of the microscope. Then the animal was ready for image capture. After all the images were collected, the wound in the skin was sutured with a 6-0 silk thread and the animal was allowed to fully recover in its home cage under a heat lamp. The same junctions were imaged at subsequent time point(s) depending on the experiment using the same procedure above.

## **Laser Ablation**

On the occasion of the capture of the first image in each animal (and only at this time), 4-Di-2-Asp, a fluorescent vital mitochondrial dye, was applied for 1 min after rhodamine-bungarotoxin (rho-BTX) to label each single muscle fiber (0.1 $\mu$ g/ml in lactated Ringer's). The whole stage with the living animal on it was then taken to Zeiss epifluorescence microscope setup with a laser ablation attachment (Photonic Instruments). I used a dye pumped Nitrogen laser (model LS 337, Laser Sciences) to ablate single muscle fibers. Coumarin 480 (Laser Sciences) in the dye cell was excited at 337nm with the pulse power of 120 $\mu$ J. The laser beam was focused through the 63X 0.9NA water objective and its intensity adjusted by a neutral density attenuator. The procedure was monitored through a SIT camera attached to the microscope and a Sony TV monitor. Each candidate fiber (also on the very surface of the whole muscle) was then irradiated 3-4 times on either side of the junction, but the endplate itself was not targeted. A plasma bubble was always visible at the time of the ablation. After all the irradiation was done, the whole stage with the animal on was then moved back to Leica microscope and CCD camera to take vital images.

## ***In Vivo* Image Capture and Analysis**

All the *in vivo* images were collected by a Leica (Nussloch, Germany) epifluorescence microscope with Nikon water immersion objectives (10X 0.3NA; 40X 0.8NA). Different filter sets were used to visualize each component with different fluorescence at the junction: CY5 620/60X, 660LP, 700/75m; TRITC 535/50x, 565LP, 610/75m; GFP 480/40x, 505LP, 535/50m; CFP 436/20x, 455DCLP, 470/40m (Chroma

Technology, Rockingham, VT). The intensity of illumination was adjusted with a combination of 4 neutral density filters. Among them, two have 50% blockage of the light and the other two 25%. Images of individual junctions were taken with a CCD camera (CoolSnap HQ, Photometrics, Huntington Beach, CA), acquired with IPLab3.5 software on a Macintosh computer. Images were captured with 1 second exposure using 2X2 binning and saved as black and white image files. Figures were then constructed using IPLab3.5 and Adobe Photoshop software with adjustments made only in image brightness and contrast.

### **Other live Staining**

To test whether the ablated fiber was dead, 0.1mM propidium iodide (PI) was applied to the living muscle 1 hour after laser irradiation for 3min. Only dead cells would be labeled by PI.

### **Histochemistry**

When needed, the animal would be sacrificed with pentobarbital (0.05-0.1ml of 5g/ml pentobarbital) after the final *in vivo* images were collected. The muscle was then dissected and fixed with 4% paraformaldehyde (PFA) in PBS (phosphate buffered saline, pH 7.4) for 30 minutes. The muscle was then rinsed with PBS for 3 times, 10mins each. A thin layer of surface fibers was then dissected from the whole muscle (“filleting”) and mounted in fluorescence mounting medium. The same endplates imaged *in vivo* were located *in vitro*, if possible, based upon the label for AChRs (almost 100% successful rate).



In some experiments, the muscle was incubated with 4',6-Diamidino-2-phenylindole (DAPI) ( $10^{-4}$  mg/ml) for 10min before filleting to label nuclei.

In other experiments, AChRs were labeled with monoclonal anti-AChR  $\beta$ 1 subunit (Sigma, N8283). In this case, the sternomastoid muscle was dissected and fixed in 1% PFA for 30min. Then it was washed with 3 times PBS for 30min in total before being transferred into goat serum blocker for 1 hour. The muscle was then incubated with anti- $\beta$ AChR (1:2000) in goat serum blocker for overnight. On the next day, the muscle was put in goat serum blocker for 1 hour before incubation with Alexa594-goat anti rat secondary antibody (1:250, Molecular Probes) for 1 hour. Finally, the muscle was washed with PBS for 30min.

### ***In Vitro* Image Capture and Analysis**

*In Vitro* images were acquired also by the Leica epifluorescence microscope but using a 40X (1.0NA) oil immersion objective. Image acquisition, filter sets (with the addition of DAPI 360/40x, 400DCLP, 450/60m and Texas Red/Alexa594 580/20X, 595LP, 630/60m), and figure construction were the same as described for the *in vivo* case above.

In some experiments, images were acquired using a Leica confocal microscope (Leica AOBS SP2 Confocal) under 63X 1.4NA oil objectives. Data was analyzed using Leica Confocal Software (Leica Microsystems), ImageJ (NIH) and Metamorph (Molecular Devices).

## **Physiology**

The sternomastoid muscle was rapidly dissected from a euthanized animal and pinned to a Sylgard-coated dish. The muscle was superfused at all time with oxygenated Ringer's solution. An electrode filled with Rhodamine-dextran was used to inject both damaged fibers and intact fibers using iontophoresis. The membrane potential was monitored on an oscilloscope (Tektronix).

## **RESULTS**

### **Individual muscle fibers can be ablated with a laser microbeam**

Neuromuscular junctions were visualized in the sternomastoid muscle of living mice using fluorescence imaging (Lichtman et al., 1987). AChRs were labeled by application of rhodamine-bungarotoxin (rho-BTX), Schwann cells by transgenic expression of GFP (Zuo et al., 2004), and the motor nerve terminal by transgenic expression of CFP (Feng et al., 2000). Prior to ablation, the preparation was briefly stained with a vital, mitochondrial dye, 4-Di-2-Asp. The labeling with this dye made visible the outlines of individual muscle fibers. A laser microbeam was then used to target individual fibers (van Mier and Lichtman, 1994). Serially, 3-4 were targeted in each experiment. For each fiber, laser pulses were focused at 3-4 sites located on each side of the neuromuscular junction. These sites were always 100-150  $\mu\text{m}$  away from the junction itself and were spaced at intervals of 100  $\mu\text{m}$  along the fiber. Observations following this procedure suggest that the targeted fibers were severely damaged and subsequently degenerated. The degeneration included the portion of each fiber underneath the motor nerve terminal, even though this region was not itself directly

targeted with the laser.

The progress of each ablation was monitored by imaging the 4-Di-2-Asp label in the muscle fibers at video rates using a SIT camera. The laser pulses produced a plasma bubble visible at the site of focus. Immediately thereafter, a bright spot of fluorescence, likely representing an aggregation of the sarcomeric components responsible for the background labeling, formed at the site of irradiation and then moved away in each direction from this site, leaving behind a black, unstained void that had the shape of the muscle fiber. As sites on both sides of the junction were ablated, the 4-Di-2-Asp fluorescence was lost from the fiber underneath the junction within 10 min, probably as that the dye-labeled components here were drawn into one of these brightly-labeled, contraction clots (Figure 2.1). The loss of fluorescence from beneath the junction was observed in all the fibers irradiated in this fashion (211 fibers in 68 animals).

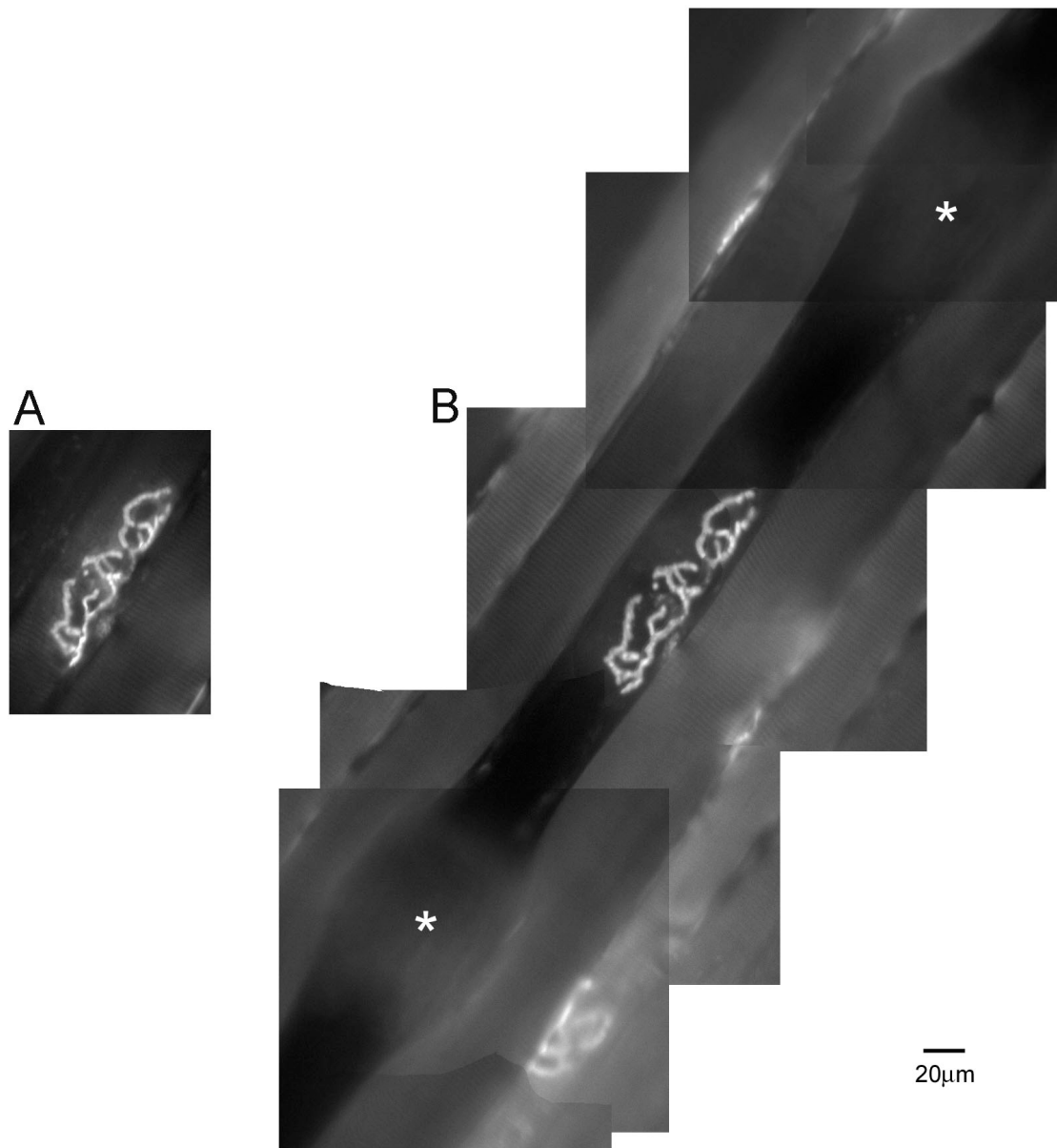


**Figure 2.1 Single muscle fiber can be ablated by laser microbeams.**

(A) After exposing the left sternomastoid muscle, the acetylcholine receptor (AChR) was labeled with Rhodamine-bungarotoxin (rho-BTX) before muscle fibers were stained with 4-Di-2-Asp, a vital mitochondria dye. Therefore, each fiber was visible with sarcomeric striations under rhodamine channel. (B) The laser was targeted to each side of the junction, about 100-150 μm away. The laser produced a plasma bubble on the membrane instantly after it was shot and afterwards, a bright spot of fluorescence, likely representing an aggregation of the sarcomeric components responsible for the background labeling, formed at the site of irradiation (asterisks) and then moved away in each direction from this site, leaving behind a black, unstained tube. For each fiber, 3-4 sites were ablated on each side of the neuromuscular junction, spaced at 100 μm between each other along the fiber. Bar: 20 μm

A second measure of fiber damage was one applied by van Mier and Lichtman (van Mier and Lichtman, 1994), namely the labeling of the sole plate nuclei with propidium iodide (PI). When applied to living tissue, this dye labels the nuclei of cells with damaged cell membranes. Application of PI to the muscle in the living animal 1 hour after laser ablation was found to label nuclei within the damaged fiber. No labeled nuclei were found outside the laser-targeted fiber with the exception of a few cells in the connective tissues over the muscle that were probably damaged during the minor surgery used to expose the muscle. Most importantly, nuclei located underneath the nerve terminal, the sole plate nuclei, were labeled. To verify that every nucleus at the endplate in the damaged fiber was labeled, the muscle was labeled with PI 1 hour after ablation. After such labeling, the animal was sacrificed, the muscle was dissected and stained with DAPI to label all nuclei present (Figure 2.2). The damaged fiber was located, and nuclei that were obviously within the damaged fiber and within 10 $\mu$ m of the endplate were counted. The nuclei of terminal Schwann cells were identified by their GFP label and were excluded from these counts. Excluding these SC nuclei, all the DAPI+ nuclei were PI+ too. Additionally, the number of sole plate nuclei counted in this fashion in damaged fibers ( $4.3 \pm 1.0$ ,  $n = 11$ ) was not significantly different from the counts made in 14 random fibers from junctions on control fibers ( $4.2 \pm 1.2$ ,  $n = 14$ ).

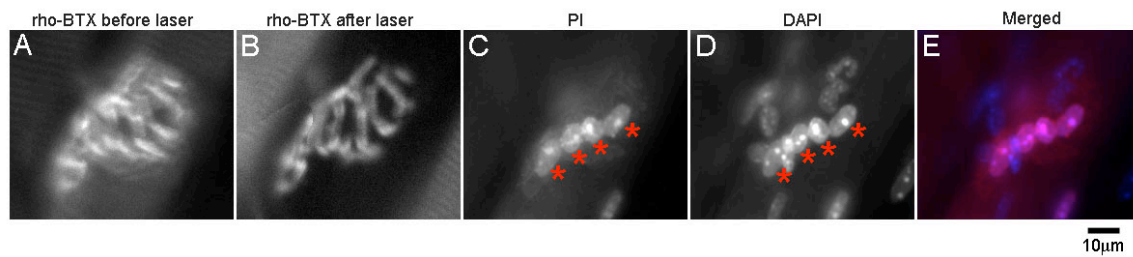


**Figure 2.2 All the sole plate nuclei in the muscle fiber are labeled by propidium iodide (PI) 1 hour after laser ablation.**

(A) AChR was labeled with rho-BTX and muscle fibers with 4-Di-2-Asp. (B) 15min after laser ablation, 4-Di-2-Asp staining was gone from the ablated spots as well as underneath the receptor. (C) 1 hour after ablation, muscle was stained with PI. Sole plate nuclei in the junctional area were labeled only in damaged fibers. PI-labeled nuclei were indicated with asterisks. Since the fluorescence intensity of PI is stronger than rho-BTX, only a faint receptor outline was seen at this time. (D) Muscle was taken out and stained with DAPI, which labels all the nuclei. DAPI positive junctional nuclei inside the fiber (asterisks) and PI positive nuclei in (C), matched, suggesting all the sole plate nuclei were labeled. Other DAPI labeled nuclei were of terminal Schwann cells or connective tissue cells. (E) Overlay of PI and DAPI staining, showing the co-labeled nuclei. Bar: 10µm

As still another assessment of the damage, microelectrodes, manipulated under the visual guidance of a compound fluorescence microscope, were used to penetrate damaged fibers 1 day after laser ablation (9 ablated fibers in 3 animals). Muscles were dissected, pinned to the surface of a sylgard-coated dish, superfused with oxygenated Ringers solution, and the laser-targeted fibers identified by the bungarotoxin-labeling of the pretzel-shaped AChR that persist immediately following the irradiation (see below). No membrane potential could be detected when attempts were made to penetrate damaged fibers in the area of the junction 1 day after laser ablation. In contrast, adjacent fibers that were not targeted with the laser had normal membrane potentials. The electrodes used for these experiments contained the dye rhodamine-dextran and this dye was ejected using iontophoresis after attempting to penetrate the damaged fiber, either a few micrometers away (2 fibers, Figure 2.3) or within the site of the former junction (7 fibers, Figure 2.4). In both cases, the dye rapidly filled a tube-like structure underneath the labeled AChR, but then quickly diffused away. In contrast, dye injected into adjacent, intact fibers was retained in these fibers for the duration of the experiment. These results, like the propidium iodide experiments described above, suggest that the sarcolemma of the damaged fibers was severely damaged. My experiments provided no evidence that a small portion of junctional sarcoplasm was quickly sealed off after the laser damage.

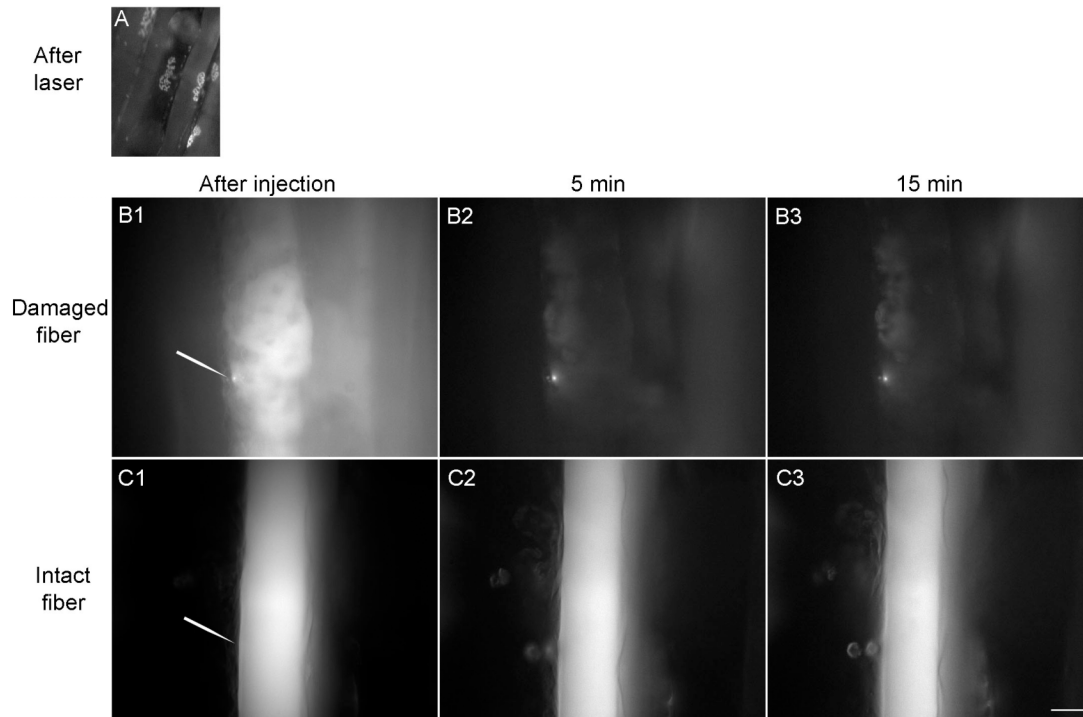


**Figure 2.3 1 day after laser ablation, injected dye quickly leaks from the damaged fiber but not from an intact fiber.**

(A) The fiber in the middle was ablated. Its rho-BTX labeled AChR stood out after 4-Di-2-Asp staining was lost from the underlying fiber. 1 day later, the muscle was taken out and pinned down in a dish supplied with oxygenated Ringer. Rhodamine-dextran, which was filled in an electrode, was injected inside the fiber but away from the junction (arrows). In (B1), the damaged fiber was fluorescent immediately after injection as was the intact fiber (C1). However, the dye quickly disappeared from the damaged fiber. Within 5min, all the dye was lost (B2) but none was lost from the intact fiber (C2). In fact, the dye remained in the intact fiber for hours (much longer than 15min shown in C3). Bar: 40 $\mu$ m



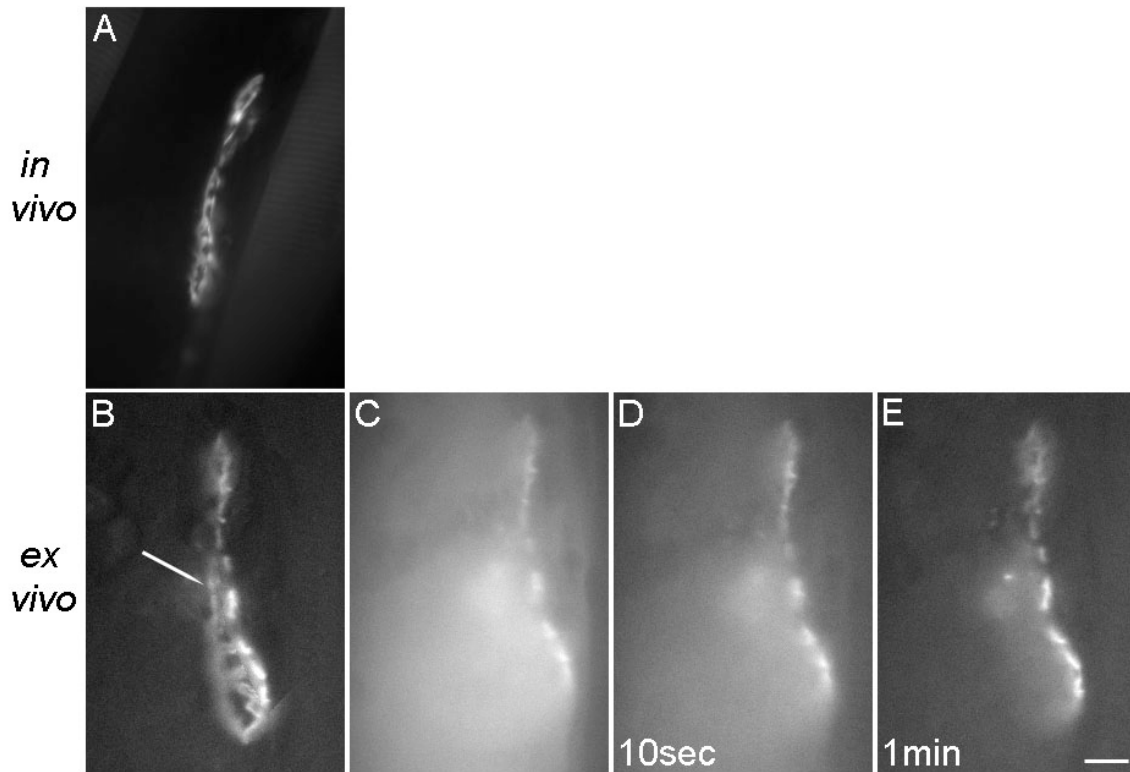


**Figure 2.4 Injected dye also can not stay in the damaged fiber if the electrode is placed on the former junction.**

(A) In vivo image of the AChR whose underlying fiber had just been ablated. The receptor was labeled with rho-BTX. (B) 1 day later, the whole muscle was taken out and placed in a petri dish. The same junction was relocated and the AChR was imaged right before dye injection. The position of the electrode was pointed by an arrow. (C)-(E) Immediately, and 10sec, 1min after dye injection, respectively. The damaged fiber was filled with the dye after continuous injection (C), but quickly lost all of it within 1min. Bar: 20 $\mu$ m

Lastly, macrophages were found to accumulate within the damaged fiber beneath the junction shortly after laser irradiation. Using a transgenic mouse line generated in the lab in which macrophages are labeled with YFP (Zuo et al., 2004), macrophages were observed to accumulate within and along the entire length of damaged fibers, including beneath the junction 1 day after laser irradiation (2 fibers, Figure 2.5). While most of the macrophages were contained within the basal lamina or endomysium of the damaged fiber, a few also accumulated outside, in the vicinity of the damaged fiber.

All the above experiments strongly suggest that laser irradiation destroys the muscle fiber underneath the junction and support the previous findings of Van Mier and Lichtman who performed muscle fiber ablations in a similar fashion.

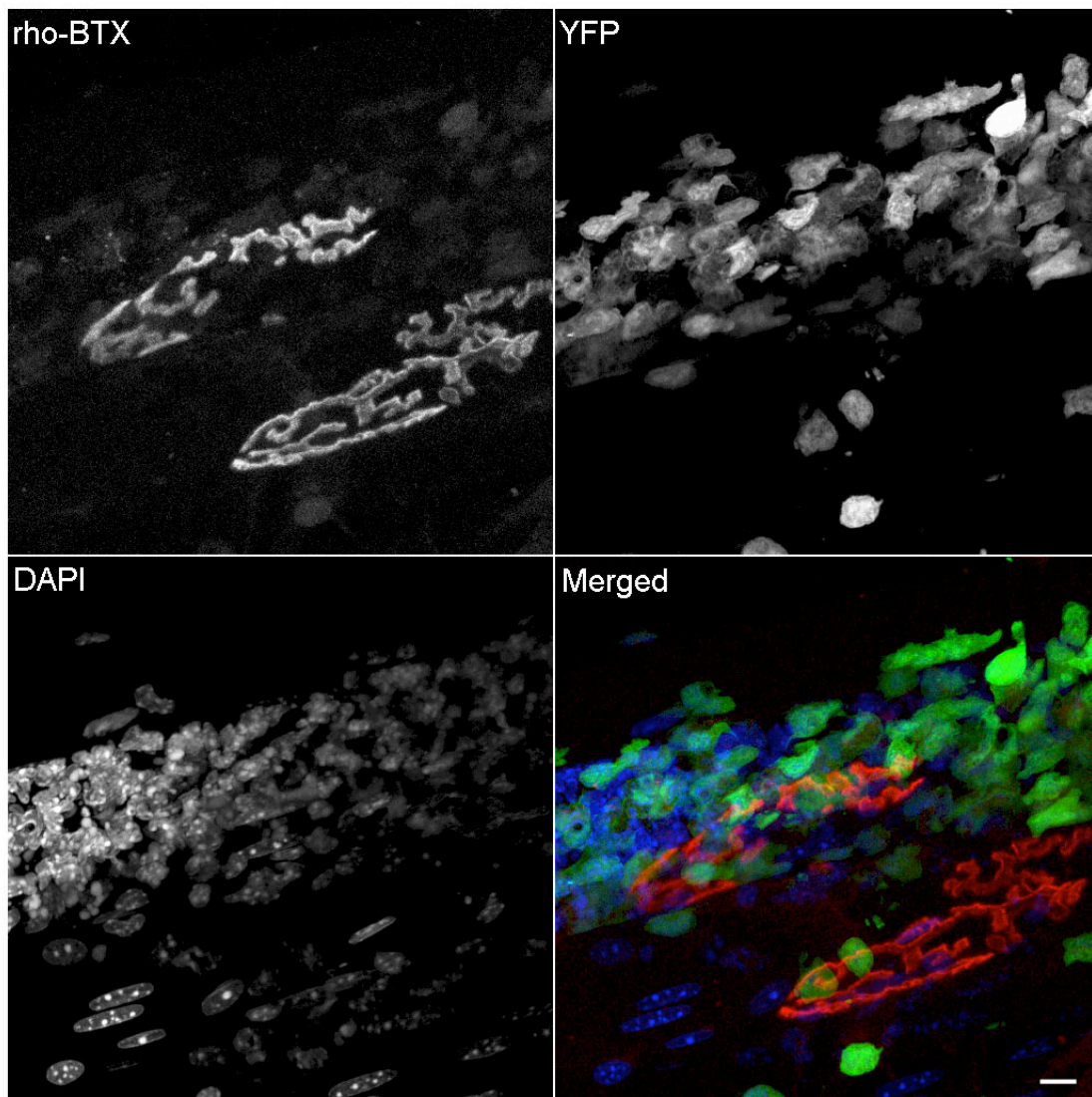


**Figure 2.5 Macrophages invade the entire damaged fiber, including underneath the junction.**

A YFP animal was used whose macrophages have yellow fluorescence protein (YFP) expressed in them. The whole sternomastoid muscle was taken out and fixed 1 day after laser ablation. Muscle was stained with DAPI before mounting onto a slide. The damaged fiber was relocated and images were acquired with a confocal microscope. Images showed here are the maximum projections of its AChR, macrophages, all the nuclei in the tissue and their colored overlay. Only the damaged fiber was filled with extra cell nuclei, including those of macrophages, both along the length of the fiber and beneath the AChR. rho-BTX: AChR; YFP: macrophages; DAPI: all nuclei. Bar: 10 $\mu$ m

**Despite the damage to the underlying muscle fiber, the nerve terminal and its SCs remain initially intact**

Before and immediately following laser ablation, fluorescence images were collected of SCs, nerve terminals, and AChR. During the laser ablation, these components underwent coordinated changes in shape, shortening along the long axis of the fiber, presumably as this fiber underwent contracture. However, they quickly re-expanded approximately to their original dimensions. All components retained their original fluorescence intensity and shape; neither the nerve terminal nor the SCs lost any branches (Figure 2.6). This suggests that these components were not damaged either as a direct or indirect consequence of the laser ablation. I then imaged these components over the course of several months to determine how they changed as the fiber first degenerated and then a new fiber regenerated.

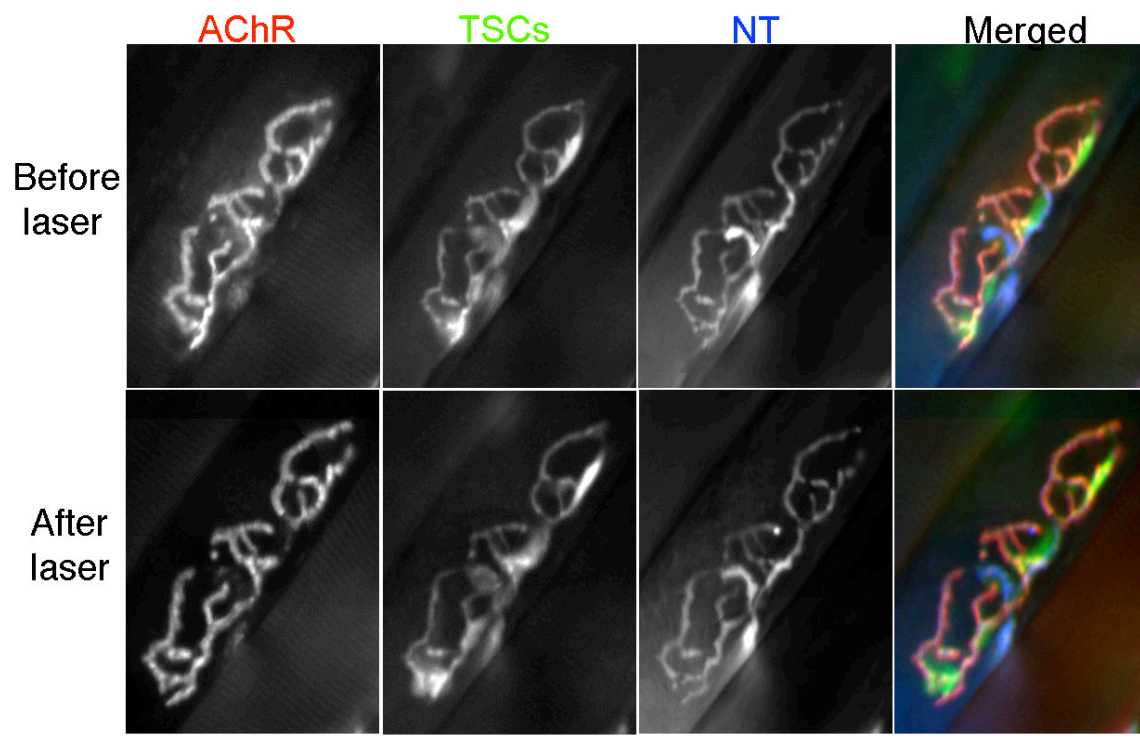


**Figure 2.6 Laser ablation itself does not disrupt the layout of AChR, terminal Schwann cells (TSCs) and nerve terminal (NT).**

AChR, TSCs and NT were viewed before and right after laser irradiation, respectively. AChR was labeled with rho-BTX, TSCs with GFP expression and NT with CFP expression. In the merged images, each of them was assigned a color as seen directly under the fluorescence microscope. AChR appears as red, TSCs green and NT blue. There were no changes to the receptor pattern, arborization of TSCs and NT. The number and position of TSCs didn't change. No retraction of nerve terminals was detected either. All three components of the junction looked exactly the same after laser ablation as before. Bar: 10 $\mu$ m

### **Repeated imaging does not induce any changes to the NMJs**

After laser irradiation, the same synapse on the damaged fiber was imaged *in vivo* for a few times at different intervals. In order to examine the possibility that repeated imaging itself might cause changes in the junctions, control experiments were performed. In double transgenic 2 months old mice, the same junctions were imaged twice, 3 days apart. Comparing each NMJ component in two sets of images, none of them showed any changes. The AChR pattern stayed the same. The branching pattern of TSCs and nerve terminal, the site where the nerve entered, and the number or position of TSC bodies, all of these remained the same (Figure 2.7). Therefore, in agreement with the *in vivo* imaging previously done in the lab, repetitive imaging does not induce any changes in the synapses. These findings agree with previous reports that adult NMJs are very stable and therefore not damaged by such imaging (Lichtman et al., 1987).

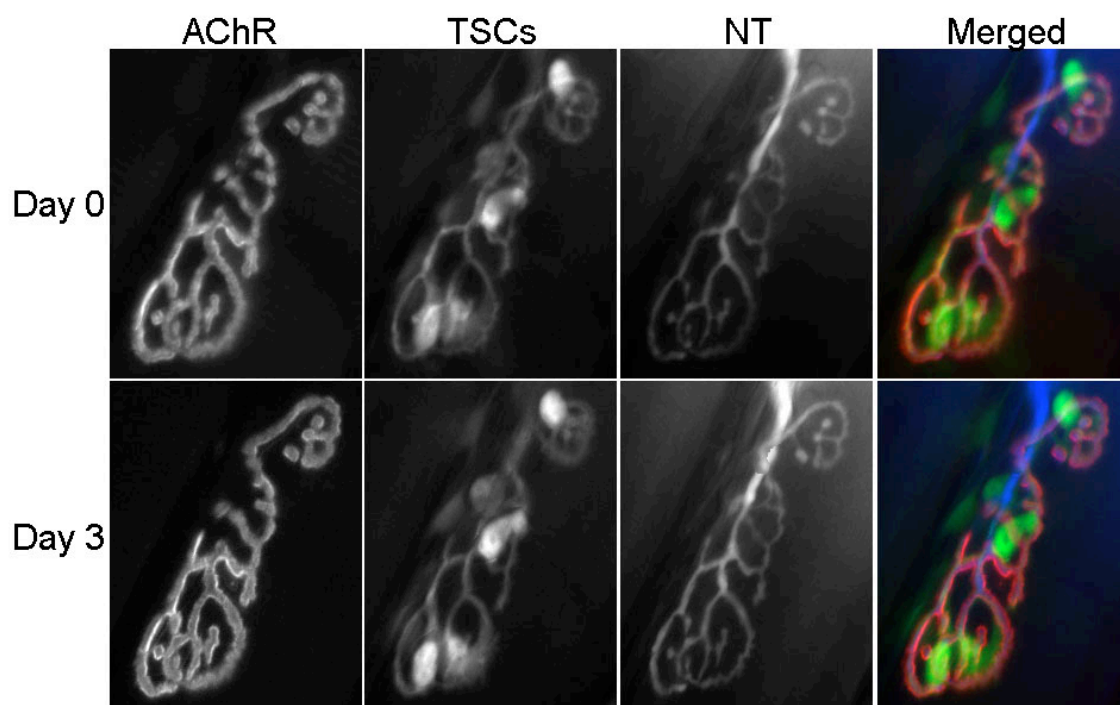


**Figure 2.7 Vital repeated imaging does not induce any changes to NMJs on intact muscle fibers.**

AChR, TSCs and nerve terminal (NT) were viewed twice with 3 days apart. AChR was labeled with rho-BTX, TSCs with GFP expression and NT with CFP expression. In the merged images, AChR appears as red, TSCs green and NT blue. Comparing the images of each component taken at different times, there were no changes to the pattern of the receptor, arborization of TSCs and NT. The number and position of TSCs didn't change, either. Bar: 20 $\mu$ m

### **Some AChRs present at the time of muscle fiber ablation persist for months**

As I imaged the synaptic elements on the ablated fibers over time in the living mice, I observed that the rhodamine label applied as rhodamine-bungarotoxin prior to laser ablation, persisted in the original, pretzel-pattern present in the first image for some time, even though its intensity markedly diminished (Figure 2.8). To examine whether the persistent label is of receptors and not just the fluorophore, I performed additional experiments.

I first asked whether fluorophore-tagged bungarotoxin would label receptors at the former synaptic sites on ablated fibers if applied for the first time after allowing a period of a few days for fiber degeneration. The synaptic site was identified *in vivo* by 4-Di-2-Asp staining and the transgenic expression of fluorescent proteins (CFP label in the motor axon and GFP in the SCs), no bungarotoxin was applied, and then the fiber was ablated. Three days later, rhodamine-bungarotoxin was applied. For 2 ablated fibers in a single animal, labeling at much diminished intensity (compared to surrounding undamaged fibers) was present in a pretzel-shaped pattern that matched the 4-Di-2-Asp labeling 3 days ago (Figure 2.9). This result suggests that components that bind bungarotoxin persist at the former synaptic site and the persistent labeling described above is not of trapped fluorophore in the absence of receptors.



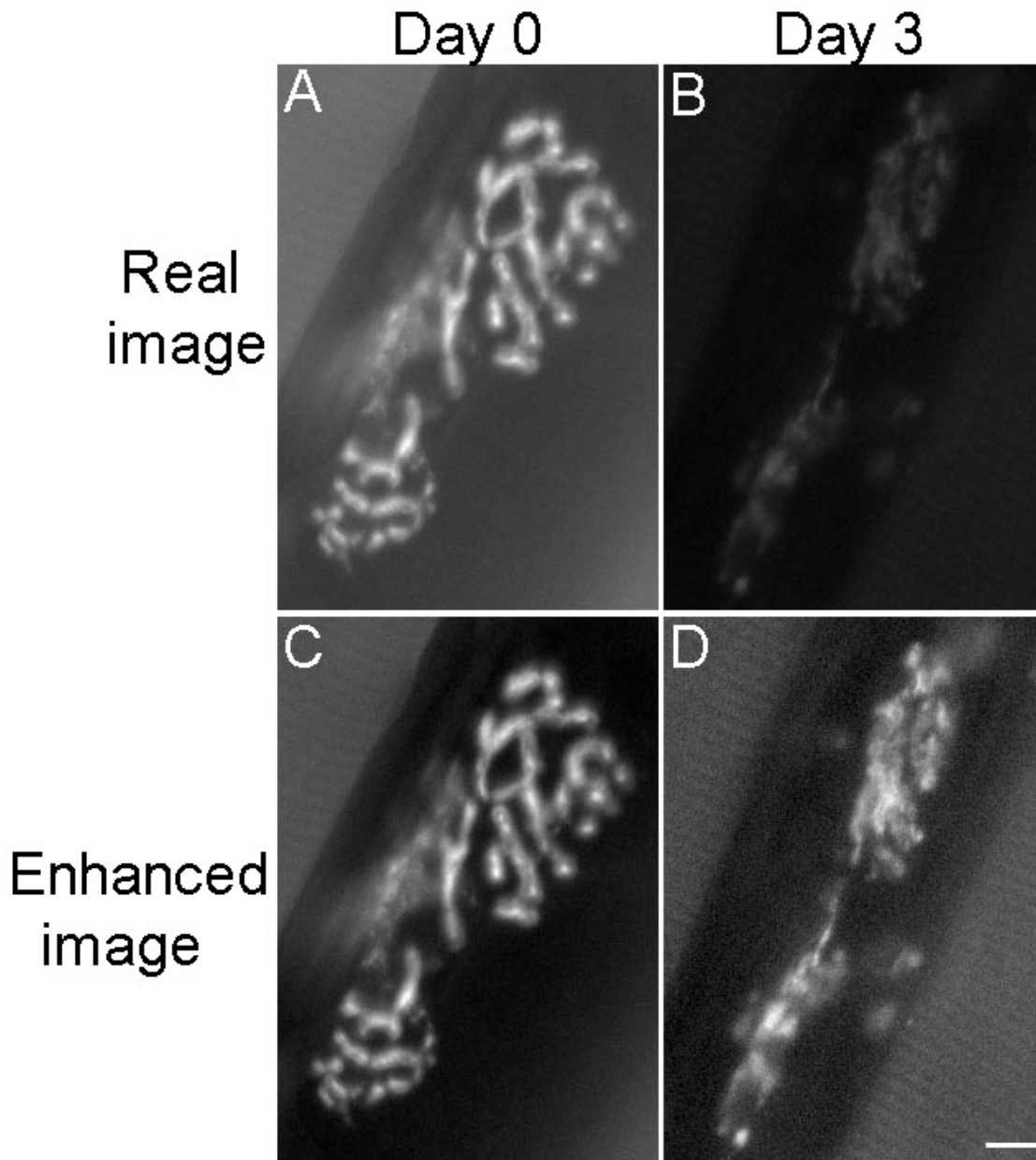


**Figure 2.8 The intensity of rho-BTX labeled AChRs is much fainter 3 days following fiber damage, but its pattern is maintained.**

AChR was labeled with rho-BTX only once before laser ablation. All the images were taken under the same illumination intensity, camera gain, and exposure time both immediately following laser ablation and 3 days later. The original images are shown in (A) day 0 and (B) day 3. Their images enhanced for brightness and contrast are shown in (C) and (D), respectively. The receptor area had shrunk considerably in diameter at day 3. Bar: 10 $\mu$ m

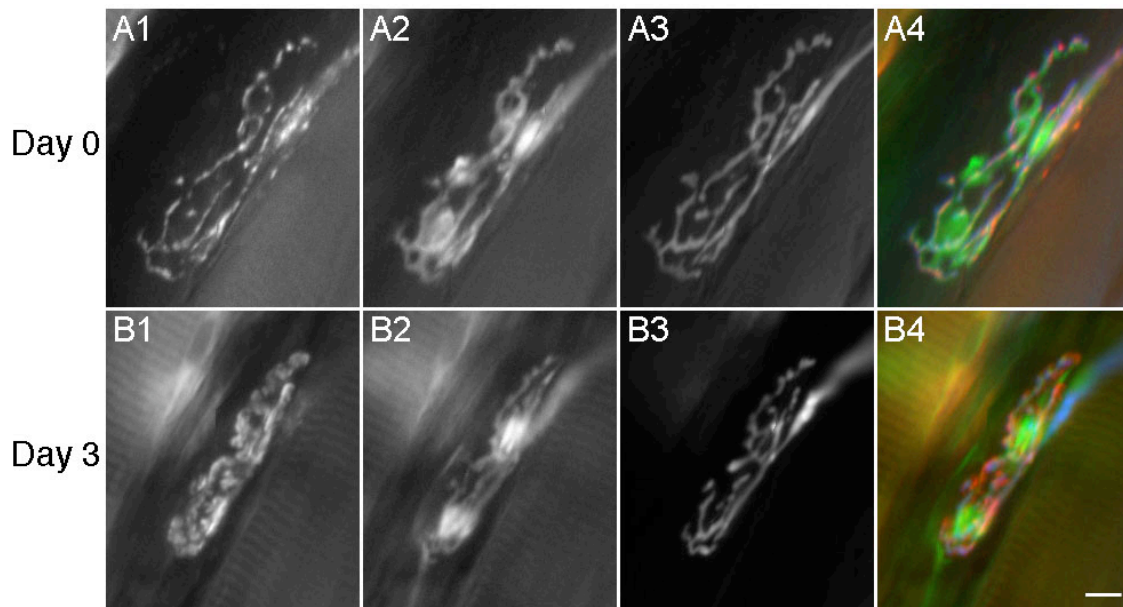


**Figure 2.9 The remaining original AChR can be revealed by rho-BTX staining 3 days after fiber damage.**

Set (A1-A3) and (B1-B3) are images acquired immediately following laser ablation and 3 days later, respectively. A4 and B4 are the merged images from A1-A3 and B1-B3, respectively. No receptors were labeled at the time when the fiber was damaged. 4-Di-2-Asp was used to label muscle fibers and it revealed the nerve terminal (A1). GFP positive TSCs (A2, B2) and CFP positive nerve terminal (NT) (A3, B3) were used to locate the same junction and relocate the same junction 3 days after ablation. Upon relocation, rho-BTX was applied. A shrunken, but full pretzel shaped receptor site was labeled (B1). In merged images, TSCs are green and the nerve terminal is blue. 4-Di-2-Asp or rho-BTX labeling is red. Note the absence of any change in the CFP image and that the bungarotoxin label is localized precisely under the branches of the nerve terminal. Bar: 10 $\mu$ m

A second approach to this same issue was to determine whether the sites on ablated fibers with persistent bungarotoxin label could also be labeled with another reagent identifying AChR. For this purpose, AChR were labeled with Alexa488- $\alpha$ BTX *in vivo* and fibers were laser ablated. The muscle was then dissected 3 days later, fixed, and a primary antibody that recognizes the  $\beta$  subunit of AChR (i.e. a subunit that does not directly bind bungarotoxin) applied. When a second antibody was used to reveal the binding of the primary antibody, the anti- $\beta$ AChR labeling was found to perfectly match the pattern of Alexa488- $\alpha$ BTX labeling (6 fibers, 2 animals) (Figure 2.10). Again, the intensity of both labels on the ablated fibers was much less than on the adjoining, undamaged fibers. Taken together, these 2 observations suggest that both bungarotoxin-binding alpha subunits and beta subunits of the AChR persist in some acellular form at the former synaptic site. However, the majority of the receptors have disappeared. This suggests that extracellular matrix/basal lamina remains attached to a small fraction of the original receptor population and that this matrix persists in association with the remaining nerve terminal following removal of the muscle fibers.

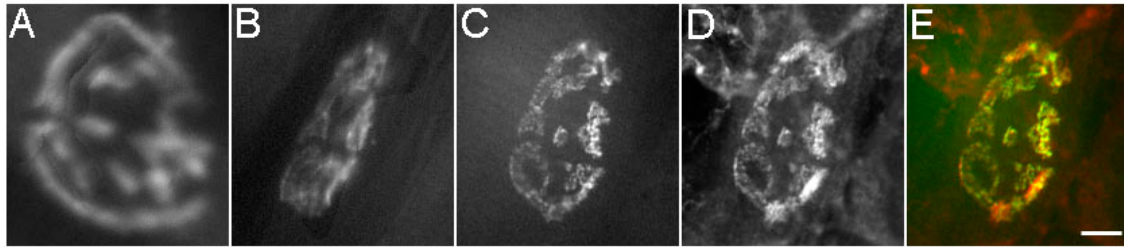


**Figure 2.10 The presence of persistent AChR at synaptic sites on ablated fibers can be verified using an antibody against another receptor subunit ( $\beta$ ).**

(A) and (B) are *in vivo* images; (C) and (D) are *in vitro* images; (E) is the overlay of (C) and (D). (A) AChR was labeled with Alexa488-BTX which binds to the  $\alpha$  subunit and its fiber was damaged. (B) 3 days later, the receptor had shrunk considerably and the intensity of its fluorescence tag was much less. After all the *in vivo* images were done, the muscle was dissected, fixed, and labeled with an antibody against the  $\beta$  subunit of the AChR. An Alexa594 conjugated secondary antibody was then used to distinguish this label from Alexa488-BTX. The remaining original AChR are shown in (C). (D) Under a TxRed filter, used to visualize Alexa594, the AChR label is also present and it matches exactly the original receptor pattern shown in (C). The merged image is shown in (E). Alexa488-BTX appears in green and the Alexa594 secondary in red. Background labeling of Alexa594 secondary was noticeable in (D). Bar: 10 $\mu$ m

The AChRs persisting at the former synaptic sites on the damaged fibers not only survived the whole degeneration process, but they remained for months following the laser damage (Figure 2.11, 2.12). To obtain a quantitative estimate of this persistence, endplates were labeled once with a non-saturating dose of rhodamine- $\alpha$ BTX in vivo before laser ablation. Images were acquired using a cooled CCD camera at the same excitation illumination, the same exposure times, and the same camera gain immediately following the laser ablation and on subsequent viewings for up to 80 days later. The average intensity at each site was compared to that present immediately following fiber ablation. In control muscles that underwent no laser ablation (n=8 fibers), the intensity of the label declined to  $79\pm 2\%$  of the original intensity on day 2 after labeling,  $66\pm 1\%$  on day 6, and  $43\pm 2\%$  on day 30. This decline in intensity can be modeled as the sum of 2 exponentials with half-lives ( $t_{1/2}$ ) of 1.3 days and 38.2 days. Such a turnover of receptors is expected at normal junctions (Loring and Salpeter, 1980) and the rate of receptor decay at a normal junction is also discussed in detail by Akkaboune et al. (1999). On ablated fibers by comparison (n=8), the intensity drop was much steeper, reaching  $41\pm 3\%$  of the original intensity on day 2,  $28\pm 2\%$  on day 6, and  $16\pm 2\%$  on day 30 (Figure 2.13). This decline is best fit as 2 exponentials with half-lives of 0.8 days and 30.6 days. A detectable amount of label was still present even 80 days later on the ablated fibers but was not detected on the non-ablated fibers. Persistence of some fraction of the original receptors at former synaptic sites was also observed if the fibers were damaged by cutting on each side of the endplate band (data not shown). Such persistence has also been observed following fiber degeneration produced by toxins (notexin, Slater and Allen, 1985). Since a new, regenerating fiber begins to form 2-3 days after laser injury and these

fibers produce their own receptors, both new and old AChRs coexist in the synaptic area for some time.

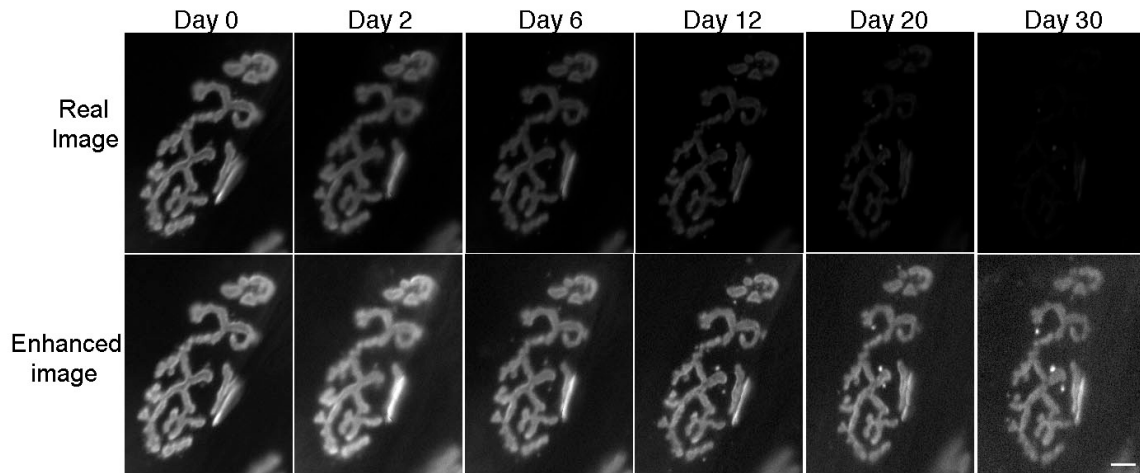


**Figure 2.11 The intensity of AChR labeling gets continuously dimmer on the intact muscle fibers because of receptor turnover.**

The same junction on the intact muscle fiber was imaged 6 times during 1 month (at day 0, 2, 6, 12, 20, and 30). The AChR was labeled with rho-BTX only once at day 0. All the images of the receptor were acquired using the same illumination intensity, camera gain, and exposure time. The images on the top panel in the figure were the real images captured by the camera. Since the intensity of the receptor staining was getting weaker and weaker with time and became impossible to detect by the naked eye, an image enhanced for brightness and contrast was prepared of each original image and is shown on the bottom panel in the same column. Bar: 10 $\mu$ m

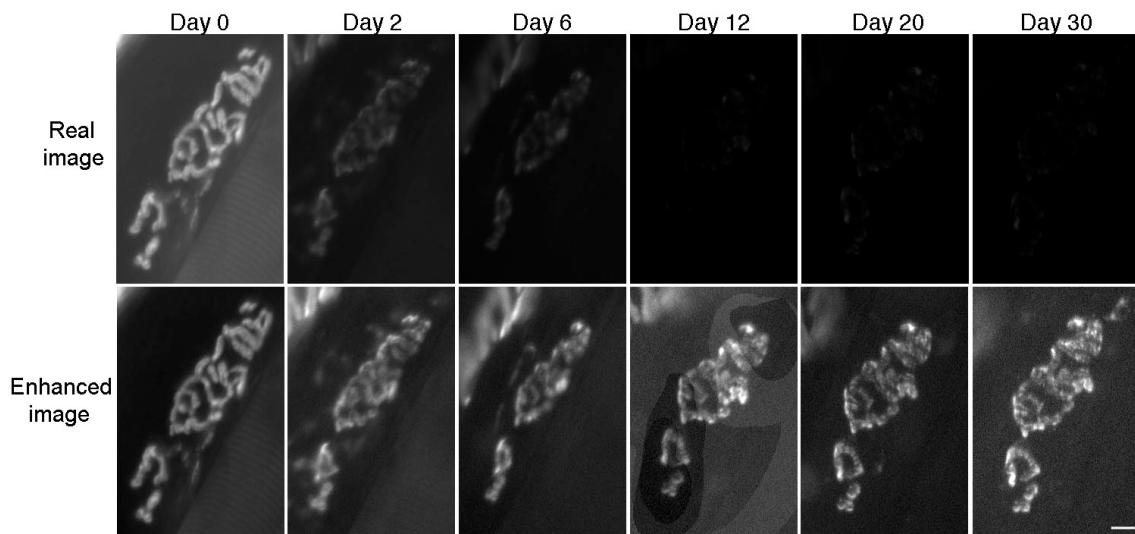


**Figure 2.12 Some of the original AChRs persist at the former synaptic sites for a long time after fiber degeneration.**

The same junction on the damaged muscle fiber was imaged 6 times during 1 month, at day 0, 2, 6, 12, 20, 30, respectively. The AChR was labeled with rho-BTX only once before laser ablation and the first image was acquired after laser ablation. All the images of the receptor were acquired using the same illumination intensity, camera gain, and exposure time. The images on the top panel were the real images captured by the camera and the images from the same day, enhanced for brightness and contrast, are shown on the bottom panel in the same column. Noticeably, the intensity of the receptor labeling had a large drop between day 0 and day 2 when the degeneration of the damaged fiber was underway. Nonetheless, the integrity of the pretzel pattern of the original receptor was preserved. Bar: 10 $\mu$ m



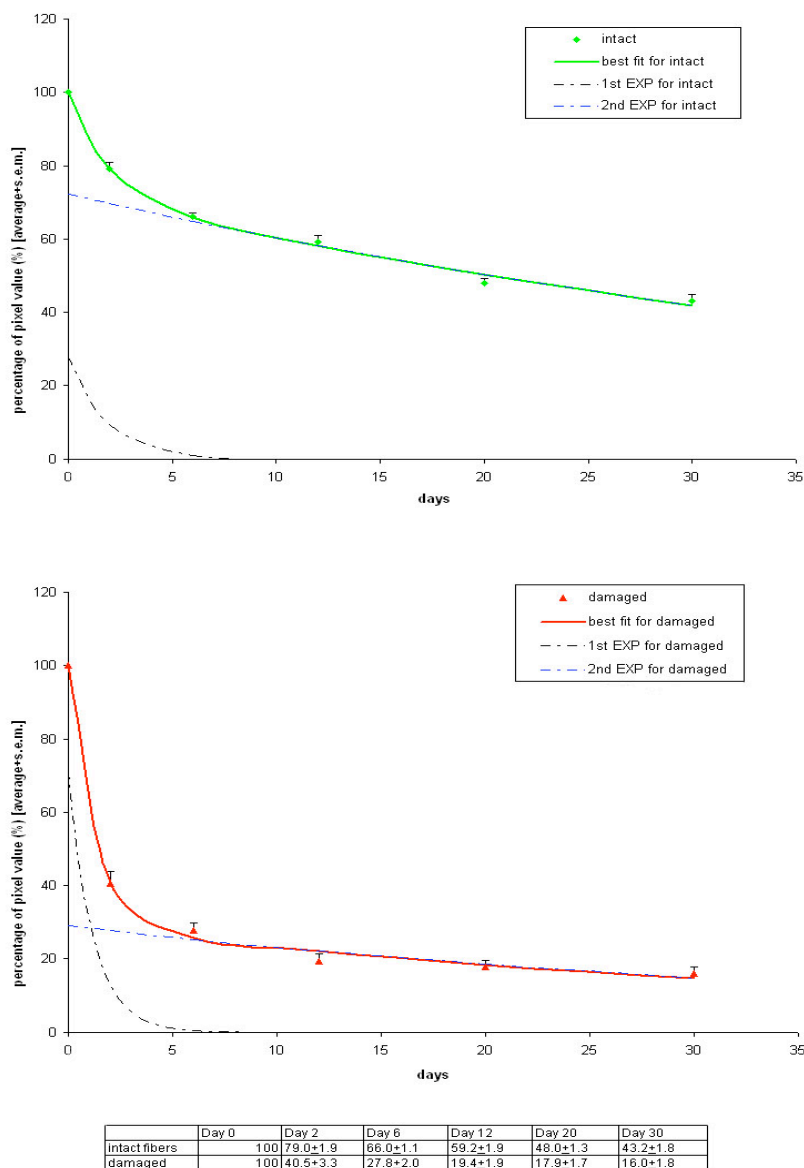


**Figure 2.13 Comparison of the intensity drop of the AChR labeling on the damaged and the intact fibers within one month.**

Quantified data for control group (8 fibers) is represented in green diamonds and damaged group (8 fibers) in red triangles. Their best fit curves are represented in lines in the same color. The AChRs were labeled with rho-BTX only once at day 0 for both groups. The intensity of the receptor staining at day 0 for each group was taken as 100% and used as a standard for that group. It is obvious that the intensity of AChR labeling on the damaged fibers dropped dramatically by day 3 following fiber injury and then it was little changed after day 12. On the contrary, the intensity of AChR labeling on the normal fibers showed a progressive loss due to the receptor turnover. The numbers [average  $\pm$  standard error of the mean (s.e.m.)] for the diagram are listed in the table underneath. Each best fit curve is the sum of 2 exponentials; 1<sup>st</sup> exponential in black dashed line and 2<sup>nd</sup> exponential in blue dashed line.

**Despite degeneration of the muscle fiber, nerve terminals and Schwann cells retain their original configurations at former synaptic sites**

As outlined above, the AChRs persist at the synaptic site following fiber ablation. As previously reported (van Mier and Lichtman, 1994), the former synaptic site shrinks considerably following ablation. During this shrinkage, many sites that could initially be viewed en face, change their orientation to lie completely or partially on the side of the muscle fiber. Therefore, in many cases, it was not possible to view the synaptic components during a second viewing in their entirety after ablation. Despite the reduced intensity in their fluorescence, a pretzel-like pattern of persistent receptors was seen in those junctions retaining an appropriate orientation. These pretzels retained their original shape over the subsequent 3 days without any obvious loss of areas (Figure 2.8).

More startlingly, both the nerve terminal and its companion TSCs persisted as well. Although they also shrank, this shrinkage was proportional to that of the persistent AChR. More importantly, wherever the former synaptic site had not shrunk so its components were distorted, the nerve terminal and its TSCs could be seen to persist without significant loss of their branches. They remained in close apposition to and alignment with the underlying, persistent AChR. All together I analyzed 23 junctions 2 days after fiber ablation; in 6 of these, the fiber had shrunk in such a manner that it was impossible to analyze whether branches persisted or were lost (Figure 2.14). However, in the remaining 17 junctions, it was possible to view all or at least a considerable portion of the branches. In 14 of these 17 junctions, the entirety of the former synaptic site could be visualized. In 10 out of these 14, all the branches of the nerve terminal and the TSC persisted in perfect alignment with the remaining AChR (Figure 2.15). The whole

apparatus was just a smaller version of that present prior to ablation. In the remaining 4 of these 14 junctions, the nerve terminal had lost 1-3 small branches, but these branches occupied on average only  $3 \pm 1\%$  (mean  $\pm$  standard error of the mean) of the receptor area (each branch of the original axon terminal was measured and compared with the image 2 days after). In the remaining 3 of these 17 junctions, only portions of the synaptic site could be visualized on the second view; the other portions were commonly on the side of the fiber. There was perfect alignment of nerve terminal and TSC to the persistent AChR on the visible portions. No terminal sprouts were visible at this time. The number and approximate location of TSC cell bodies remained the same.

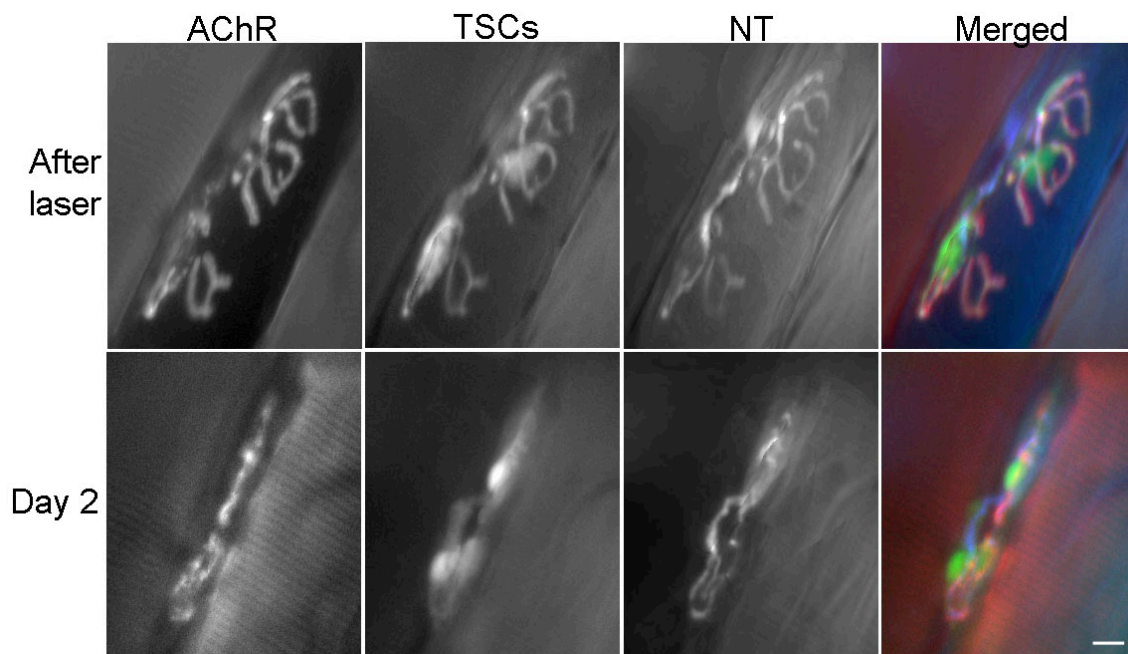


**Figure 2.14 In many cases the original junction collapses dramatically following fiber degeneration.**

AChR was labeled with rho-BTX, TSCs with GFP expression and nerve terminal (NT) with CFP expression. The images were acquired immediately after laser ablation and 2 days later from a living mouse. On day 2, all the components of the previous junction, AChR, TSCs and NT had shrunk so much that it was impossible to make a detailed comparison with the images acquired right after ablation. The physical pressure from the surrounding fibers may account for such results. In merged images, AChR appears as red, TSCs green and NT blue. Bar: 10 $\mu$ m

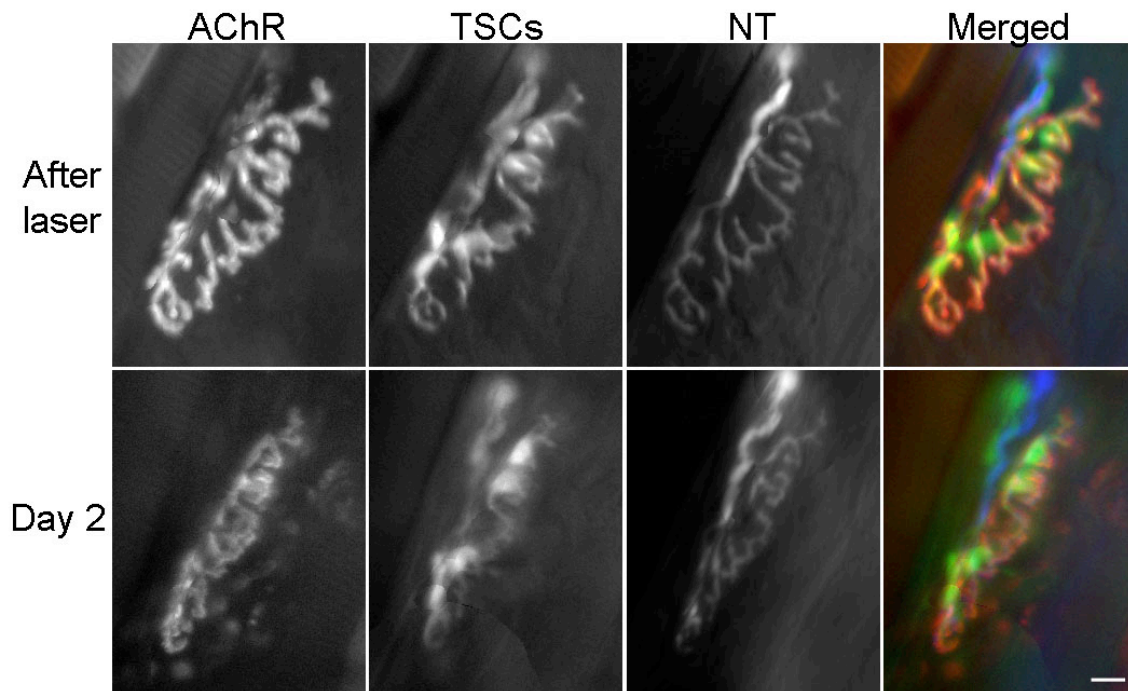


**Figure 2.15 The arborization of both TSCs and the nerve terminal is fully preserved despite the degeneration of its underlying fiber.**

AChR was labeled with rho-BTX, TSCs with GFP expression and nerve terminal (NT) with CFP expression. The images were acquired immediately after laser ablation and 2 days later. In merged images, AChR appears as red, TSCs green and NT blue. In some cases, fiber degeneration did not destroy the visibility of the whole former junction at day 2. All the branches of TSCs and the NT persisted at the junction with no signs of retraction. They also aligned with the remaining AChR perfectly as shown in the merged images. No changes were detected to the former junction except the shrinkage. Bar: 10 $\mu$ m

Another set of sites were re-imaged 3-4 days after damage. The fibers and their former synaptic sites had shrunk still further. Notably, 3 junctions were found among 23 ablated fibers viewed at this time in which all the components of the former synaptic site could still be viewed. In these cases all of the nerve terminal branches and their associated TSCs were intact. For the remaining 10 junctions in this set the shrinkage resulted in only a portion of the former site being visible. For those portions that could be re-viewed, none showed any misalignment of nerve terminal, TSCs, and persistent receptors or any obvious change from the previous pattern. TSCs began to grow early processes from the endplate area around this time (8/15, 53.3%), and nerve terminals also extended short sprouts (4/15, 26.7%) [discussed in detail in Chapter 3] (Figure 2.16). These terminal sprouts suggested that the regeneration of damaged fibers had already begun by this time (Van Mier et al., 1994). The combined data is summarized in Table 2.1.

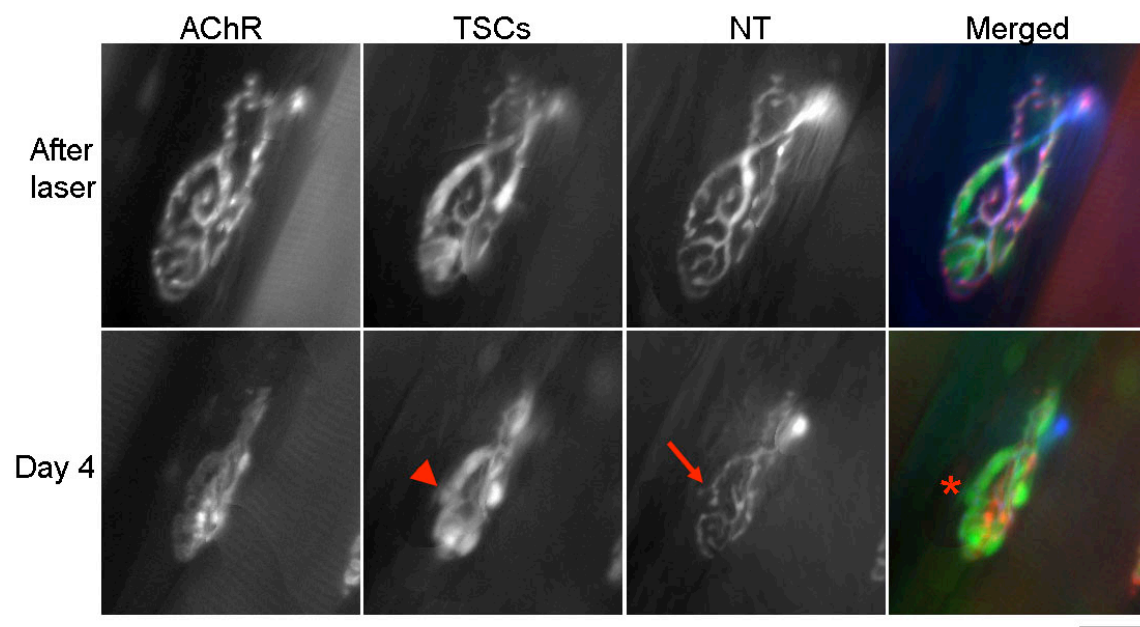


**Figure 2.16 Short TSC processes and terminal sprouts are sometimes detected 4 days after fiber damage.**

AChR was labeled with rho-BTX before laser ablation. The images were acquired immediately after laser ablation and 4 days later, respectively. In merged images, AChR appears as red, TSCs green and nerve terminal (NT) blue. At day 4, all the branches of TSCs and NT were still in alignment with the remaining AChR as shown in the merged images. At the same time, one short TSC process (arrowhead) and one terminal sprout (arrow) which accompanied this process (asterisk) were seen extending out of the original junctional area. Bar: 20 $\mu$ m

Table 2.1 Summary of data: Comparison of the properties of AChR, TSCs and nerve terminal (NT)  
of the former junction 2 or 3-4 days after fiber damage.

	branches of terminal	terminal sprouts	terminal SC number	new SC processes	AChR area change(loss or addition)	alignment of TSCs&NT	alignment of NT&AChR
2 days after laser	whole junction can be analyzed (14mmis)	10/14(71.4%) no change; 4/14(28.6%) missing 1-3 small twigs due to position change;	12/14(85.7%) no change; 2/14(14.3%) can't decide	10/14(71.4%) no; 3/14(21.4%) had 1 or 2 short ones; 1/14(7.1%) can't decide	10/14(71.4%) no change; 4/14(28.6%) can't decide	10/14(71.4%) aligned well; 4/14(28.6%) can't decide	11/14(78.6%) aligned well; 3/14(21.4%) can't decide
	portion can be analyzed (3mmis)	3/3(100%) visible portion no change;	2/3(66.7%) no change; 1/3(33.3%) can't decide	0/3(0%)	2/3(66.7%) visible portion no change; 1/3(33.3%) can't decide	3/3(100%) totally align;	3/3(100%) totally align;
	no part can be analyzed (6mmis)	6/6(100%) can't decide	5/6(83.3%) no change; 1/6(16.7%) can't decide	4/6(66.7%) no; 2/6(33.3%) can't decide	6/6(100%) can't decide	4/6(66.7%) visible portion align; 2/6(33.3%) can't decide	4/6(66.7%) visible portion align; 2/6(33.3%) can't decide
3-4 days after laser	whole junction can be analyzed (3mmis)	3/3(100%) no change	3/3(100%) no change	1/3(33.3%) had 1 twig; 2/3(66.7%) no	2/3(66.7%) no change; 1/3(33.3%) can't decide	3/3(100%) align	2/3(66.7%) align; 1/3(33.3%) can't decide
	portion can be analyzed (10mmis)	10/10(100%) visible portion no change; invisible portion can't decide	3/10(30.0%) had 1 short twig; 1/10(10.0%) had 1 pre-terminal 6/10(60.0%) no	4/10(40.0%) had 1 or 2 short ones; 3/10(30.0%) no; 3/10(30.0%) can't decide	4/10(40.0%) visible portion no change; 6/10(60.0%) can't decide	9/10(90.0%) align; 1/10(10.0%) can't decide	6/10(60.0%) visible portion align; 1/10(10.0%) portion doesn't align; 3/10(30.0%) can't decide
	no part can be analyzed (10mmis)	10/10(100%) had 1 short; 1/10(10.0%) no;	4/10(40.0%) no change; 6/10(60.0%) can't decide	3/10(30.0%) had 1 short; 2/10(20.0%) no;	1/10(10.0%) no change; 9/10(90.0%) can't decide	1/10(10.0%) align; 8/10(80.0%) can't decide	2/10(20.0%) don't align; 8/10(80.0%) can't decide



In the case of 4 ablated fibers in 2 animals, viewing was discontinued 3 days after ablation, the animal sacrificed and the synaptic sites reconstructed from confocal stacks. Examination of these stacks showed that fluorescently marked axons and TSCs persisted above the persistent AChR at all levels (Figure 2.17). Taken all together, these observations strongly suggest that, other than the changes due to shrinkage, the nerve terminal and its Schwann cells remain morphologically intact over the 3-4 days immediately following ablation of the underlying muscle fiber.

One striking difference between the junctions on the damaged fiber and the intact fiber is in the organization of the junctional components. Normally, when a NMJ is viewed from the side, TSCs (outer layer) cover axon terminal (middle layer) and terminal makes synapses with AChRs on the muscle fiber (inner layer) (Figure 2.18A). This structure is usually destroyed in the junctions on the degenerated fibers. 3 days after fiber ablation, TSC processes can now be seen on both sides of the remaining receptor and its nerve terminal (Figure 2.18B). In fact, such organization is also seen in the reformed NMJs after the fiber regenerates (data not shown). It will be interesting to find out in the future by electron microscopy whether this is due to the growth of TSCs into the junctional folds or the convolution of the junction after the collapse of the underlying fiber, since the resolution of confocal microscopy is not high enough to address this issue.

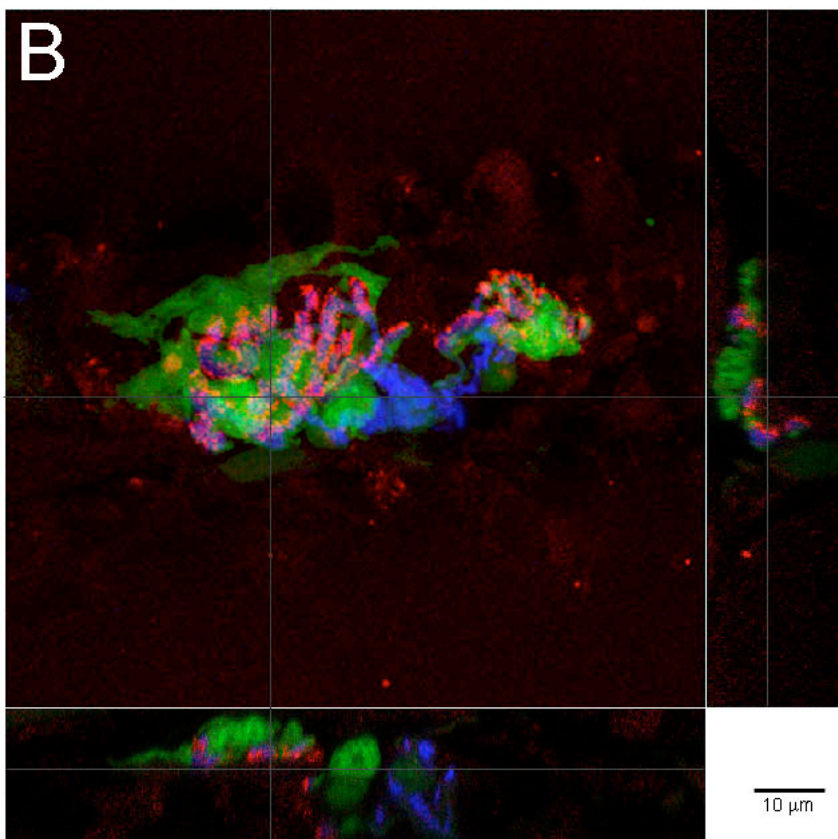
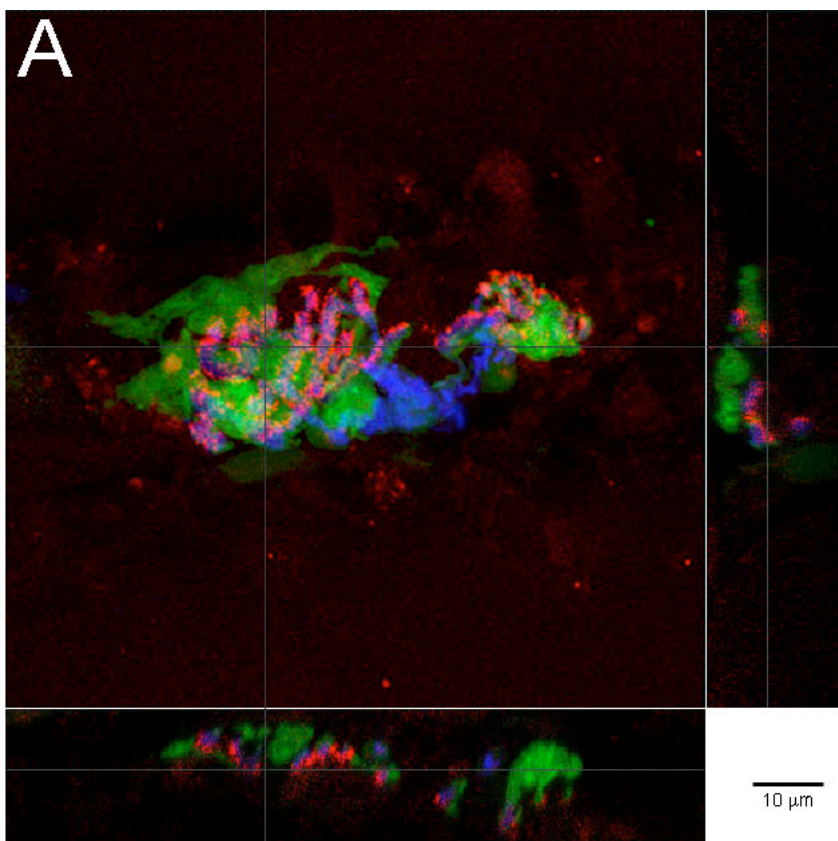


**Figure 2.17 TSC processes and nerve terminal (NT) are seen apposing the AChR at all levels 3 days after fiber damage by confocal microscopy.**

The AChR was labeled with rho-BTX before laser ablation. 3 days later the whole sternomastoid muscle was taken out, fixed and made into a slide. The former junction was relocated and scanned by a confocal microscope. In both A and B, AChR appears as red, TSCs in green and NT in blue. Example Z sections at two different positions on this junction from the confocal stacks are shown in A and B, respectively. In either A or B, the superimposed image of the maximum projections of all 3 junctional components is placed at the upper left; X-Z section is on the bottom and Y-Z section on the right. The lines represent the place where the sections were cut. Both Z sections in A or B show that red receptor sites were always present together with green TSC process and blue nerve terminal. Bar: 10 $\mu$ m

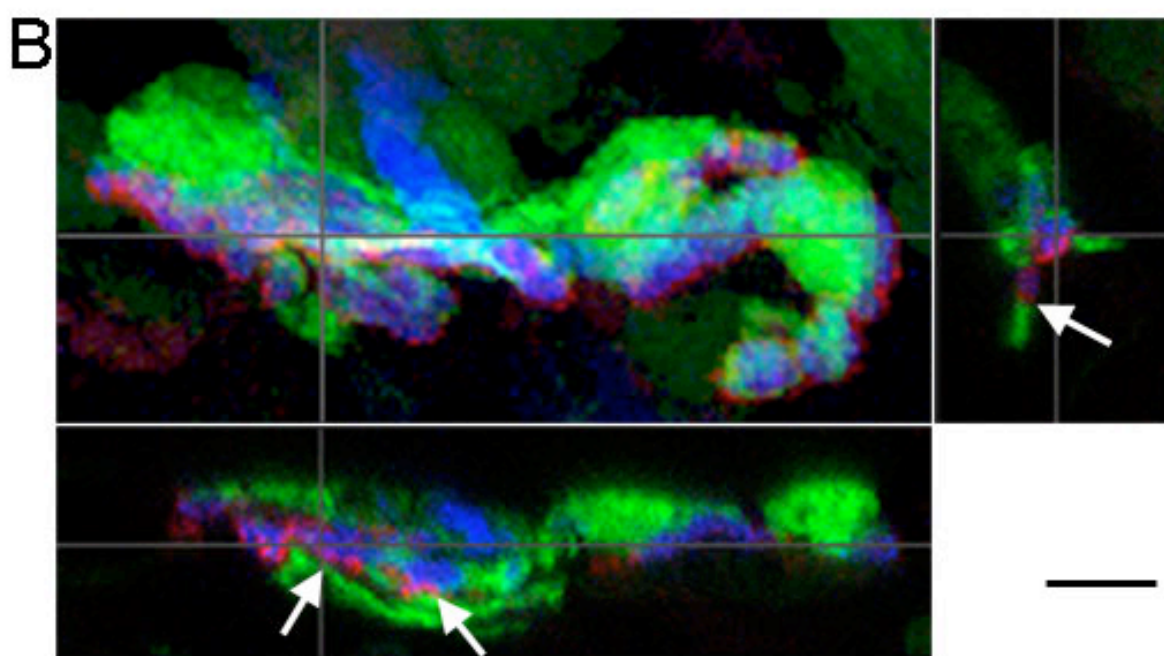
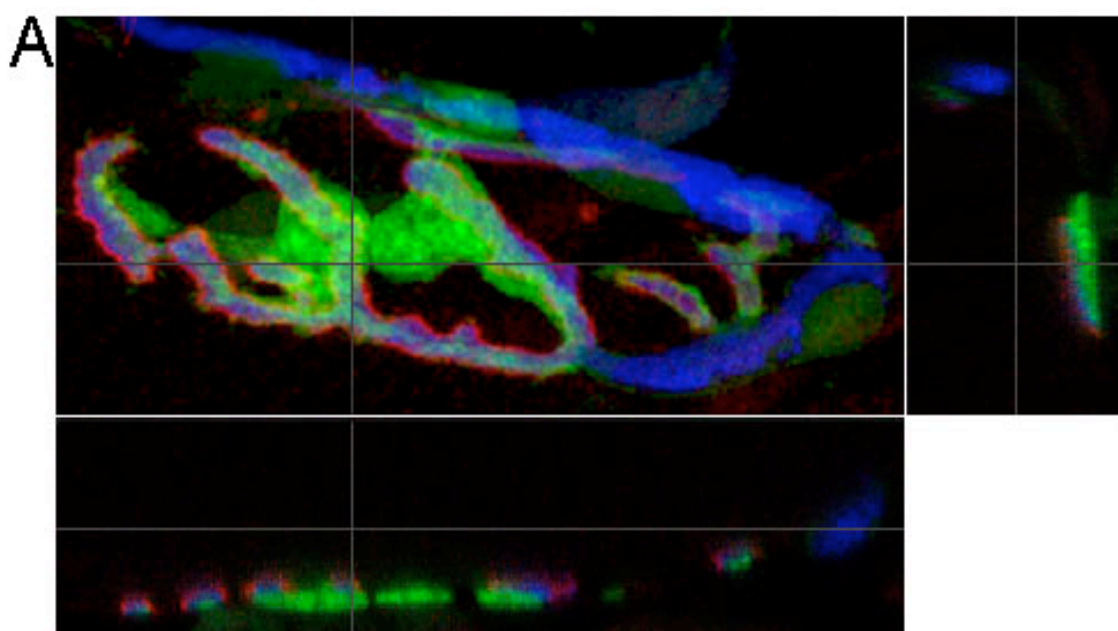


**Figure 2.18 The order of the apposition of the junctional components is changed on the damaged fiber in Z axis after fiber degeneration.**

A. A normal junction on an intact fiber. B. A junction on a damaged fiber 3 days after laser ablation. Both junctions were imaged with a confocal microscope. In both A and B, AChR appears as red, TSCs in green and nerve terminal (NT) in blue. The arrangement of the images in both of them is as follows: the merged image of the maximum projections of AChR, TSCs and NT is placed at the upper left; X-Z section is at the bottom and Y-Z section at the right. The lines represent the place where the sections were cut. In Z sections of a normal junction shown in A, TSC processes (green on the bottom) always cover the NT (blue in the middle) which then apposes postsynaptic receptor sites (red on the top). This order is always observed. However, a difference is noted in the corresponding Z sections from the junctions on the damaged fibers. In B, fiber degeneration disrupted the normal order. Red receptor sites were seen in between green SC process and blue NT (arrows) in this case. Bar: 10 $\mu$ m in A and 7.6 $\mu$ m in B

## DISCUSSION

The primary functions of skeletal muscle are posture maintenance, movement, and breathing. However, skeletal muscle is susceptible to injury. It can be caused by direct trauma (e.g., intensive physical activities, lacerations) (Fry et al., 1991; Helveston and Grossman, 1976) or indirectly such as neurological dysfunction or innate genetic defects (Martin et al., 2000; Morgan, 2005). Since muscle activities are controlled by nerves, it is important to understand how nerves react to muscle injury at the NMJ.

For decades, people have believed that once the muscle fiber is gone, the nerve terminal also rapidly disappears from the synapse. Nerves are reported to not regrow to form the new synapse until muscle fiber regenerates (Rich and Lichtman, 1989b). At the same time, AChRs that are located on the plasma membrane of the fiber disappear as well with fiber degeneration. However, my results strongly support different conclusions. Receptors do not totally disappear from the junction following fiber degeneration. Instead, there are always some receptors that remain and they also maintain their original pretzel shape. In other words, the density of the whole receptor area just becomes less without losing any of its parts. Furthermore, there are no signs of axon terminal loss following fiber degeneration. Both TSC processes and nerve terminal branches just shrink with the receptor plaques, without losing any of their arborization. These observations were obtained by *in vivo* imaging and confocal microscopy at the time of the terminal experiment. It seems that the presence of a healthy fiber is not crucial for maintaining the complete arborization of the nerve terminal at the synapse, at least for a short period of 3-4 days.

## **The maintenance of some AChR sites at the original NMJ following muscle degeneration**

That receptors do not completely disappear from the NMJ following muscle fiber degeneration has been reported before. In frogs, 10% of the original AChRs remained 4 days after damaging and denervating the muscle (Burden et al., 1979). In rat soleus muscle, some original AChRs also persisted for some days at the junction after new muscle fibers regenerated from notexin-induced muscle damage (Slater and Allen, 1985). In addition to laser ablation, I also copied the method that Rich et al used to damage the fibers, that is, to damage the fibers on both sides of the endplate band with forceps. In this case, the damage to the muscle would be more extensive compared to single fiber ablation. However, I still detected faint, yet well conserved whole receptor pretzel, 3 days after muscle damage for all the junctions I had examined (data not shown). Therefore, despite the conventional belief, muscle degeneration does not mean total loss of AChRs from the synaptic sites. This persistence has nothing to do with how the muscle is damaged. Rather some receptors can stay in an acellular state for a long time.

How come the receptors behave like this? What do they cling to? When the muscle fiber degenerates, its basal lamina sheath is left behind. Basal lamina is a layer comprised of proteins, including collagen, agrin, laminin, fibronectin, entactin, and perlecan (Sanes, 1982; Patton, 2003). It also contains AChE and neuregulin (Anglister, 1991; Loeb, 2003). Whereas some of these components are present all along the muscle fiber, others are only localized at the junctional area. Those junction specific proteins are believed to be crucial in maintaining the function of NMJs, providing a means of cell adhesion and signaling among NMJ components. We have known that AChRs do not

cluster at the junction without the presence of a mature basal lamina, and my results suggest that receptors can survive without the underlying membrane. All of these imply that there is some kind of adhesion between basal lamina and AChRs at the junction, either directly or indirectly. It was shown that laminin  $\beta 2$  inside basal lamina binds directly to voltage-gated calcium channels on the pre-terminal membrane and this interaction is required for neurotransmitter release from the synaptic terminal (Nishimune et al., 2004). Therefore, I suspect that there are also molecule(s) in the basal lamina that tightly binds AChRs directly or binds another molecule that is connected with AChRs. In doing this, the basal lamina acts as a scaffold to hold the presynaptic terminal and the postsynaptic receptors together to facilitate the neurotransmission.

### **The maintenance of TSCs and nerve terminals following muscle fiber degeneration**

The observation that TSCs and nerve terminals are both maintained at the junction even as the muscle fiber degenerates is surprising. It has long been believed that terminal branches withdraw from the endplate following fiber degeneration (Rich and Lichtman, 1989b). The previous workers suggested that either the sustenance of nerve terminal at the junction requires some factors be released from living fibers or that degenerating muscle fibers release some destabilizing factors causing nerve retraction. In other words, it was proposed that the basal lamina is not sufficient to maintain nerve terminal completely at the junction.

However, my experiments show this is not true. Following muscle fiber degeneration, both TSCs and nerve terminals just shrink in all directions with the collapse of the fiber, but neither of them shows retraction of their branches. Their processes still



match the remaining of the AChR pretzel, which is preserved as well. Why are my results totally different from the previous ones? What truly happens at the junction following muscle fiber degeneration? By comparing the different ways of addressing this question (*in vivo*, *in vitro* and confocal scanning), I am confident that my results reflect the true phenomenon, that basal lamina is sufficient to maintain the structure of the NMJ in the absence of the postsynaptic cell. There are three main reasons that could account for the discrepancy between previous results and mine. First, they used 4-Di-2-Asp to label the nerve terminals. 4-Di-2-Asp is a vital mitochondrial dye. When the fiber collapsed during degeneration, the nerve terminal shrank with it. The dotted-line of 4-Di-2-Asp staining was now so folded that it may have been really hard to identify each terminal branch. In addition, cutting the muscle fibers in a big area raises the background labeling. This, in turn, blurs the 4-Di-2-Asp images. Loss of functional synapses due to fiber degeneration might also cause reshuffling of mitochondria in the nerve terminals. Therefore, the loss of mitochondrial staining might not precisely represent the loss of the nerve terminal. I mimicked their experiments using the same method and I compared the 4-Di-2-Asp staining with the CFP labeling in the axon. I saw that 4-Di-2-Asp staining was indeed lost from some of the terminal branches while CFP was still present (Figure 2.19). CFP is a small fluorescent molecule that is expressed only in the axon. It should be able to diffuse to all the tips of the axon and it is far easier to visualize than 4-Di-2-Asp. In my experiments, I always used CFP transgenic mice. Therefore, except for the difficulties in relocating the synaptic structures due to fiber collapse, CFP should reflect the position of the nerve terminal more precisely than 4-Di-2-Asp. Second, in order to verify the physical absence of the nerve terminals at the junction, they stained the muscle with anti-

cholinesterase. It was suggested that cholinesterase staining was present in parallel tracks where the nerve was present and continuous staining where the nerve was absent (Rich and Lichtman, 1989a). However, this argument holds when the muscle fibers are intact. When the underlying fiber is gone, staining reagents now also have access to the whole basal lamina, not just from above but also from below. Therefore, the presence of continuous cholinesterase in the synaptic gutter might not necessarily reflect the absence of nerve terminals in this case. Third, the muscle has already begun regeneration 3 days after damage. As a result, all the changes that occur should not be attributed to degeneration per se. Actually, I occasionally observed that nerve terminals do not totally match the remaining receptors around this time. All these findings suggest that it is fiber regeneration that causes the nerve terminal to change, not degeneration.

In fact, the maintenance of nerve terminals at the previous junction after fiber degeneration is not only suggested in the frog (Dunaevsky and Connor, 1998), it is also shown before in rat when its anterior tibial muscle was damaged by bupivacaine injection (Sadeh et al., 1985). Since acetylcholinesterase staining was used as a standard to identify the pattern of the former junctions after fiber damage, these researchers compared acetylcholinesterase staining and silver impregnation of the nerve at the junction at different time point after bupivacaine injection. They showed that axon arborization was well preserved above the necrotic fibers. Therefore, I believe my interpretation of my results is justified.

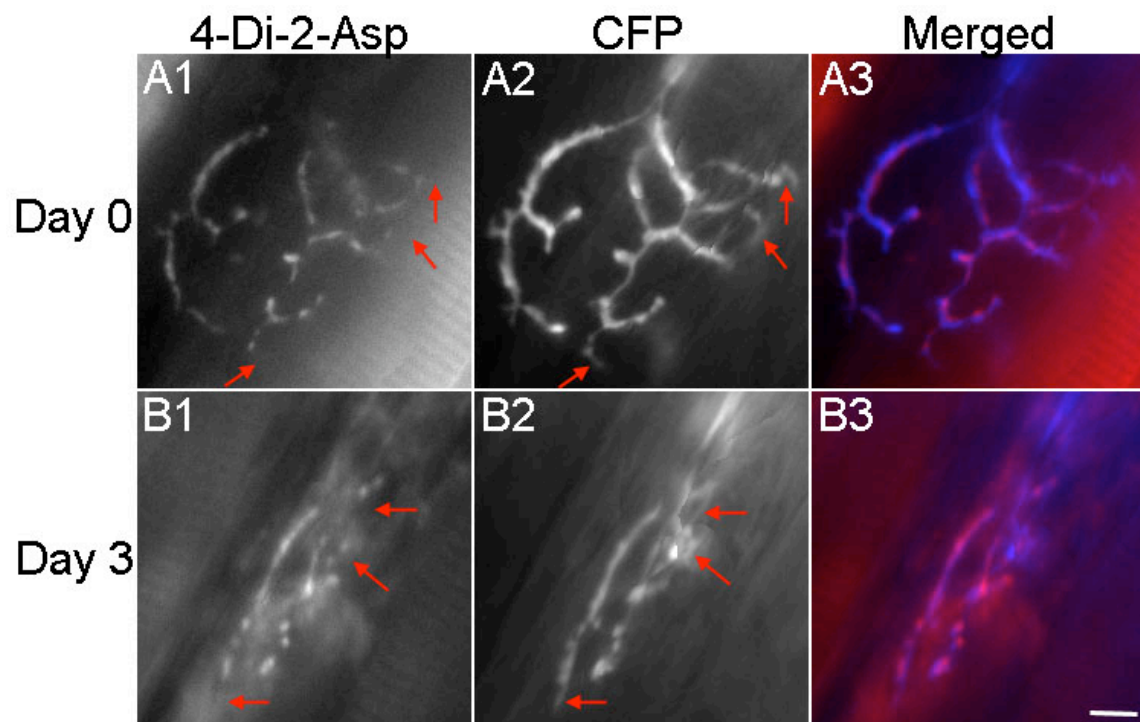


**Figure 2.19 4-Di-2-Asp staining does not reflect the position of the nerve terminals as faithfully as CFP transgene expression.**

Nerve terminals were labeled with 4-Di-2-Asp before laser ablation and 3 days after. The images were acquired immediately after laser ablation and 3 days later, respectively. In merged images, 4-Di-2-Asp staining appears as red and CFP expression in axon blue. Note that 4-Di-2-Asp labeling was absent at some places while CFP was indeed present. This was true not only in day 0 images (arrows in A1, A2), but also in images 3 days after fiber damage (arrows in B1, B2). Bar: 10 $\mu$ m

## **CHAPTER 3**

### **TERMINAL SCHWANN CELL PROCESSES ARE INDUCED BY REGENERATING MUSCLE FIBERS DURING THE FORMATION OF NEW NMJs**

#### **ABSTRACT**

Regeneration of the muscle fiber and the reestablishment of new synaptic connections happen quickly after muscle damage. It has been shown in both adult amphibians and mammals that new receptor sites accumulate at the original synaptic sites in the absence of the nerve (Burden et al., 1979; McMahan and Slater, 1984; Slater and Allen, 1985; Brenner et al., 1992). Furthermore, a regenerating axon can grow back to the original synaptic sites even when fiber regeneration is prohibited (Sanes et al., 1978). The above findings suggest that either the expression of new AChR sites or the differentiation of the nerve terminals on the regenerated fibers is determined by the components in the synaptic portion of the remaining basal lamina.

However, what has not been addressed in the previous studies is the case of what happens to the nerve if it is undamaged and the fiber it previously innervated begins to regenerate, as is the case in my experiments (Chapter 2). Will the nerve terminal play a role in accumulating new AChRs, or is the regenerating synaptic site directed only by the remaining basal lamina? By studying the reformation of the NMJs on regenerated fibers, I found that a majority of the new receptors do not overlap with the original receptors. In about 90% of the cases, new synaptic sites are added to the original sites but they do not completely cover the area occupied by synaptic sites before damage occurred. They are also situated at shifted locations from the original sites and nerve terminals are seen in adjacent to them at all places. This implies that nerve terminals play a role in determining the AChR distribution on the regenerating muscle fibers. Another important observation is that TSCs were seen growing processes along the regenerating fiber. Terminal sprouts follow these processes and induce new receptor accumulation. TSC processes were also present on the surrounding intact muscle fibers around the same period, although terminal sprouts were not seen growing on them. My results suggest that nerve terminals are able to induce AChR expression and their growth is guided by TSC processes, whose own growth is induced by signals secreted by the regenerating muscle fibers.

## **METHODS**

Several different procedures were used to try to saturate the original AChRs before laser ablation. 1) 2 $\mu$ g/ml Rho-BTX was applied for 10min followed by 25 $\mu$ g/ml unlabeled-BTX for 1 hour. After laser ablation (done in Ringer's if not specified), 5 $\mu$ g/ml Alexa647-conjugated bungarotoxin (Alexa647-BTX, Molecular Probes) was applied for

10min to determine whether there was any staining then and 2 days later. 2) 2µg/ml Rho-BTX was applied for 10min which was followed by 25µg/ml unlabeled-BTX for 2 hours. Laser ablation was done in the 25µg/ml unlabeled-BTX solution afterwards. Then 5µg/ml Alexa647-BTX was applied for 10min to determine whether saturation had been accomplished. 3) 2µg/ml Rho-BTX was applied for 10min and laser ablation was performed. After that, 25µg/ml unlabeled-BTX was applied to the muscle for 2 hours. Then 5µg/ml Alexa647-BTX was applied to check the status of saturation.

*In vivo* imaging in Chapter 3 was done as described in Chapter 2, except that Alexa647-BTX (2µg/ml in sterile lactated Ringer's) was applied to the living muscle during fiber regeneration to reveal the newly expressed AChRs.

*In vitro* processing was also similar to that described in Chapter 2. The confocal imaging was also accomplished as described in Chapter 2.

## RESULTS

### **As ablated muscle fibers regenerate, newly synthesized receptors can be detected by applying a second color of fluorophore-tagged BTX**

As shown in the previous chapter (Chapter 2), a fraction of the rho-BTX applied to label AChR prior to muscle fiber ablation persisted at the former synaptic site following fiber degeneration. Muscle fibers regenerate following this type of ablation (van Mier and Lichtman, 1994), and the expectation was, as reported before (Slater and Allen, 1985), that new AChR would appear at the previous synaptic sites as synapses became re-established on the regenerating fibers. To examine this issue, I made an

attempt to compare the AChR present at the time of ablation and those that appeared during regeneration. To distinguish the new AChR from those persisting from the time of ablation, I needed to apply a bungarotoxin conjugated to a second fluorophore. However, since this second color bungarotoxin would also be expected to label a portion of the AChR present initially that were not saturated with the original toxin, I first attempted to saturate the labeling of the original AChR prior to ablation.

Receptor saturation was previously shown to be achievable at the mouse NMJ with application of a single saturating dose of 5 $\mu$ g/ml of any fluorophore-tagged bungarotoxin for 1 hour (Akaaboune et al., 2002). Therefore, I first used this procedure in my experiments before ablating a muscle fiber. If, immediately following the ablation, I applied a second color of bungarotoxin (2 $\mu$ g/ml Alexa647-BTX for 5min), I could detect no receptor labeling. However, when I re-imaged the junctional area on the damaged fiber or the junctions on the adjoining, undamaged fibers 2 days later, I was surprised to find labeling for the second color even though no additional bungarotoxin was applied. The labeling was present both at the junctional site on the ablated fiber and also at the junctions on the intact fibers. The label in each case took the pattern of the receptors labeled with rho-BTX applied initially. This result was paradoxical. While I would expect that some receptor turnover occurs on the intact fibers and these could be labeled by some of unbound Alexas-647 bungarotoxin that persisted in the area and was not washed away, such a result would not be expected in the case of the ablated fiber as no new receptors should be added to this junction during the 2 day period. The simplest explanation for these observations is that the first bungarotoxin application failed to saturate all the receptors and a small amount of the Alexa 647 bungarotoxin bound to

these unsaturated receptors. That this Alexa 647 labeling was not detectable immediately after its application but only 2 days later is probably explained by the low labeling intensity and the high background present immediately after application. So this first attempt at saturating receptors at the time of ablation, that was repeated several times, failed.

As a next attempt at achieving saturation, I raised the concentration of bungarotoxin. However, no matter what concentration of bungarotoxin I used or time of incubation (application of non-labeled BTX 25 $\mu$ g/ml for 1-2 hours following 10min rho-BTX before laser ablation, or performing laser ablation in the presence of non-labeled BTX), I still found it is impossible to totally saturate the original AChRs. Alexa 647-BTX which was applied immediately following ablation could still be seen to label receptors on the damaged and the surrounding, unablated fibers when these fibers were viewed 2 days later (Figure 3.1). Part of the explanation for this labeling is undoubtedly the camera gains and exposure times necessary to see the persistent receptors at the endplate on the ablated fiber. A similar result of inability to completely saturate AChR has been reported previously (Fertuck and Salpeter, 1976).



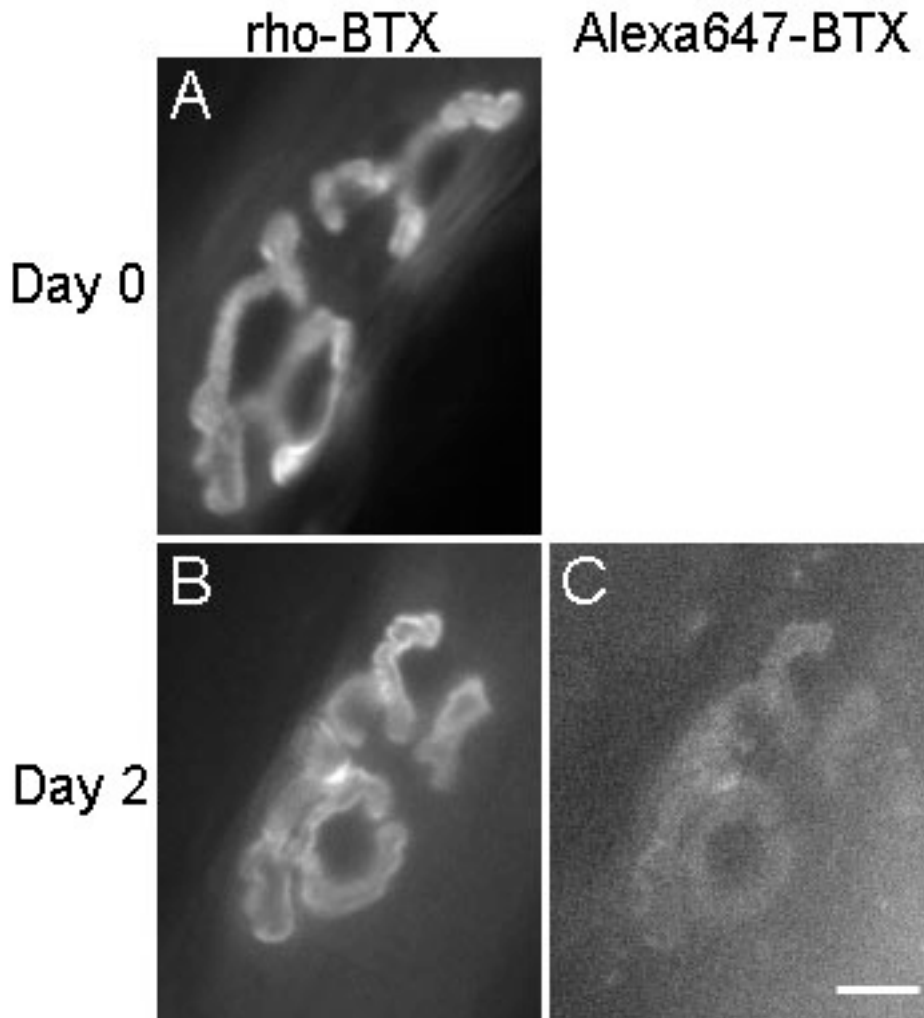


**Figure 3.1 AChR can not be saturated with bungarotoxin using conventional methods.**

The sternomastoid muscle was exposed in the anaesthetized animal and labeled with  $2\mu\text{g/ml}$  rho-BTX for 10min followed by  $25\mu\text{g/ml}$  of unlabeled-BTX for 1 hour. Laser ablation was then performed on 3 fibers after which muscle fibers were labeled with 4-Di-2-Asp. Images were acquired afterwards from both damaged and intact fibers. Then  $5\mu\text{g/ml}$  Alexa647-BTX was applied to the muscle for 10min and imaged at the conclusion of washing after this application. 2 days later, this label was imaged again under the same fluorescence intensity. rho-BTX labeled AChR from an intact fiber are shown in A and B at day 0 and day 2, respectively. Alexa647-BTX labeling was undetectable at day 0 (image not shown), but appeared at day 2 as shown in C. Bar:  $10\mu\text{m}$

Failing in my attempt to completely saturate receptors, I investigated whether it still might be possible to obtain strong evidence about how new receptors are added to the synaptic sites on regenerating fibers. I labeled AChR *in vivo* as I normally would for vital imaging (5min 2 $\mu$ g/ml rho-BTX). I then labeled subsequently after fiber regeneration with the second color of bungarotoxin (5min 2 $\mu$ g/ml Alexa647-BTX). Despite the fact that some AChR present at junctions remain unlabeled by rho-BTX applied before fiber damage but are then subsequently labeled by Alexa647-BTX, I believe that the great majority of the labeling with Alexa647-BTX is of new receptors on the newly generated fibers. First of all, the labeling with Alexa647-BTX becomes progressively stronger with time, suggesting the accumulation of new receptors (details seen below). Within a few days, the labeling with Alexa647-BTX eclipses that of the rho-BTX applied initially. Secondly, as shown below, the receptors labeled with Alexa647-BTX most commonly do not overlap in their position with those labeled with the original rho-BTX, suggesting that receptors are commonly at slightly different locations. This is particularly obvious in confocal micrographs made after sacrificing the animal and examining the muscle in detail *in vitro* (see below). Therefore, I continued the above labeling for all my experiments.

**New AChRs on regenerating muscle fibers are added gradually to the synaptic sites and take the general pattern of the original one**

To examine how the synapse on the regenerating fiber is laid down, I imaged the ablated fiber, not only during and immediately following ablation, but also at 4, 6, and 12 days later. At each view I applied Alexa647-BTX so as to label new receptors. Fiber

regeneration began shortly (2-3 days) after muscle damage (d'Albis et al., 1989; Whalen et al., 1990). A thin myotube was sometimes visible at the injured site on day 4, although sarcomeric striations were not detectable at this time, even if 4-Di-2-Asp was also applied to the muscle (data not shown). At day 4, the intensity of the new AChR was usually very low (6 fibers in 2 animals). These new receptors were commonly uneven in their distribution. They were often present in more intense foci situated close to persistent old receptors, but did not mirror the entire pattern of old receptors (Figure 3.2 panel B2). When the same junction was imaged 2 days later, the new receptors appeared to have filled in the gaps between these initial foci, and the intensity of the label increased and became more uniform (Figure 3.2 panel B3). Overall, the pattern of the new receptors came to resemble that of the collapsed older pattern, with some exceptions noted below. Following an additional 6 days (12 days following ablation), the application of Alexa647-BTX yielded an even more intense, uniform label (Figure 3.2 panel B4). The most obvious change visible at 40X magnification *in vivo* was that the entire receptor area appeared to have expanded, an effect expected as the regenerating fiber grows in diameter with time.

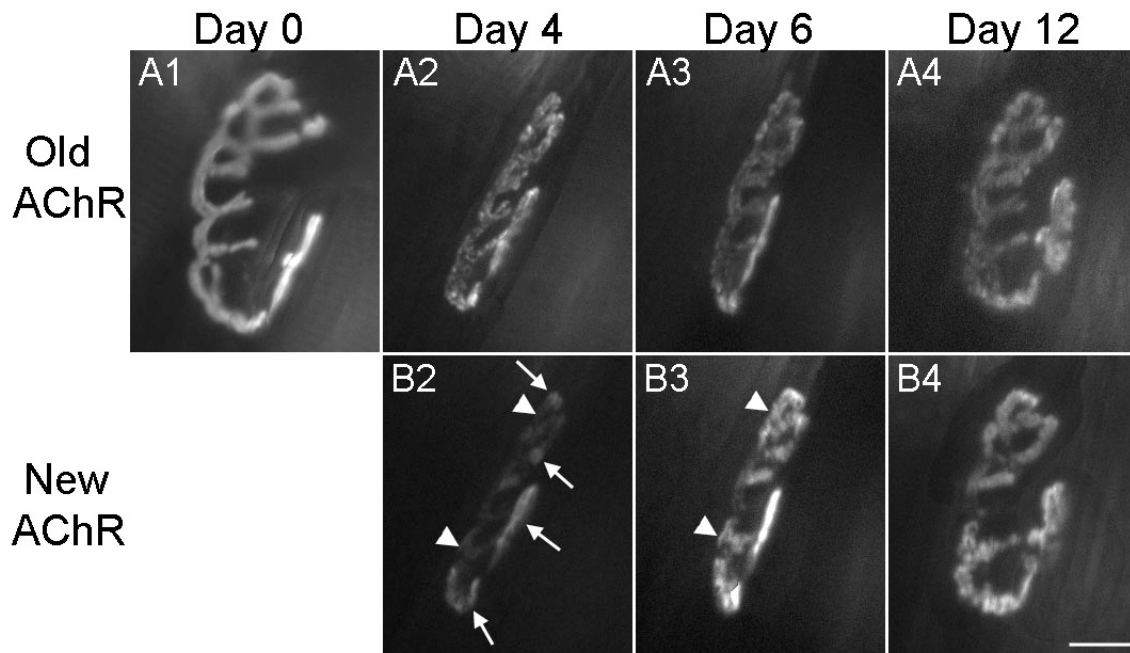


**Figure 3.2 New AChR sites appear gradually at the junction on a regenerating fiber.**

The distribution of new AChRs was examined over the course of 12 days. The original AChR was labeled by rho-BTX once before laser ablation at day 0. Alexa647-BTX was applied on day 4, 6 and 12 to label the new AChR. The images of the original AChR are shown in A1-A4 and those of the new AChR are shown in B2-B4. The original AChR and the new AChR correspond at each time point. New AChR was first detectable at day 4 after fiber damage (B2), but the sites were usually uneven in their distribution with some in more intense foci (arrows). 2 days later, new AChR sites were present in the space between the initial foci (arrowheads in B2 and B3) and the intensity of label became more even throughout the whole area. The intensity of the new AChRs kept on increasing between day 6 and day 12, usually at sites already seen earlier (B4). The growth in their diameter was most obvious between days 6 and 12. Bar: 20 $\mu$ m

**New AChRs commonly do not overlap with the original AChRs viewed en face and they are situated at a different plane in the Z axis**

To investigate the similarities and differences in the pattern of new receptors relative to those present at the time of ablation, I examined the AChR distribution *in vivo*, as described above. However, to obtain a more thorough analysis, I sacrificed the animals, dissected their muscles and captured images from the same junction using high resolution confocal microscopy.

In total, 11 regenerated fibers from 3 animals were analyzed. My observations show that new receptor sites tend not to match the original sites at many places. When the receptors were viewed en face (i.e. in the X-Y dimension), sites of new AChRs were present where no original AChRs were present (see asterisks in Figure 3.3). This was the case for areas within 10 of the 11 junctions. If I examined the old receptors and asked whether new receptors were present at these same sites, I found the colocalization of such receptors in 10 of the 11 junctions. However, for most junctions this colocalization was only partial as a portion of the sites containing old receptors in 10 of 11 junctions (arrows in Figure 3.3) had no new receptors. Only in 1 case was colocalization of old and new receptors complete (Figure 3.4). The percentage of the area of new junction containing entirely new receptor sites varied from ca. 0-50%. The range of areas of the old sites unoccupied by new receptors varied over the same range. When the receptors were viewed under 100X magnification, new AChR did not have the smooth and regular stripes of staining attributable to folding of the postsynaptic membrane (Marques et al., 2000) as was present in junctions on adjacent, unablated fibers (Figure 3.5).

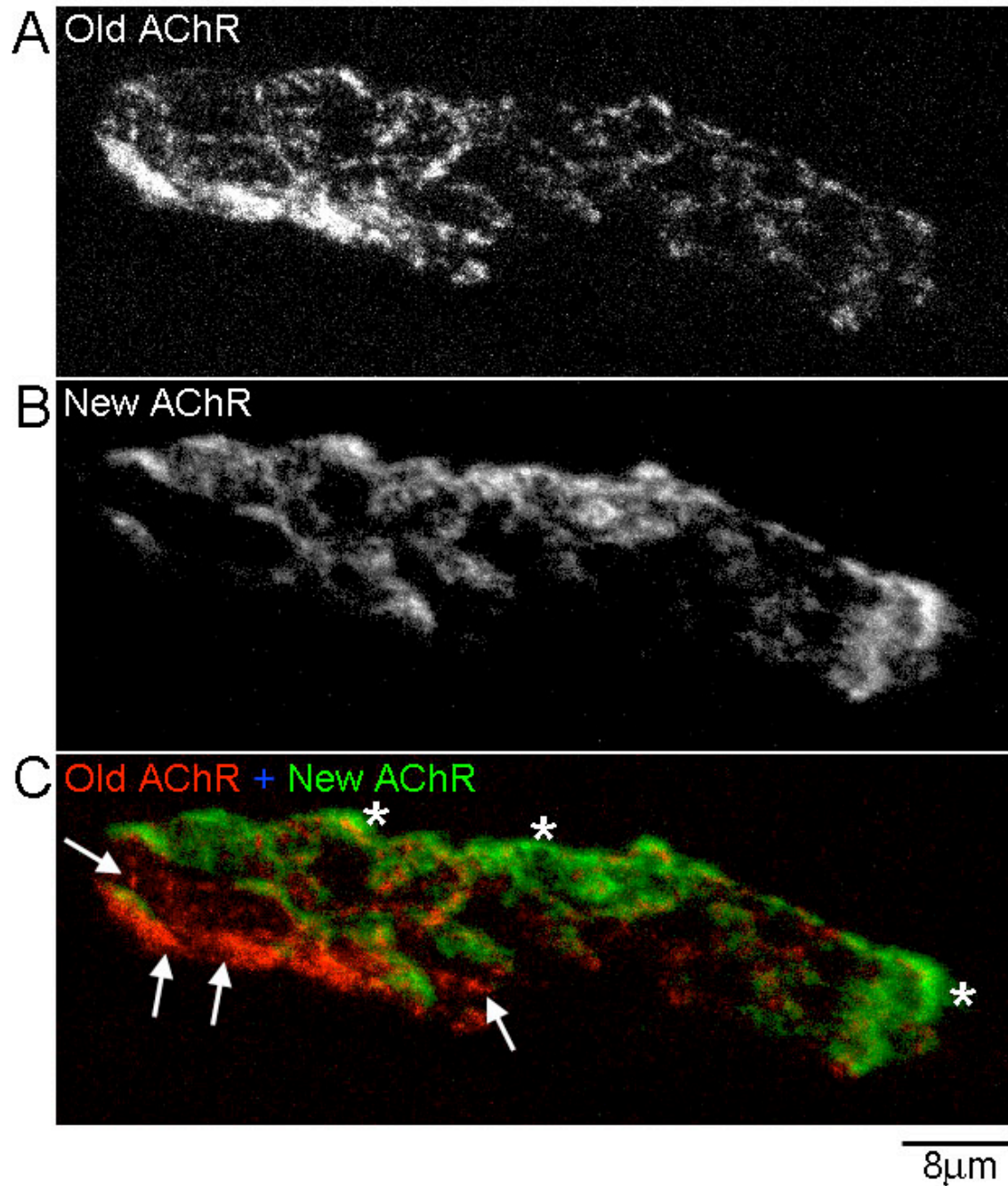


**Figure 3.3 New AChR sites are added to the original AChR area at some places but not at others.**

The original AChR was labeled with rho-BTX and the new AChR was labeled with Alexa647-BTX. Muscle was dissected 6 days after laser ablation, fixed and prepared for confocal imaging. Maximum projections of the original AChR, new AChR and their overlay are shown in A, B and C, respectively. In C, original AChR appear red and new AChR green. Sites of newly added receptors were found outside the original receptor area (asterisks). At the same time, many original AChR sites were not filled by new AChRs (arrows). Bar: 8μm

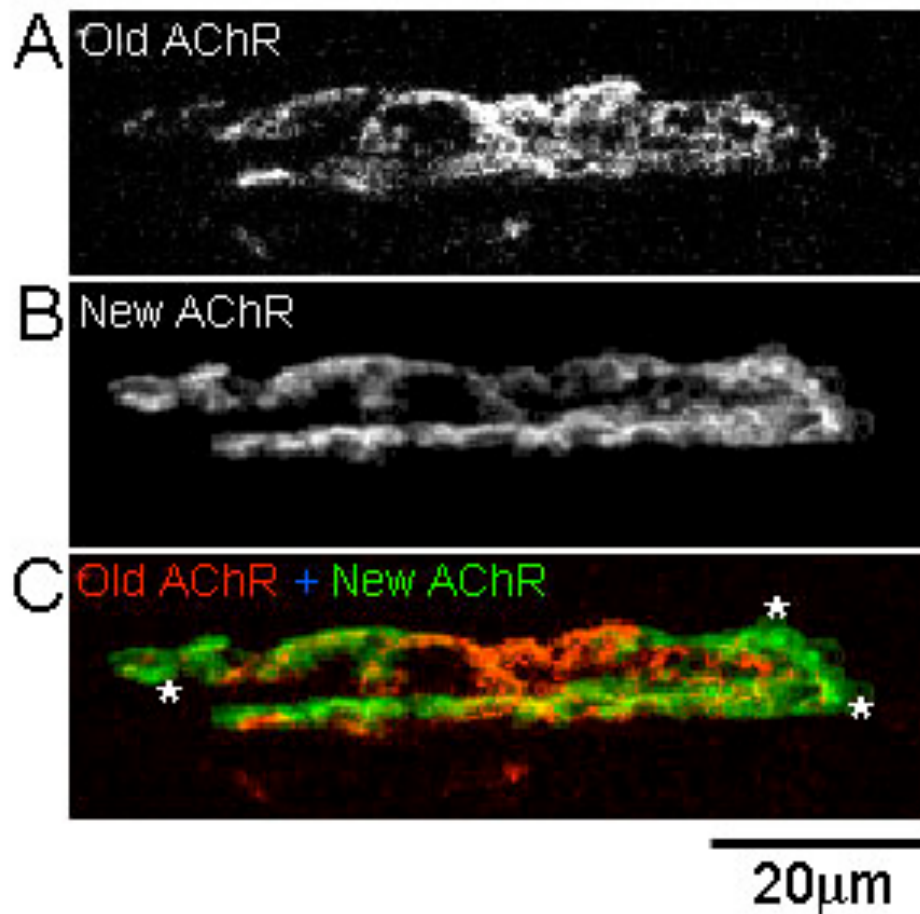


**Figure 3.4 In one case, new AChRs appeared to occupy all of the original AChR sites**

The original AChR was labeled with rho-BTX and the new AChR was labeled with Alexa647-BTX. Muscle was dissected 6 days after laser ablation, fixed and prepared for confocal imaging. Maximum projections of the original AChR, new AChR and their overlay are shown in A, B and C, respectively. In C, original AChR appears red and new AChR green. While the new receptor sites were found outside the original receptor area (asterisks), they also filled all of the original receptor sites. Bar: 20μm

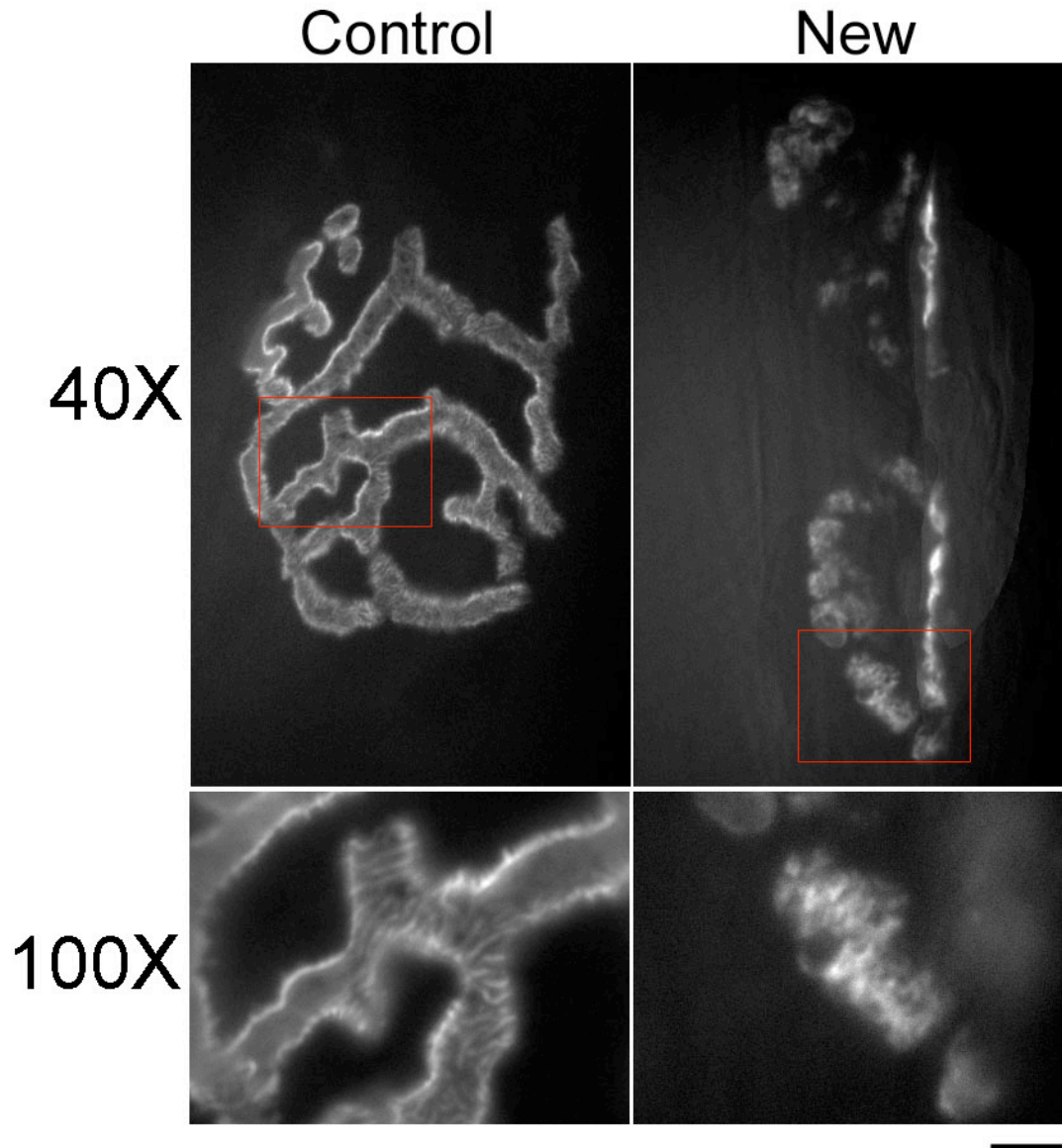


**Figure 3.5 Higher magnification shows that the structure of the junctional folds of the new NMJ is different from those of the intact NMJ.**

Alexa647-BTX was applied to the sternomastoid muscle 6 days after laser ablation to label all the AChRs. Then the muscle was dissected and fixed. AChRs from the intact fiber (upper and bottom left panels) and the regenerating fiber (upper and bottom right panels) were examined under both 40X and 100X oil objectives. The squares in the 40X images represent the area magnified at 100X in the lower panels. AChR labeling on the intact fiber appeared with regular parallel striations in the high magnification image (bottom panel on the left). However, such striations were not seen under the same magnification from the new AChRs on the regenerating fiber (bottom panel on the right). The organization of their layout was very irregular and they didn't have a smooth outline. Bar: 20 $\mu$ m for 40X images and 8.5 $\mu$ m for 100X images



The differences between the new AChR and the original AChR sites are more striking in their Z sections from the confocal stacks. In 5 of the above 11 junctions (45%), the new receptor sites were very close to the remaining old sites at most places when viewed en face, but they were not at the same location when examined from image to image in the Z stack. Instead, the new receptors seemed to be in a plane that was parallel to the plane of the original receptors (Figure 3.6). Moreover, this new plane was invariably located deeper into the fiber than the old one. In two additional cases, the new receptor sites were so close to the old sites that they appeared to overlap each other. In the case of another 2 regenerating fibers, the pattern of receptor distribution was mixed in the same junction, with about half of the junctional area having the receptors in parallel planes and about half overlapping. The most interesting cases are the last 2. One had a totally new AChR pattern and the other one had a similar pattern compared to the original plaque, but both of them had their new receptor sites separated from the original sites with a large gap in the Z axis (as far as ca.  $6.3\mu\text{m}$ ) (Figure 3.7). In contrast, the AChRs on the intact fibers showed a complete overlap between the initial label and the new label (Figure 3.8). To my knowledge, while others have observed the receptor distribution in en face views of the junctions on regenerating fibers, my observations are the first to examine the distribution in detail and in particular in the Z axis.

My observations suggest that, despite the presence of the remaining original AChRs at the junction, newly expressed AChRs on the regenerating muscle fiber are not commonly established at the same exact sites.

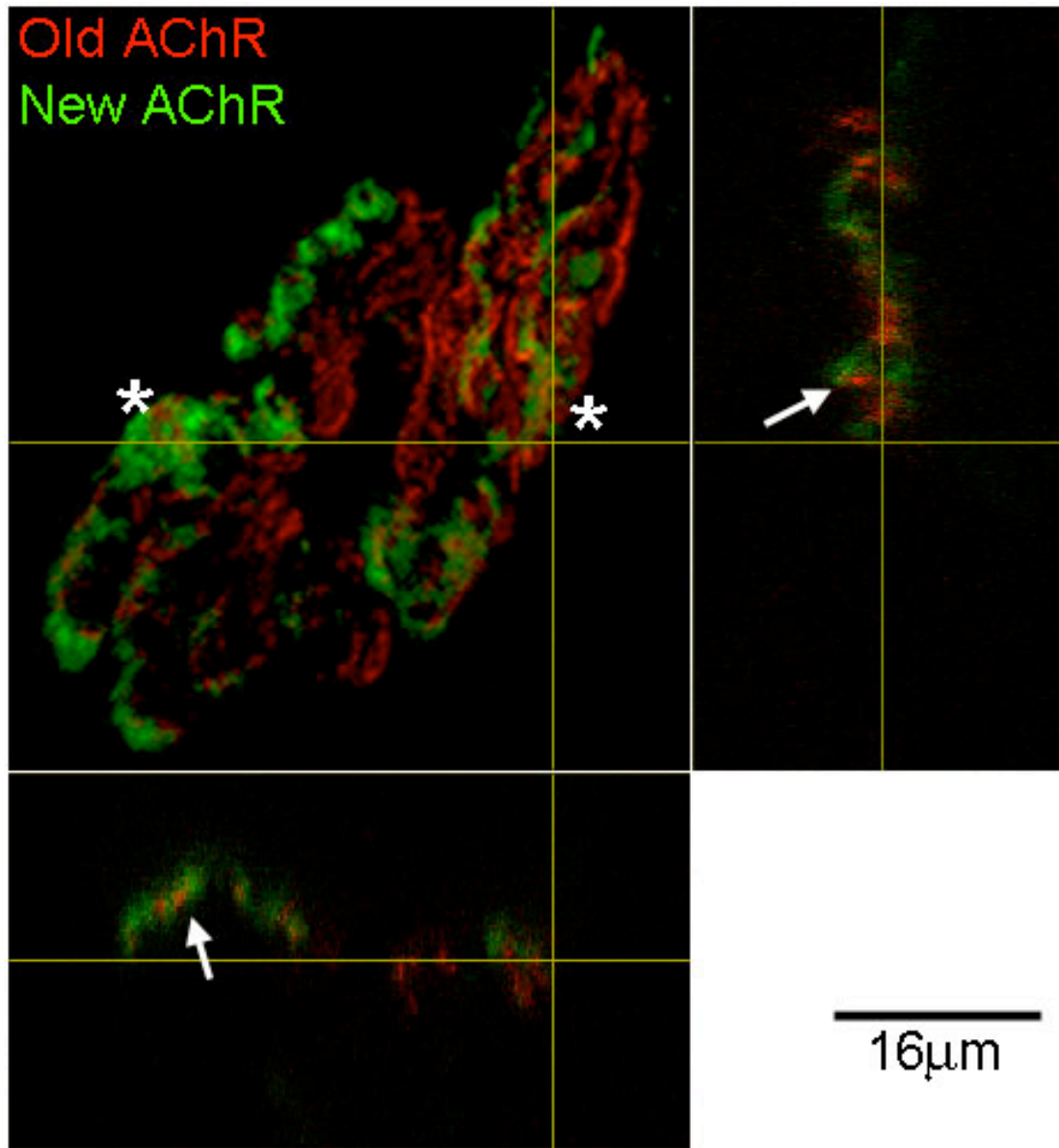


**Figure 3.6 New and old AChR sites are present at the same position in an en face view but are not at the same location when viewed 3 dimensionally.**

The original AChR was labeled with rho-BTX and the new AChR was labeled with Alexa647-BTX. Muscle was dissected 6 days after laser ablation, fixed and prepared for confocal imaging. Sections in the Z axis were analyzed. Here, old AChR appear red and new AChR green in all three panels. The overlay of the maximum projections is shown in the upper left panel. One X-Z section is shown at the bottom and the corresponding Y-Z section is at the right. The lines represent the place where the sections were cut. At places where the new AChR sites seemed to overlap with the original AChR sites in the maximum projection (asterisks), the receptors were actually separated in the Z axis (arrows). Green-pixels of the new receptor sites seemed to be interrupted by red-pixels of original receptor sites and vice versa. This was true in most of the Z sections where new and old receptor sites were found be close. Bar: 16µm

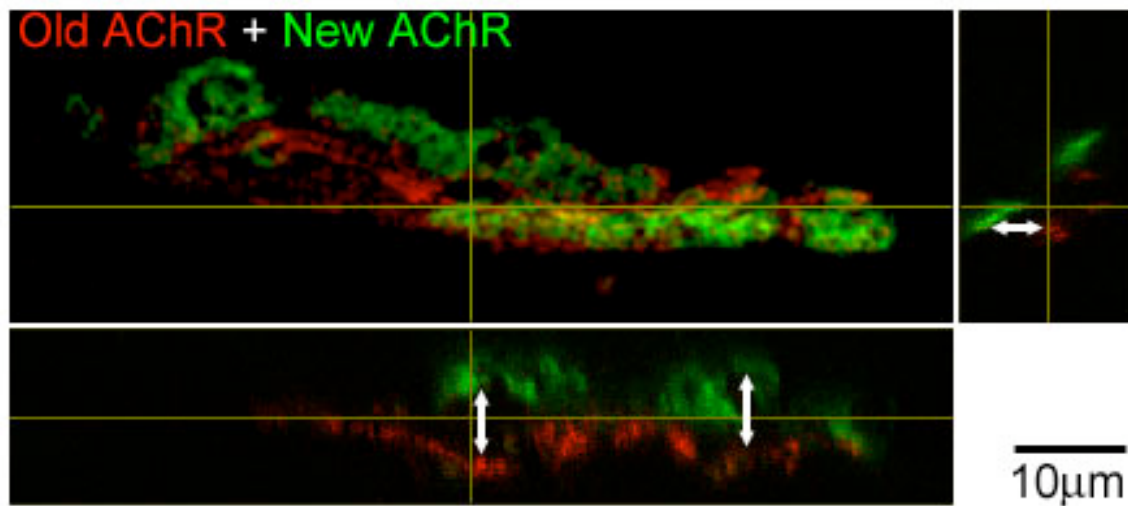


**Figure 3.7 New AChR sites can sometimes be found to be situated beneath the original AChR sites**

The original AChR was labeled with rho-BTX and the new AChR was labeled with Alexa647-BTX. Muscle was dissected 6 days after laser ablation, fixed and prepared for confocal imaging. The overlay of the maximum projections of the new and old AChRs (in the upper left panel) and one group of the Z sections (X-Z section in the bottom panel and Y-Z section in the right panel) are shown. The original AChR appears red and the new AChR green. The lines represent the place where the sections were cut. In most places with both Z sections, green-pixels representing new receptor sites are located far away from red-pixels representing original receptor sites. The gap between the new and old AChRs can be estimated from the scale bar. Noticeably, the pattern of the new AChR looked very different from that of the original AChR in this case. Bar: 10µm

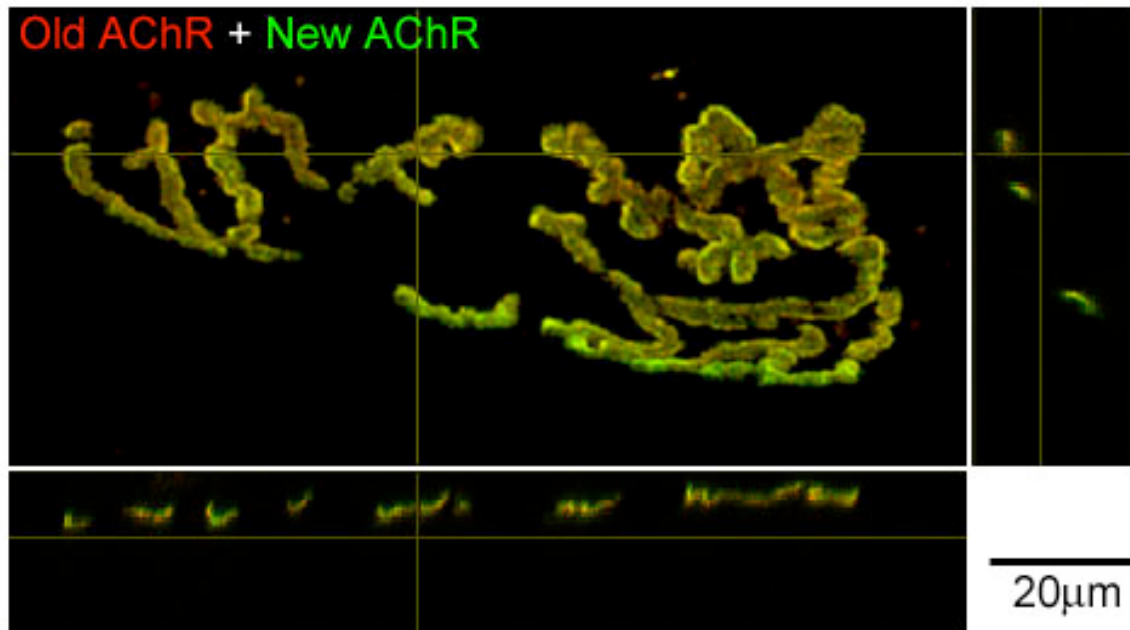


**Figure 3.8 New AChRs and old AChRs always overlap with each other in all dimensions on fibers that were not ablated.**

AChRs on the intact fibers were labeled with rho-BTX at day 0 and Alexa647-BTX at day 6, the time at which AChRs on the regenerating fibers were first observed. Confocal stacks were then acquired from these intact endplates after the whole muscle was dissected, fixed and mounted onto a slide. The old rho-BTX label appears in red and the new Alexa647-BTX label in green in all three panels. The upper left panel is the overlay of the maximum projections from both labels and the bottom and left panels are X-Z and Y-Z sections sliced at one location within the endplate area. The lines represent the place where the sections were cut. In contrast to the case for regenerating fibers, new and old labels on these intact fibers always overlapped with each other at all locations. Therefore, their overlay produced a yellow color. Noticeably, receptor clusters on the intact fibers were always confined to a thin line in the Z axis, very different from the clusters on the regenerating fibers (see Figure 3.6, 3.7). Bar: 20μm

### **Nerve terminals are associated with all the sites of new receptor deposition**

The fact that new AChR sites do not commonly overlap with the original AChR sites suggests that the accumulation of the new receptor sites is not under the influence of the remaining basal lamina. Instead, the nerve terminals at the synaptic sites after fiber degeneration might play a role here. In order to determine whether this might be the case, I examined the association of the nerve terminals with the AChR sites in the same 11 junctions above.

In all 11 junctions, nerve terminals were still seen overlaying the remaining old synaptic sites 6 days after fiber damage. A few original receptor sites (approximately 1-2%) were not apposed by nerve terminals in four of these junctions. At the same time, nerve terminals were indeed seen adjacent to the new receptor sites in all of the cases (Figure 3.9).

More interestingly, in those 2 junctions that had their new receptor sites completely separated from the original sites by a large gap in the Z axis, nerve terminals were not only seen associated with the old AChR sites, but also were found present on top of the newly expressed receptor sites (Figure 3.10). I presume that the persistent old receptors remain associated with the original synaptic basal lamina (discussed in Chapter 2). This suggests that in some cases, as the fiber regenerates, its plasma membrane is not in contact with the old synaptic basal lamina. Growths from the nerve terminals then penetrate through the old basal lamina to the regenerating muscle fiber. Clearly, this does not occur in all the cases. I suggest that in these other cases the regenerating fiber comes into contact with the old synaptic basal lamina.

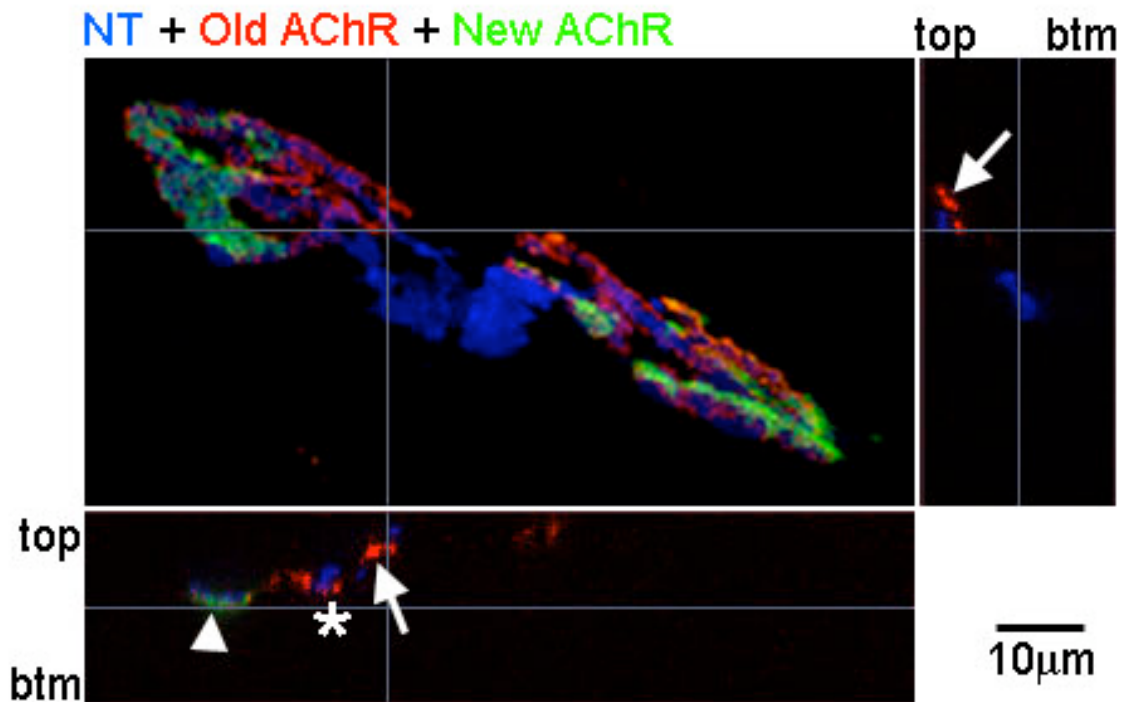


**Figure 3.9 Nerve terminals are associated with new AChR sites as well as old AChR sites during early fiber regeneration.**

The original AChR was labeled with rho-BTX and the new AChR was labeled with Alexa647-BTX. Nerve terminal (NT) was visualized by CFP expression. Confocal stacks were acquired from this regenerated endplate after the whole muscle was observed in vitro 6 days after fiber ablation. The original AChR appears red, the new AChR green and the NT blue in all three panels. The upper left panel is the overlay of the maximum projections from all three labels and the bottom and right panels are X-Z and Y-Z sections sliced at one location within the endplate area. Btm or top refers to the position of the fiber. Top means above the fiber and btm on the other direction. The lines represent the place where the sections were cut. At day 6 in this regenerating junction, the NT was associated with old receptor sites at most places (asterisk, arrowhead); but it was also missing at some other sites (arrows). Meanwhile, new AChR sites were seen close to where the NT was (arrowhead). Bar: 10µm

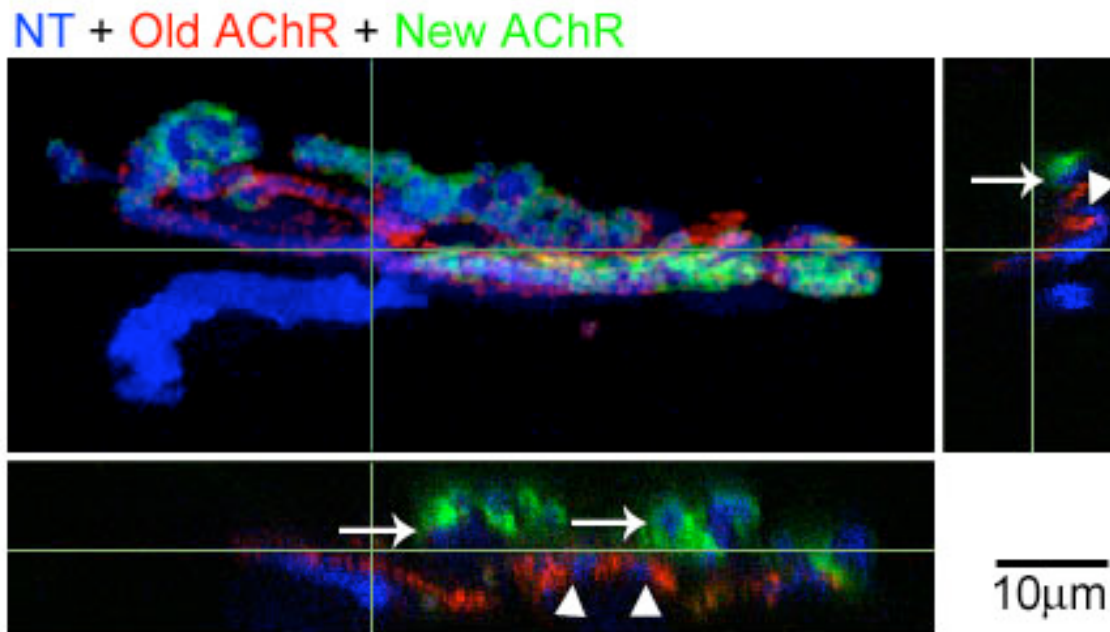


**Figure 3.10 New receptor sites located far beneath the original sites are apposed by nerve terminals during early fiber regeneration.**

The original AChR was labeled with rho-BTX and the new AChR was labeled with Alexa647-BTX. Nerve terminal (NT) was visualized by CFP expression. Confocal stacks were acquired from the new endplates after the whole muscle examined in vitro 6 days after fiber damage. The original AChR appears red, the new AChR green and the NT blue in all three panels. The upper left panel is the overlay of the maximum projections from all three labels and the bottom and right panels are X-Z and Y-Z sections sliced at one location within the endplate area. The lines represent the place where the sections were cut. At day 6 in this regenerating junction, the NTs were seen still associated with old receptor sites (arrowheads). Meanwhile, they were also present far away from the original AChR sites, at places where the new AChR sites were located (arrows). This suggests that NTs have extended sprouts and penetrated the original basal lamina sheath to innervate the receptor sites on the regenerating fibers. Bar: 10µm

### **Terminal Schwann cells extend processes along the regenerating fibers and guide terminal sprouts that establish new synaptic sites**

As described above, all the new receptor sites that are outside the original receptor area are apposed by nerve terminals, some of which were presumably formed as sprouts from the original nerve terminal. Previous results from this lab suggest that TSCs should be involved in these cases of sprouting (Son and Thompson, 1995a,b).

To find out if SC processes are present at the endplate area and when they appear following fiber damage, I examined TSCs at different times after laser ablation. Short TSC processes were detected as early as 3 days after fiber damage, but not before (8 out of 15 junctions, reported in Chapter 2). From day 4-6, short processes were still common in the vicinity of the original junctional area in most of the endplates I examined (10 of 11 junctions). Because the synaptic region tended to collapse/shrink following fiber ablation (Figure 3.11), these observations were also verified from fixed tissue examined under the confocal microscope. Occasionally, TSCs were found to have grown long processes beyond the endplate area along the regenerating muscle fibers around the same period. This was seen in 4 out of another 37 junctions imaged only *in vivo*. In 3 of these 4 junctions, only one long SC process was detected at the junction. The last junction showed 2 processes. All of the above processes were detected around 4 or 5 days following fiber degeneration with the exception of one not seen until after day 6. The time frame detection of these SC processes at the synapse from both *in vivo* and confocal observations suggests that TSC processes are induced by regenerating fibers.



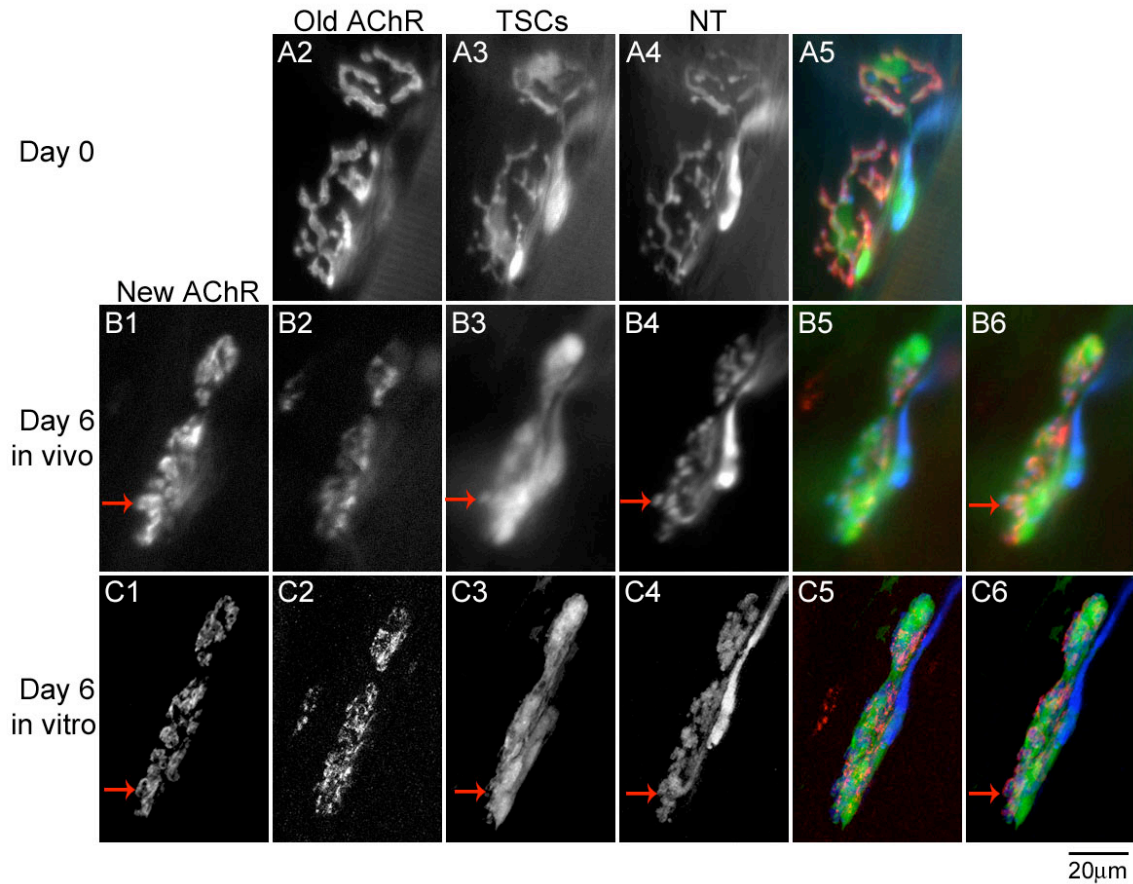


**Figure 3.11 Short TSC processes are present with terminal sprouts on regenerating fibers.**

AChR, TSCs and nerve terminal (NT) at an endplate on a damaged fiber were viewed immediately following laser ablation (A2-A4) and 6 days after (B1-B4) in a living animal. The original AChRs were labeled with rho-BTX at day 0 and new AChRs were labeled with Alexa647-BTX at day 6. The same endplate was also viewed after the muscle was dissected at day 6 with a confocal microscope. Maximum projections for each label are shown in C1-C4. In the color images, A5, B5, C5 are the overlays from the old AChR (red), TSCs (green) and NT (blue) acquired at the same time; B6, C6 are the overlays from the new AChR (red), TSCs (green) and NT (blue). A short TSC process (arrow in B3) and a short terminal sprout (arrow in B4) were both visible 6 days after fiber damage. The two were the same length (arrow in B6). New AChR clusters were also present at the same place (arrows in B1, B6). The regenerating fiber looked quite squeezed at this moment compared to the images at day 0. To verify the results from *in vivo* images, the muscle was fixed and viewed with a confocal microscope for precise alignment of all three components at the junction. The same results were obtained in the individual maximum projection (arrows in C1, C3, and C4) and their overlay (arrow in C6). Bar: 20µm

Therefore, both TSC processes and terminal sprouts respond to regenerating muscle fibers. To determine whether these two are associated in the same way as they are during nerve regeneration and sprouting after partial denervation, I examined their relative positions at different time points. At day 3, terminal sprouts were seen associated with TSC processes, but their number is smaller (4 sprouts vs. 8 processes out of 15 junctions, see Chapter 2). Their lengths were about the same as SC processes (Figure 2.16). Then at day 6, TSC processes were also found to be associated with the new synaptic terminals where new receptor sites were added in the vicinity of the original endplate area on the regenerated fiber. In addition, TSC processes were associated with those terminal sprouts that had penetrated through the original basal lamina (Figure 3.12). This implies that in order to establish new synaptic sites, both SC processes and nerve terminals are present.

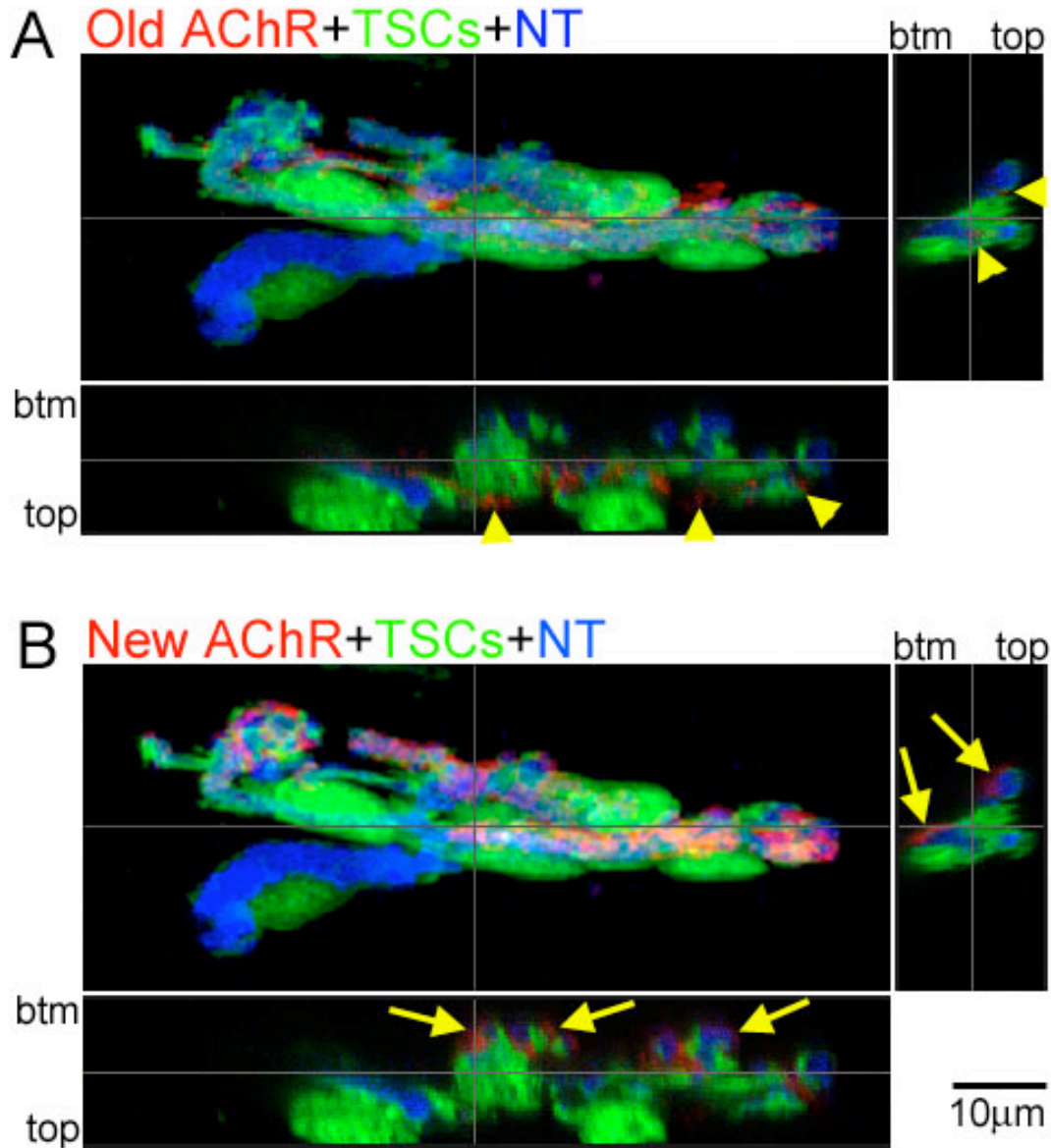


**Figure 3.12 TSC processes accompany terminal sprouts that are underneath the original basal lamina sheath.**

Confocal microscopy was performed on an endplate from a regenerating fiber 6 days after laser ablation. The old AChR was labeled with rho-BTX in A and the new AChR was labeled with Alexa647-BTX in B. In all 3 panels in both A and B, AChR appear red, TSCs green and nerve terminal (NT) blue. In both A and B, the merged maximum projection of AChR (old or new), TSCs and NT is on the upper left and X-Z section on the bottom, Y-Z section on the right. Btm or top refers to the position of the fiber. Top means above the fiber and btm the other direction. The lines represent where the section was cut. In the Z axis, the tips of the TSC processes and terminal sprouts were present underneath the plane of old AChRs (A), but associated with new AChRs (B). Arrowheads: position of the old AChR; arrows: position of the new AChR. Bar: 10µm

As mentioned above, 4 out of 37 junctions (10.8%) that were traced by repetitive *in vivo* imaging showed a long TSC process extended during fiber regeneration. Without exception, all these TSC extensions were found to be accompanied by sprouts from the axon terminal at some point. In 1 of these 4 junctions, a long TSC process was visible 5 days after fiber damage, but no terminal sprout was present at this time (Figure 3.13 panel C3, C4). Then, 4 days later, a fine terminal sprout was present and it followed exactly the path of the preexisting SC process. When Alexa647-BTX was applied to the muscle at this time, new AChR clusters were found to have accumulated underneath the sprout (Figure 3.13 panel D1-D4). No terminal sprouts on regenerating muscle fibers were ever seen in my experiments that were longer than SC processes. This clearly suggests that TSC processes are induced by the regenerating fibers first, and then serve as a substrate to guide the growth of the terminal sprouts to recruit new receptor sites. This observation is consistent with the findings during fiber denervation and reinnervation (Son et al., 1996).

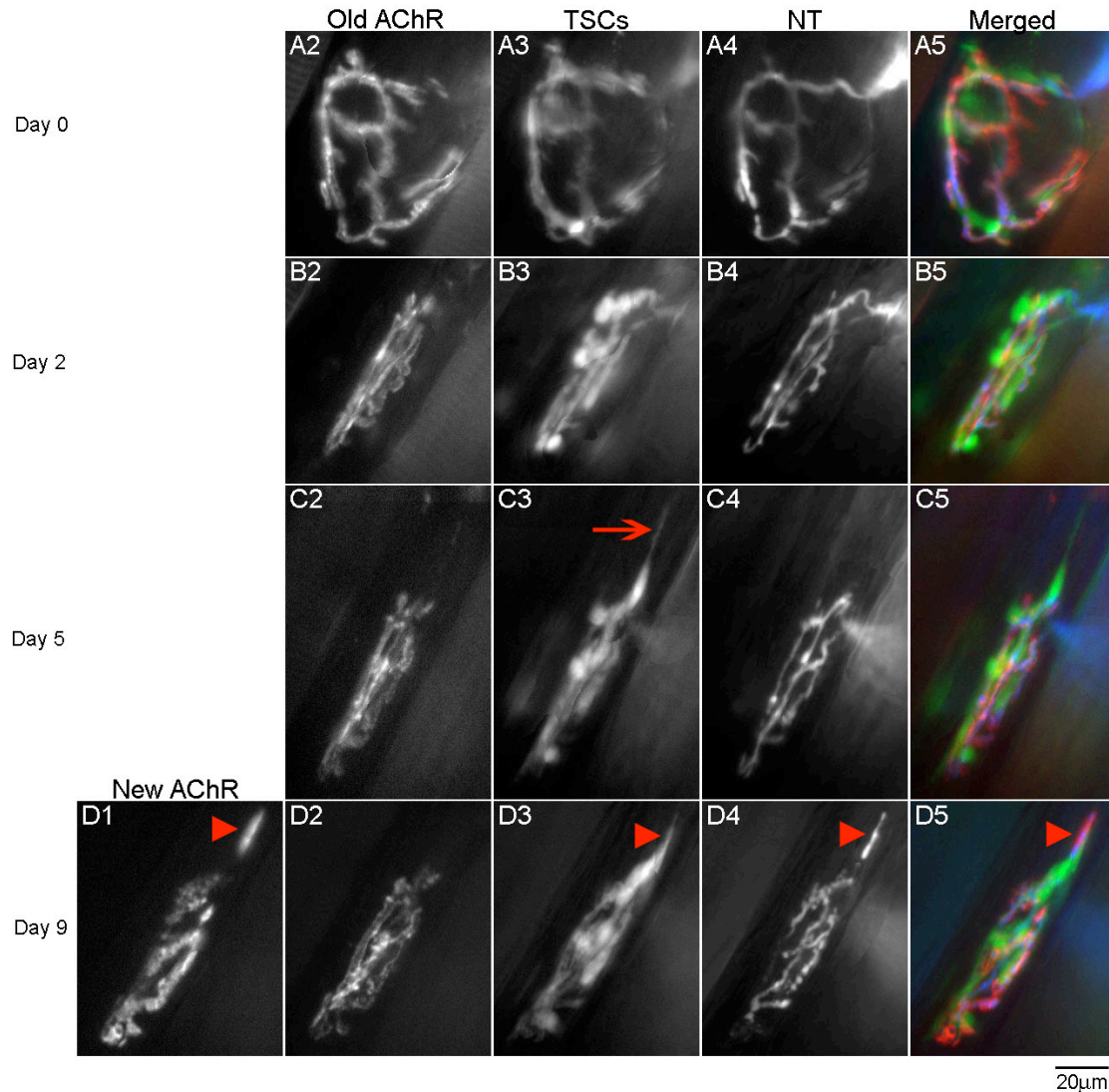


**Figure 3.13 TSC processes induce and guide terminal sprouts that then recruit new AChR clusters during muscle fiber regeneration.**

AChR, TSCs and nerve terminal (NT) at an endplate on a damaged fiber were viewed 4 times over the course of 9 days. AChRs were initially labeled with rho-BTX. Images were acquired immediately following laser ablation (day 0), day 2, 5, and 9 afterwards. Alexa647-BTX was applied on day 9 to reveal the position and the pattern of the new AChR sites. In the merged images, A5, B5, C5 are the overlays from the old AChR (red), TSCs (green) and NT (blue) acquired at the same time; D5 is the overlay from the new AChR (red), TSCs (green) and NT (blue). At day 2, both TSCs and NT have shrunk considerably following fiber ablation. A long SC process was present at day 5 along the regenerating fiber (arrow in C3), but no terminal sprout was visible at this time. However, a terminal sprout did appear 4 days later (arrowhead in D4) and exactly followed the path of the preexisting SC process (arrowhead in D5). At the same time, new AChR clusters were accumulated underneath the sprout (arrowheads in D1, D5). The SC process also seemed to have retracted slightly at this time. Bar: 20µm

### **Terminal Schwann cells also extend processes from nearby intact fibers during muscle fiber regeneration**

My experiments above suggest that some signal arising from regenerating muscle fibers can induce the growth of Schwann cells and motor axons on these fibers. If this signal is diffusible, it might be expected to affect the endplates on adjoining muscle fibers. To examine if this is the case, I observed the junctions on the nearby intact fibers at the same time I was observing those on the damaged fibers.

Indeed, TSC processes were sometimes detected on the intact muscle fibers near the new fiber (arrow, Figure 3.14 panel C2). Such processes were observed in about 14% of the cases (4 out of 29 nearby fibers). In 2 of these 4 cases, the intact fibers were adjacent to the regenerating fiber; in another 1 case, the intact fiber was one fiber away from the regenerating fiber and in the last case the intact fiber was two fibers away from the regenerating fiber. Additionally, in these 4 cases the SC processes were relatively thinner and shorter than the ones on the regenerating fibers. They also appeared about 1 to 2 days later than the processes on the new fibers. Among the 4 cases, two showed an inclination toward the regenerating fiber and the others grew along the length of the fibers. After comparing the time point at which TSCs extend processes on the regenerating fibers and the ones on the nearby intact fibers, I suggest that the regenerating fiber is the source of this growth and the signal is likely diffusible.

Although terminal sprouts were reported before to be present on these nearby intact muscle fibers (van Mier and Lichtman, 1994), in no cases did I detect such sprouts for the duration of every experiment. In Figure 3.14 panel C2 and C3, TSC grew a process along the intact fiber, but the nerve terminal did not follow it at day 12 after the

damage of the surrounding fiber, and it continued axonless for the next 8 days (Figure 3.14 panel D2, D3). Furthermore, no new AChR clusters were visible under this SC process. This SC process became much fainter and was eventually lost from the junction (Figure 3.14 panel E2). At no time did the apposition of nerve terminals, AChR, and SCs change at this junction.



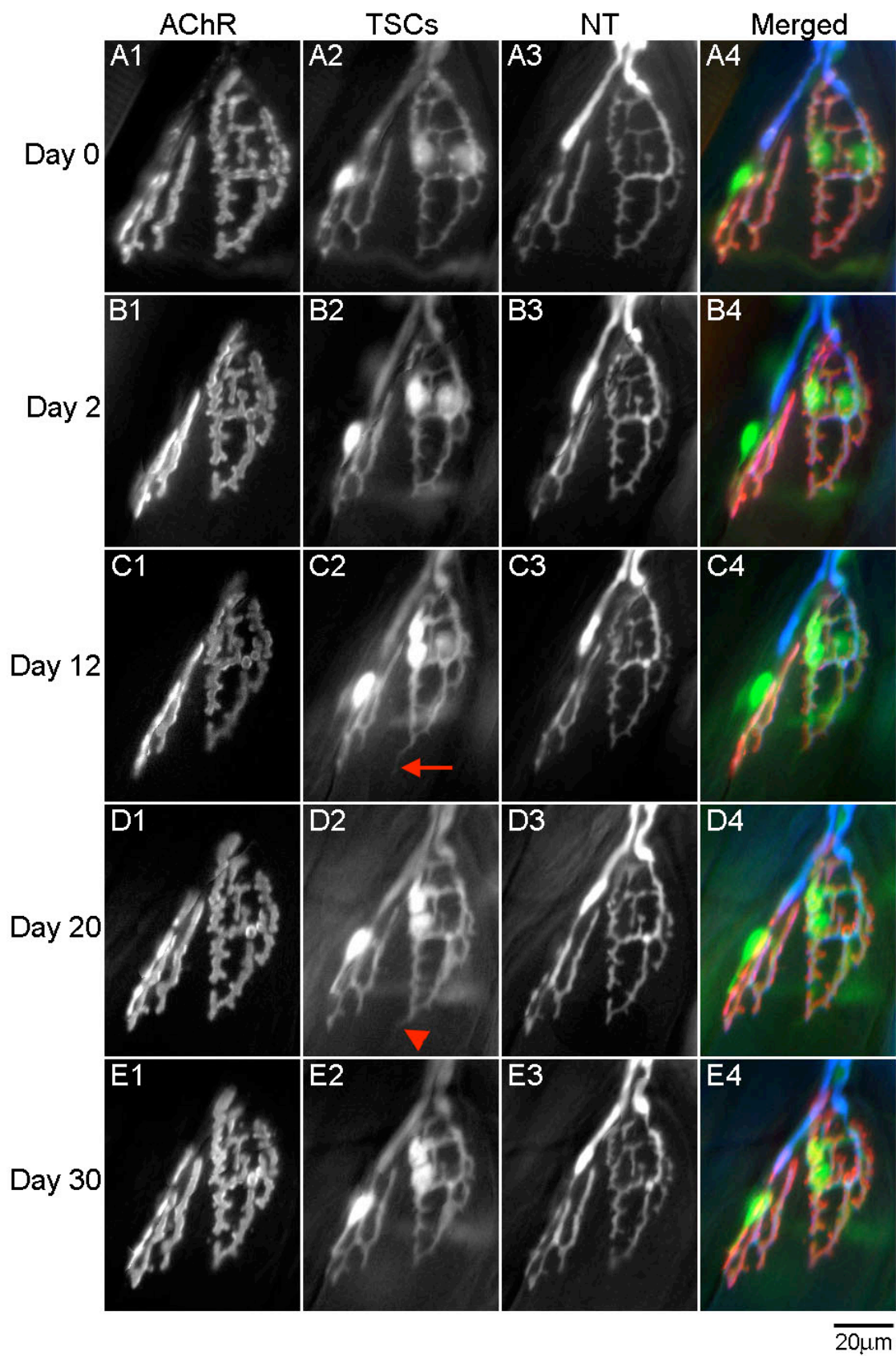




**Figure 3.14 TSCs also extend processes on the nearby intact muscle fibers during fiber regeneration.**

AChR, TSCs and nerve terminal (NT) of an endplate on an intact fiber were viewed repeatedly over the course of 30 days following the ablation of the nearby fiber to its right. AChRs were initially labeled with rho-BTX at day 0 and relabeled with Alexa647-BTX at day 20. In the merged images (A4, B4, C4, D4 and E4), AChR appears in red, TSCs in green and NT in blue. No changes were detected in either TSCs (B2) or NT (B3) at day 2 after the degeneration of the nearby fiber. The endplate was then viewed at day 6, but all components appeared unchanged (images not shown). A SC process appeared later by day 12 (arrow in C2), yet no terminal sprout was present (C3). When the endplate was imaged at day 20, the SC process seemed to have retracted and looked fainter (arrowhead in D2). There was still no sign of any terminal sprout. Newly labeled AChR also appeared the same as before. At day 30, the SC process had totally retracted and the junction had the same appearance as in the first images. Bar: 20 $\mu$ m

## DISCUSSION

Skeletal muscles are involved in all kinds of activities in animals; as a result, they are susceptible to injury. To compensate for injuries, muscle cells maintain a powerful ability to regenerate even after they mature. Once injured, the damaged segment will undergo necrosis (Carpenter and Karpati, 1989) and satellite cells will be activated to form a new fiber within the original basal lamina sheath (Carpenter, 1990). All the above events are apparently well orchestrated to make the repair as complete as possible. If the degeneration includes the muscle fiber underneath a neuromuscular junction, the components of the NMJ respond as well. My results show that new AChRs are added gradually to the original endplate area. Although they appear similar to the original AChRs, new receptor sites do not overlap with the original sites at many places in most cases. Most commonly, new sites are added in the vicinity of the original endplate area or new sites are a far distance away from the original sites. In all cases, new receptor sites are mostly apposed by the original nerve terminals or their small extensions no matter where they are. This implies that the distribution of the new AChR sites is more influenced by the nerve terminals than the remaining basal lamina as previously suggested. At the same time, TSC processes are found to be always accompanying terminal sprouts, either short or long. Further experiments have shown that, consistent with what happens during reinnervation, terminal sprouts always follow the path of TSC processes and later induce AChR clusters underneath. TSCs on the nearby intact muscle fibers also grow processes around this time period, with a slight inclination to grow toward the regenerating fibers. However, no terminal sprouts are seen associated with

them. These results imply that regenerating muscle fibers produce diffusible signals that induce TSC processes and use them to establish new synaptic sites.

### **Accumulation of new AChR sites by nerve terminals on the regenerating muscle fibers**

When muscle fibers were damaged and denervated at the same time in the frogs, new AChRs accumulated at the original synaptic sites, even in the absence of the nerve (Burden et al., 1979; McMahan and Slater, 1984). The same phenomenon apparently exists in mammals. In rats in which the sternohyoid muscle was grafted to a new site, the new AChR clusters and synaptic folds colocalized with acetylcholinesterase staining (Hansen-Smith, 1986). Since AChE persists in the original synaptic basal lamina even in the absence of the nerve, it serves as an enduring marker of the previous synaptic site (McMahan et al., 1978). In addition, if ectopic NMJs were induced by nerve implantation, only mature NMJs that had been forming for at least 2 weeks could induce new AChR clusters in the same region when muscle fibers were damaged and the nerve was severed (Slater and Allen, 1985). All of these results suggest that basal lamina directs the structural organization of the postsynaptic receptors. The cues lying inside the basal lamina are sufficient to guide the growth of the presynaptic terminals (Sanes et al., 1978) and induce the expression of AChR genes (Brenner et al., 1992) at the original synaptic sites.

However, my results suggest that this may not be totally true if the nerve is present at the synapse when new receptors are being inserted onto the surface of the regenerating muscle fibers. New receptor sites do not overlap with the original synaptic

sites at many places within the original endplate area. New receptor clusters are commonly added in the vicinity of some of the original receptor sites or permanently lost from others. The discrepancies in the location of the new and the old receptors are not likely to be caused by the inaccessibility of the remaining old receptor sites to the new receptor label. Such an inaccessibility might be caused by internalization of the remaining old receptors by other cells (for example, by macrophages or Schwann cells). If the fluorescence-tagged BTX is not applied before performing laser ablation but applied for the first time to label the remaining old receptors after fiber degeneration, a whole pretzel receptor pattern is revealed at the original synaptic sites (see Chapter 2). Therefore, no internalization of the original receptors is suggested in this case. Instead, the lack of a complete overlap between new receptor sites and old receptor sites implies that the original basal lamina sheath does not determine the location of AChR sites on the regenerated muscles under all circumstances. In fact, I found that nerve terminals are around the new receptor sites in most of the cases. Therefore, combining the previous findings and mine, it seems that if the nerve is severed at the time of fiber damage, new AChRs are inserted at the original synaptic sites; however, if the nerve is preserved at the time of fiber damage, new AChR sites will be modified and align with nerve terminals. This indicates that nerve terminals can override the signals residing in the basal lamina to direct AChR expression. This conclusion is not really at odds with the results of McMahan and colleagues (Burden et al., 1979; McMahan and Slater, 1984) who argued that signals in the basal lamina direct receptor insertion on newly regenerating muscle fibers, since they never performed experiments in which muscle fibers regenerated in the absence of the nerve.

Evidence from confocal stacks also supports my conclusion above. When viewed from the top, some new and original receptors appear to overlap. However, when viewed from the Z sections, it is clear that they are in close proximity but do not overlap. New receptor sites are not directly underneath the original sites. Instead, they are usually next to the original sites. In other words, the two run parallel with each other. Occasionally, new receptor sites are seen directly beneath the original receptor sites, but at a far distance from the original sites. Since the position of the original basal lamina sheath is reflected by the remaining original receptor labeling, these observations suggest that the original basal lamina is not a deciding factor here for new receptor accumulation. At the same time, nerve terminals are present where the new receptor sites are, whether they are next to the original sites or far apart. Therefore, such observations reflect the process that occurs during synaptogenesis in normal development (Dahm and Landmesser, 1991; Grinnell AD, 1995). This, once more indicates that accumulation of new AChR sites is under the influence of the nerve terminals that persist on the regenerating muscle fibers. It also implies that the cues in the original basal lamina sheath do not necessarily trigger the formation of functional synapses.

### **Induction of terminal sprouts by regenerating muscle fibers**

Whether new receptor clusters are found to be outside of the original receptor area or directly beneath them at some distance, they are apposed by nerve terminals. On one hand, this suggests that new AChR sites are induced by nerve terminals on the regenerating fiber; on the other hand, more interestingly, this shows that the original nerve terminals which are maintained after fiber degeneration become active during fiber

regeneration and are able to extend sprouts around the original endplate area or even penetrate through the original basal lamina sheath.

Noticeably, the distance between the original basal lamina sheath and the new fiber membrane is related to where the nerve terminal ends. It seems as if the new plasma membrane rises up to the level of where the original junctional basal lamina is, the persisting nerve terminals can directly induce new AChRs there. This would explain why new and old AChR sites are so close at many places and their pattern is similar. However, if the new fiber membrane fails to rise to the proximity of the original basal lamina, or the original basal lamina is ruptured too much during fiber degeneration for the new membrane to reach; nerve terminals will then grow sprouts, cross the old basal lamina sheath and induce new receptor sites on the new membrane. In this case, the new AChRs would take on a completely new appearance from the original AChRs. This actually raises another interesting question. That is, why can't the new fiber membrane rise up to the proximity of the original basal lamina sheath when the nerve is present during regeneration? It seems that this problem does not exist if the nerve is severed while fiber regenerates. In that case, new AChRs seem to always appear at the endplate sites and totally fill in the original receptor area (Rich and Lichtman, 1989b). Such discrepancy may be partly explained by 2 mechanisms.

First, as shown here, regenerating muscle fibers can induce terminal sprouts. The new fiber membrane fails to get close to the original basal lamina sheath because the growing nerve sprouts reach the new fiber membrane first. This nerve terminal induces the formation of the new synaptic sites. However, if the nerve is absent, then the new fiber membrane will always grow to lie close to the original basal lamina sheath and

express new AChRs under the influence of the cues inside the sheath. The second mechanism is that when the nerve is present, the growth of the regenerating fiber is heavily pressured physically from all directions by the surrounding intact fibers because of the muscle activity; therefore their membrane sometimes can not get close to the original basal lamina. Then nerve terminals will have to send out sprouts to induce new synaptic sites. If the nerve is absent, then all the surrounding intact fibers would become more and more atrophic while the regenerating fiber grows. Therefore, this would relieve the physical pressure caused by the surrounding fibers and the new fiber membrane could get close to the original basal lamina sheath.

Although the first mechanism is more easily justified by my results, the second mechanism cannot be excluded at the present time. In any case, regenerating muscle fibers are able to induce terminal sprouts to produce new synaptic sites.

### **Induction of Schwann cell processes by regenerating muscle fibers and their leading role in synapse formation**

In normal adult neuromuscular junctions, TSC processes cover and align precisely with the nerve terminal branches and the AChR pretzel. Morphologically they are stable. However, they do grow extensively beyond the junctional area in response to denervation and paralysis (Son and Thompson, 1995a; O'Malley et al., 1999). Later on these processes serve as the substrate for regenerating axons to follow during reinnervation. The importance of TSCs in synapse restoration and their relationship with nerve terminals has been well studied and discussed under those scenarios (Son et al., 1996). However, it is unknown whether this is true in other cases. More interestingly, the cause

of the extension of TSC processes is unclear. When a junction is denervated, the loss of nerve terminals might be the signal for SC growth, but the denervated and inactive muscle fibers could also play a role in this growth.

I didn't examine whether the denervated muscle can induce TSC processes per se (this was studied by a former student in the lab and she found this to be true, Love et al., 2003); instead, I looked at fiber degeneration and regeneration. I found that both TSCs and nerve terminals are maintained at the previous junctional area without losing any branches or gaining any extensions following fiber degeneration. However, things start to change during fiber regeneration. The frequency of seeing TSC processes suddenly increases. Nerve sprouts are sometimes seen running alongside them at the same length if not shorter. Especially in one case, it appears clearly that terminal sprouts follow the path of TSC processes. Therefore, it seems that both TSCs and nerve terminals send out extensions in response to regenerating fibers. Yet terminal sprouts are again found to follow the path of TSC processes. All this suggests that the first step to induce new synaptic sites on the regenerating fiber is the induction of TSC processes by the regenerating fiber. In addition, the fact that TSC processes are detected not only on the regenerating fibers but also on the nearby intact fibers indicates that the signal(s) from the regenerating fiber are diffusible in a short range.

My experiments seem to offer answers to the above questions. In order to restore or induce new synaptic sites in adult animals, TSCs need to create a path for nerve terminals to follow. This is true no matter whether it is the presynaptic terminal or the postsynaptic cell that is damaged. Signals to induce SC processes at least partly (if not totally) come from the postsynaptic cell during reinnervation. In fact, it is more



reasonable that muscle fibers induce the growth of TSCs when the synaptic connection is interrupted. If the presence of nerve terminals at the synapses normally suppresses the growth of TSCs, then denervation would cause TSCs to grow randomly in all directions. However, results from partial denervation suggest that TSCs grow preferably from the denervated junction to the innervated junction (Son and Thompson, 1995a,b). Such directionality also implies that denervated fibers are the source of TSC growth.

Why then do muscle fibers induce SC processes either after denervation or their own regeneration? It seems that rapid restoration of the synaptic connection would be nature's priority under all circumstances. However, for the axon to get to the place where it can most easily form a synapse, it needs a path to guide it. Therefore, induction of SC processes by denervated or regenerating muscle fibers becomes necessary. *In vitro* studies have implied that muscle fibers are able to secrete a large number of trophic factors, including insulin-like growth factor (IGF), fibroblast growth factor (FGF), interleukin-6 (IL-6) family of cytokines and nitric oxide (Allen and Boxhorn, 1989; Austin and Burgess, 1991; Balon and Nadler, 1994). It has been reported that the mRNA levels of IGF1 and IGF2 in denervated or paralyzed muscles increase several fold and they can induce nerve sprouting in innervated fibers (Caroni and Grandes, 1990). Since not many factors have been tested *in vivo* so far, future studies will be needed to reveal the identity of such molecules.

### **The absence of terminal sprouts from surrounding intact fibers**

Terminal sprouts were previously reported to be present on the nearby intact fibers (van Mier and Lichtman, 1994) during muscle regeneration. However, I have not

detected any in my experiments. I think this discrepancy again lies in the method of axon labeling as discussed in Chapter 2. They used 4-Di-2-Asp to label the possible terminal sprouts during fiber regeneration. Yet TSCs at the junction and some other unidentified cells around it also possess mitochondria in their processes. It is possible that these cells would be labeled by 4-Di-2-Asp as well. In fact, I did see 4-Di-2-Asp stained processes occasionally on the nearby intact fibers (separate experiments, Figure 3.15). As a result, 4-Di-2-Asp staining does not necessarily reflect only the presence of nerve terminals. On the contrary, CFP expression inside the axon is controlled by an axon-specific promoter. Therefore, the internal CFP fluorescence should more accurately represent the real position of the terminals.

At the same time, it is not unreasonable that the junctions on the nearby intact fibers only have SC processes and not terminal sprouts. Since the synaptic transmission is maintained normally at those junctions, it is not necessary for nerve terminals to extend sprouts as they have a tendency to induce new synaptic sites. However, this does not stop their TSCs from sensing the growing signals from the regenerating fiber in the vicinity. A path is there, but this doesn't necessarily mean that the nerve has to follow.

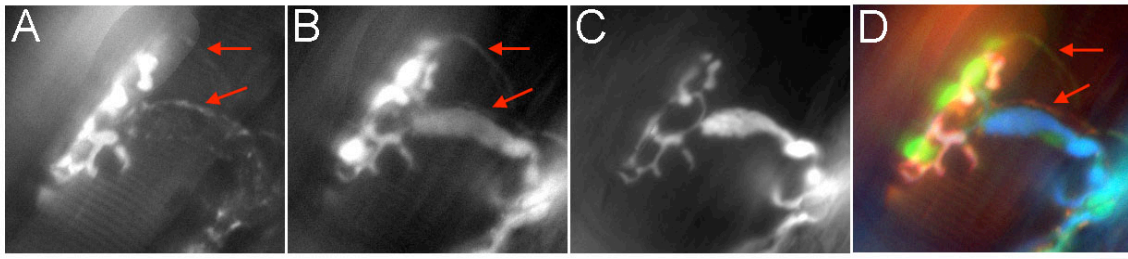


**Figure 3.15 4-Di-2-Asp staining is sometimes seen present in unknown cell processes around the junctional area.**

A junction on an intact muscle fiber (it was adjacent to the damaged fiber) was viewed after its AChR was labeled with rho-BTX and 4-Di-2-Asp was applied in addition. Their combined image is shown in A. TSCs were viewed by GFP expression (B) and nerve terminal (NT) by CFP expression (C). D is the merged image of A (red), B (green) and C (blue). Noticeably, processes labeled by 4-Di-2-Asp (arrows in A) were GFP positive (arrows in B, D) but CFP negative. Bar: 10 $\mu$ m

## **CHAPTER 4**

### **NEW NMJs ON REGENERATED MUSCLE FIBERS UNDERGO CONSTANT, LONG TERM REMODELING**

#### **ABSTRACT**

Once the animal reaches adulthood, most of its neuromuscular junctions remain stable apart from overall growth in accordance with growth in the size of the muscle fibers (Lichtman et al., 1987). However, the situation is quite different for neuromuscular junctions reforming on regenerated fibers. As reported in Chapter 3, although new AChR sites do not overlap with the original AChR sites at many places on the early regenerating fibers, their overall pattern still resembles the original one. This chapter deals with the stability of the pattern that is formed upon reconnection of the nerve with the regenerating fiber. Interestingly, I find the receptors on the regenerating fibers are much less stable than those on the undamaged fibers right next to them. The newly formed NMJs constantly remodel themselves for months when observed by repetitive *in vivo* imaging. AChRs seem to break into many small pieces with time. A lot of these pieces have ‘ring’ shapes with a bright circumference. TSC processes and nerve terminals also

extend branches and recruit new receptor clusters at some sites or retract some branches that are associated with the loss of AChR sites at other parts of the endplate. I usually observe that, in this remodeling, the loss of receptor territory is usually a little bigger than the addition. Furthermore, nerve terminals seem to become swollen at their endings in all the cases. In months, this continuous remodeling of NMJs always produces an ‘en grappe’ pattern on the regenerated fibers, making them stand out among the surrounding intact fibers. This suggests that the nature of the synaptic connections on the regenerated fibers is different from that on the intact fibers.

## **METHODS**

The methods used in the studies in this Chapter are the same as those described in Chapter 2.

## **RESULTS**

### **Newly formed NMJs on regenerated fibers start to change around 2 weeks after fiber damage**

Previous studies have shown that junctions on the regenerated fibers are abnormally complex. They are usually divided into numerous sub-units. Their nerve terminals are usually enlarged at the tip (Duchen et al., 1974; Minatel et al., 2001). However, my imaging shows that they do not appear abnormal, at least during early fiber regeneration. To determine the reason for this discrepancy, I followed the newly formed NMJs on the regenerated fibers for a few months.

As described in Chapter 3, the early pattern of the new AChRs on the regenerating fibers was established around day 6 after fiber damage. Both TSCs and nerve terminals still appeared to have long and smooth branches (panel B1-B3 in both Figure 4.1 and 4.2). Then, from day 6 to day 12, new receptors were primarily added to the early pattern, mainly increasing the receptor density. Usually, the new endplate area was expanded at day 12 due to the growth of the underlying fiber, but this enlarged site still had a pattern similar to the original one (Figure 4.1 panel C1). The arborization of TSCs and nerve terminals also seemed normal (Figure 4.1 panel C2, C3). However, some changes were observed in about 50% of the cases at this time. At those junctions, AChRs seemed to be losing their earlier uniformity and became fragmented (Figure 4.2 panel C1). Although branches of TSC processes looked approximately unchanged, nerve terminals started to acquire bulbous endings at some sites (Figure 4.2 panel C3).

No matter whether changes were detected at the new NMJs on the regenerating fibers or not at day 12, all of them would have fragmented AChR sites and swollen nerve terminals at some area within the endplate in the next week or two (Figure 4.1 panel D1, D3). What's more, the ones that had already shown those characteristics would become more prominent later on (Figure 4.2 panel D1, D3). New receptors also began to acquire 'ring' shapes which had a bright circumference and a black hole inside (arrowhead in Figure 4.1, 4.2).

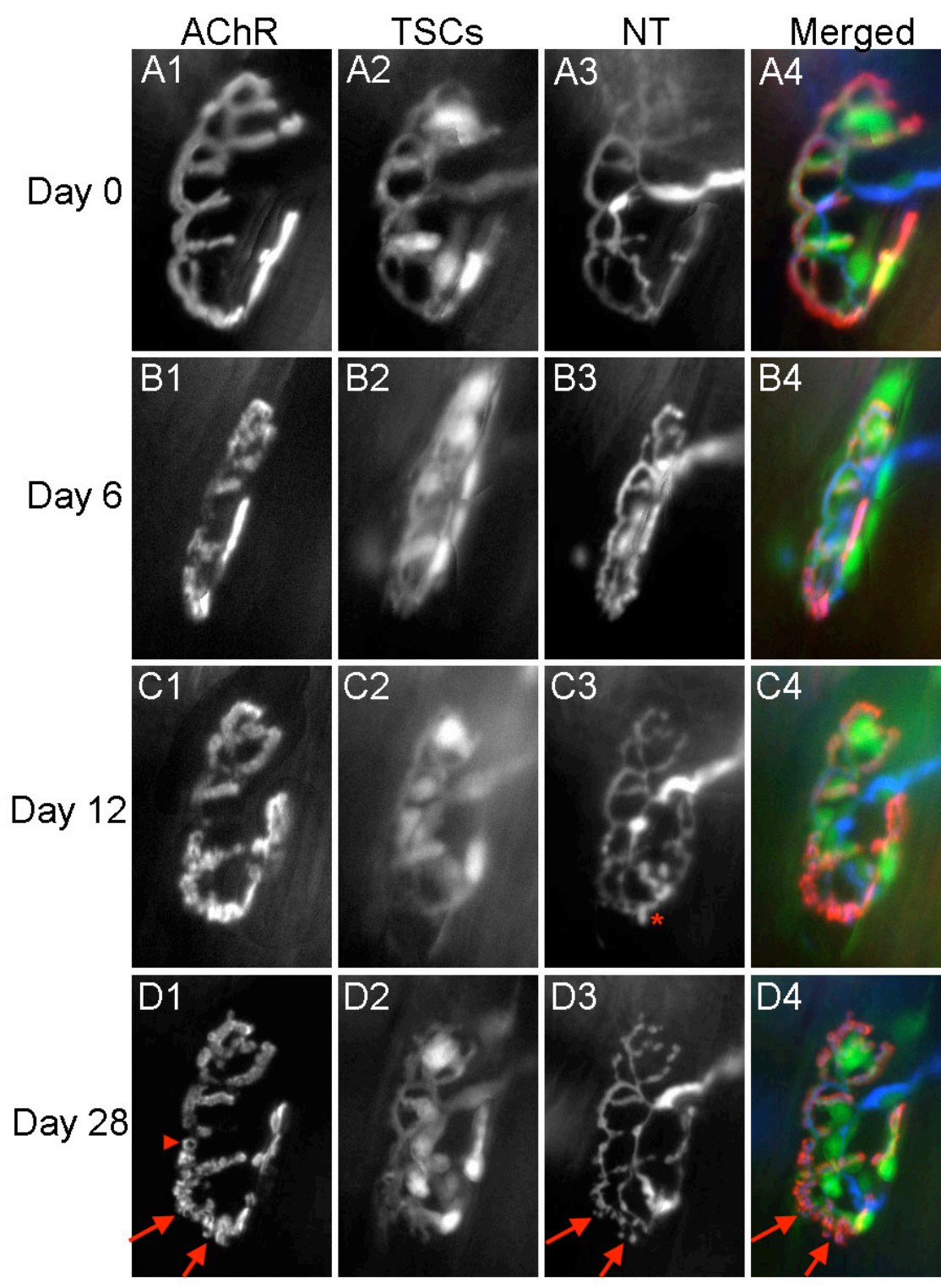


**Figure 4.1 Newly formed NMJs on the regenerated muscle fibers show some morphological abnormalities around 1 month after fiber damage.**

AChR, TSCs and nerve terminal (NT) of an endplate on a damaged fiber were viewed repeatedly at day 0, 6, 12 and 28, respectively, after laser ablation. The original AChR was labeled with rho-BTX (A1) at day 0 before laser ablation and the new AChR was labeled with Alexa647-BTX at each observation on day 6, 12 and 28 (B1, C1, D1). In the merged images (A4, B4, C4, D4), AChR appears red, TSCs green and NT blue. All three components of the junction were still very collapsed at day 6, but their outlines appeared to be smooth at the moment (B1, B2, B3). They all expanded over the next 6 days (C1, C2, C3) and showing a branching pattern similar to the original one. There was a short terminal sprout present (asterisk in C3). At day 28, changes in AChR and NT were especially obvious. At the bottom part of this junction, AChR sites seemed to have separated into several small aggregates (arrows in D1) and the corresponding nerve terminals had bulbous endings (arrows in D3, D4). AChRs also showed a 'ring' pattern (arrowhead in D1) which is very common later on the regenerated fibers. Bar: 20 $\mu$ m



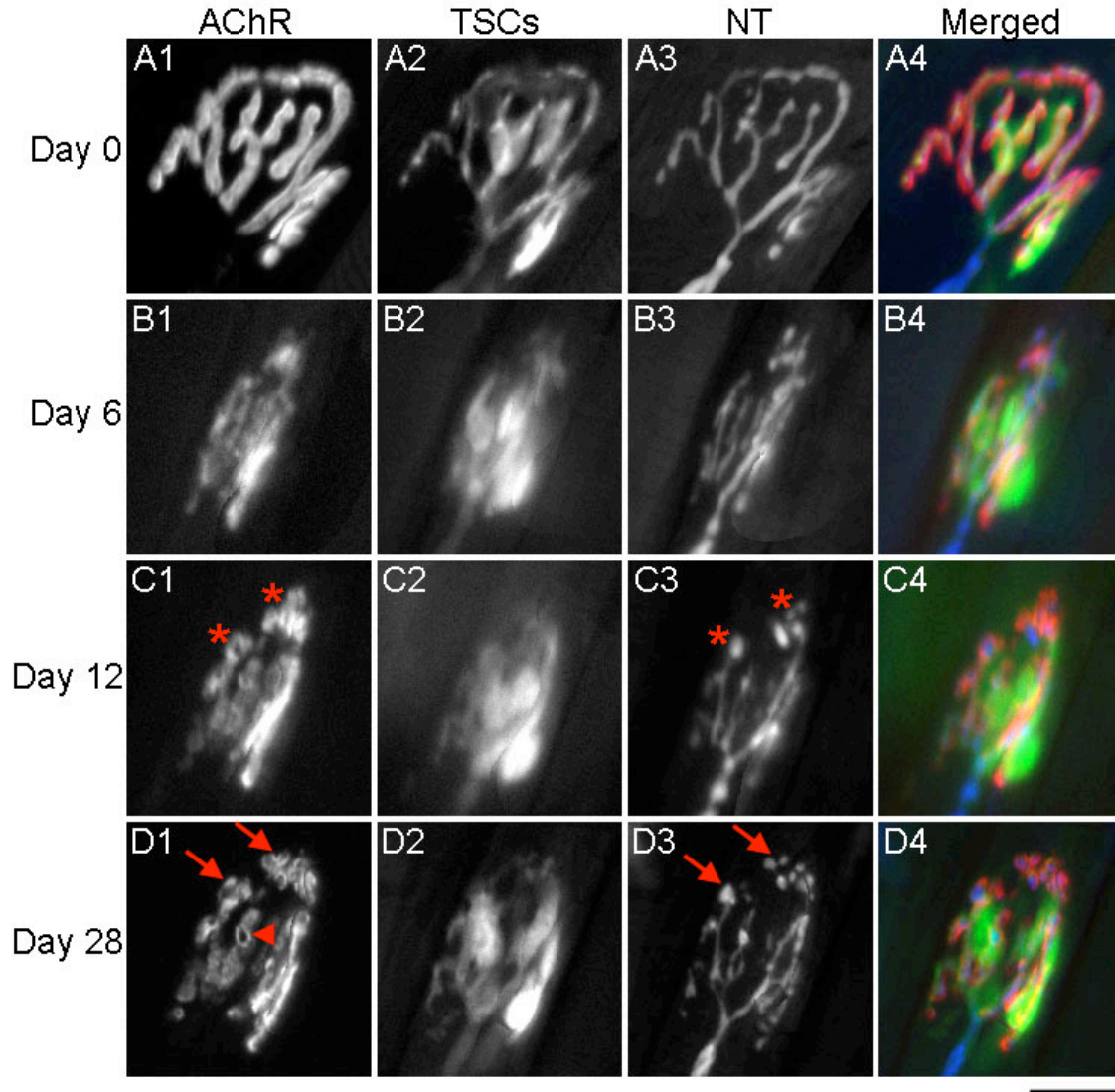


**Figure 4.2 Sometimes the morphological abnormalities appear early in the NMJs on regenerated fibers and progressively get more distinct over time.**

AChR, TSCs and nerve terminal (NT) of an endplate on a damaged fiber were viewed repeatedly at day 0, 6, 12 and 28, respectively, after laser ablation. The original AChR was labeled with rho-BTX (A1) at day 0 before laser ablation and the new AChR was labeled with Alexa647-BTX each time the junction was imaged on day 6, 12 and 28 (B1, C1, D1). In the merged images (A4, B4, C4, D4), AChR appears red, TSCs in green and NT blue. At day 6, the branches of both AChRs and NTs were still relatively smooth (B1, B3) compared to those at day 0 (A1, A3). However, receptors had already appeared non-uniform (asterisks in C1) and nerve terminals had a few enlarged tips (asterisks in C3) at day 12. At day 28, same places where changes were seen in AChR and NT before became much more obvious (arrows in D1, D3). At the same time, AChR fragmentation of the whole endplate area seemed prominent (D1) and the nerve terminal tips were also swollen at many places (D3). Again, the AChR showed a 'ring' pattern (arrowhead in D1) in this case. Bar: 20 $\mu$ m

### **Continuous remodeling is common for the NMJs on regenerated fibers**

Changes to the new NMJs on the regenerated fibers are not limited to fragmentation of the AChRs. Usually starting at about one month after fiber damage, loss or addition of the synaptic sites began to take place (6 fibers in 2 animals). In 3 of these 6 junctions, TSC processes and nerve terminals were seen to have retracted from some endplate areas at one to two months (Figure 4.3 panel C2, C3). The AChRs underneath these previous terminals were fainter than before (Figure 4.3 panel C1). As time went by, these receptor sites were eventually totally lost from the initial endplate area (Figure 4.3 panel F1). Although TSCs retracted their branches, the number of their cell bodies remained the same (one of them seemed to have one addition) and their position did not change either. Besides retraction, TSCs and nerve terminals also extended new branches at other locations with time (2 out of the above 3 junctions) (Figure 4.3 panel F2, F3). Application of Alexa647-BTX revealed that new AChRs had already been added underneath the terminal (Figure 4.3 panel F1). Nonetheless, whether retraction or extension of TSC processes and nerve terminals occurred at the junction, their tips were found to be of the same length. Since the interval between the subsequent images is relatively long in all these cases (2 weeks to a month), it is hard for me to tell which one changed first. The other 3 of these 6 junctions didn't show any obvious loss or addition to the endplate area, but fragmentation occurred.

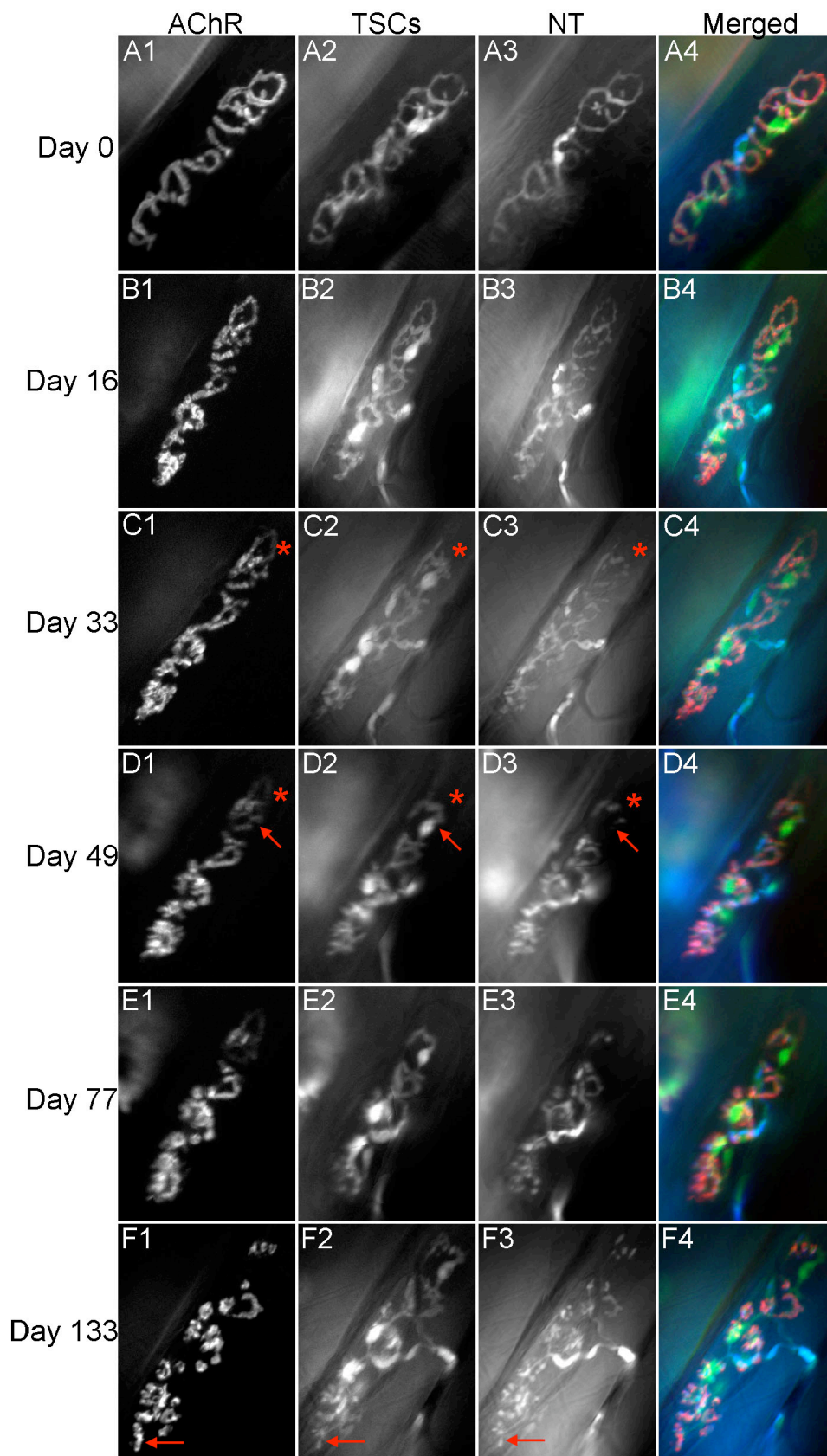


**Figure 4.3 NMJs on the regenerated fibers undergo slow but continuous remodeling.** AChR, TSCs and nerve terminal (NT) of an endplate on a damaged fiber were viewed repeatedly over the course of 133 days. The original AChR was labeled with rho-BTX (A1) at day 0 before laser ablation and the new AChR was labeled with Alexa647-BTX each time the junction was imaged on day 16, 33, 49, 77 and 133, respectively (B1, C1, D1, E1, F1). In the merged images (A4, B4, C4, D4, E4, F4), AChR appear red, TSCs green and NT blue. At day 16 after fiber damage, the new junction had some uneven receptor sites within the endplate, particularly at the bottom, but the arborization of the TSCs and NT looked similar to the original. However, when the junction was viewed again at day 33, both TSC processes and NT had lost a branch at the top (asterisks in C2 and C3). The AChR sites underneath the lost NT branch also seemed slightly faint (asterisk in C1). Then, over the next 17 days, these faintly labeled AChRs that were not covered by both TSC process or NT became even fainter (asterisk in D1). At the same time, both TSC processes and NT had retracted more branches (arrows in D2 and D3), and the receptors beneath those retracted branches became dimmer still. All these faintly labeled AChRs were eventually lost by day 133. In addition, both TSCs and NT extended one new branch at another area of the endplate after day 77 and new receptor sites were accumulated underneath when viewed together at day 133 (arrows in F1, F2, and F3). Noticeably, in the final view, AChRs appeared very fragmented and the swelling of nerve terminal tips was also prominent. Bar: 20 $\mu$ m

**Nerve terminals extend many fine processes and take on an ‘en grappe’ appearance on long-term regenerated fibers**

As the regenerated fiber grows bigger with time, fragmented AChR sites become more and more prominent (Figure 4.3 panel F1). Ring-shaped receptor clusters also seem to become dominant at the endplate. Combined with the remodeling described above, the pattern of the new AChRs 3 or 4 months after fiber damage looks totally different from that of the original receptors (Figure 4.3 panel A1, F1). Another example is shown in Figure 4.4. Meanwhile, in accordance with receptor fragmentation, their nerve terminals seem to grow a lot of small twigs off the main trunks, making their branching pattern look abnormal and complex. Furthermore, the tips of those twigs become swollen in most cases. As a result, the arborization of the presynaptic terminals takes on an ‘en grappe’ appearance (Figure 4.4 panel B3) and each ‘grape’ is in alignment with each receptor ring (Figure 4.4 panel B4). Such alignment is also verified by confocal imaging when the muscle was taken out after the final set of *in vivo* images (Figure 4.5).

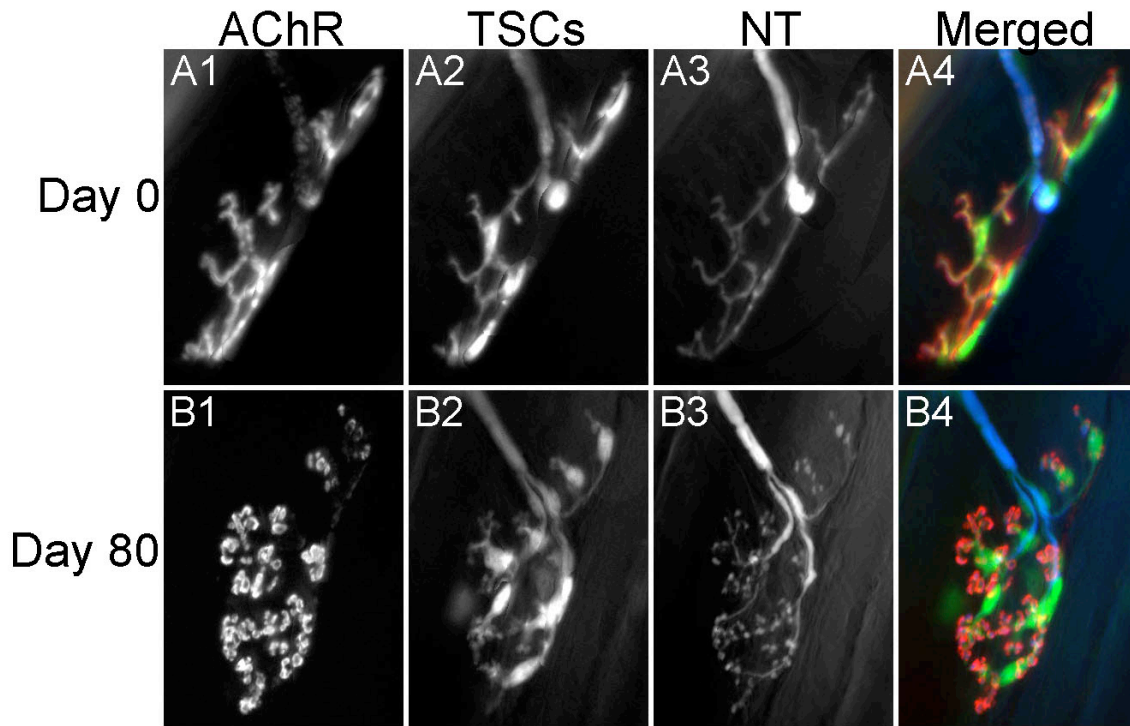


**Figure 4.4 NMJs on the regenerated muscle fibers are transformed into an ‘en grappe’ pattern in months.**

An endplate on a damaged fiber was followed for 80 days. Only the first and final sets of images were shown for the comparison. The original AChR was labeled with rho-BTX (A1) at day 0 before laser ablation and the new AChR was labeled with Alexa647-BTX (B1) at day 80. In the merged images (A4, B4), AChR appear red, TSCs green and NT blue. TSCs and NT on the original fiber had the normal smooth arborization (A2, A3) and the whole endplate had an ‘en plaque’ pattern. However, 80 days after fiber damage, new AChRs were totally segregated into many small islands and the density was uneven within each island (B1). Although the main branches of both TSCs and NT didn’t change, they extended many short twigs (B2, B3). Especially, nerve terminals were full of swelling endings. The whole junction looked like an ‘en grappe’ now. Bar: 20μm

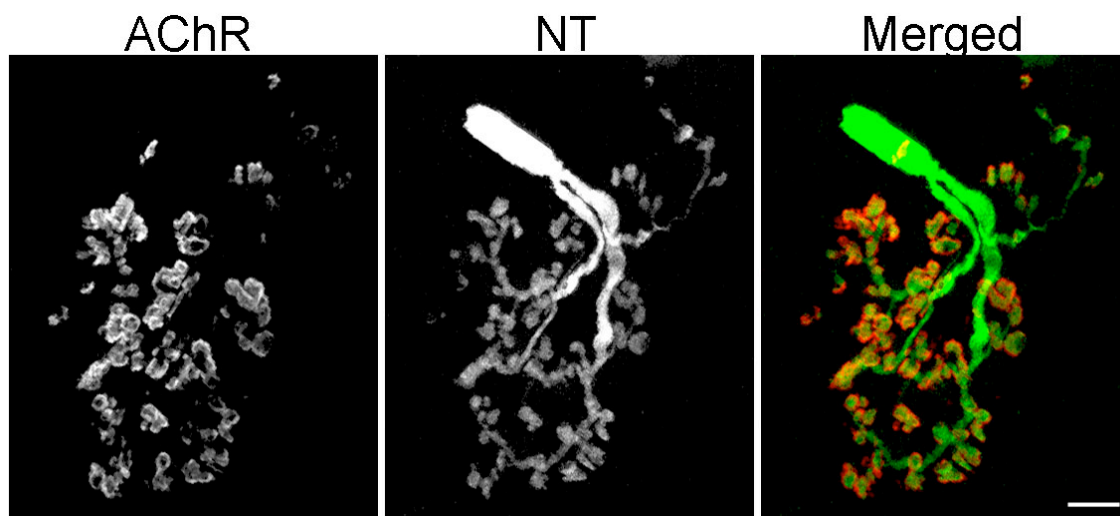


**Figure 4.5 Each nerve terminal bulb is aligned with each receptor island.**

After the final *in vivo* imaging, the animal was sacrificed and the muscle was dissected and fixed. Maximum projections were acquired from the confocal stacks of the junction in Figure 4.4. In the picture, AChR was labeled by Alexa647-BTX and NT was labeled with CFP expression. In the merged image, AChR appear in red and NT in green. The merged maximum projections of AChR and NT showed that each red receptor island was apposed by a green bulbous nerve terminal ending. Bar: 10 $\mu$ m

**The distribution of AChR sites and their alignment with the nerve terminals are changed in the 3-D space on long term regenerated fibers**

In normal junctions, nerve terminals should be right above and apposing the AChRs on the crests of the postsynaptic membrane. However, as described above, on regenerated fibers some swollen tips of the nerve terminals were found to be facing the dark hole inside the receptor ring. Does this suggest that the alignment between the nerve terminals and AChRs is changed on the regenerated fibers? In order to investigate this problem, I examined the relationship between these two in the Z axis in their confocal micrographs.

For junctions on the intact fibers, receptors are distributed in smooth thin lines in their side views (Figure 4.6), which suggests that they are located at about the same level on the fiber membrane. Nerve terminals are only on top of the receptor sites (Figure 4.6). This is definitely not the case on the regenerated fibers. When their junctions were viewed from the side, the outline of the AChR sites was very rugged and irregular. In addition, receptor sites seemed to be on the side of the nerve terminals as well as underneath (Figure 4.7). Particularly at those places where the ring-shaped receptor clusters were, receptors were not organized in rings as their top view revealed. They were actually shaped like a 'well' on a 3-D structure. Receptors were not only located on the top, they were also located on the 'wall' of the 'well' with a certain depth. Only the bottom of the 'well' was really devoid of receptors (Figure 4.7). At the same time, the swollen nerve terminal was enclosed inside the receptor 'well' (Figure 4.7).



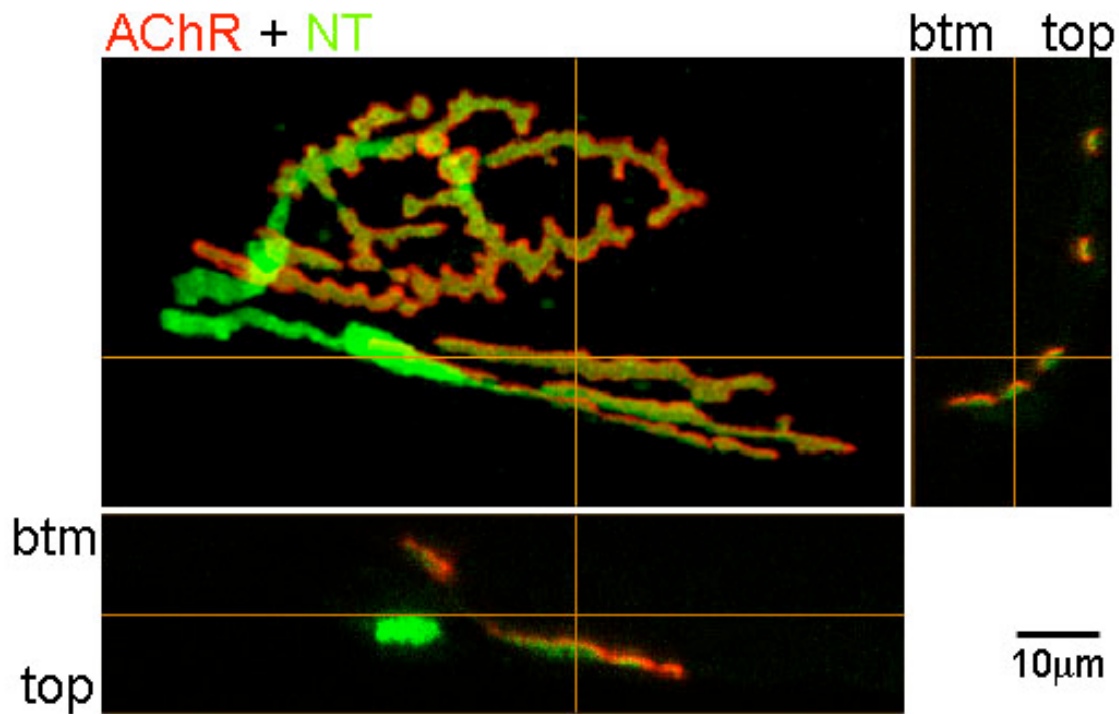


**Figure 4.6 Endplates on the intact fibers have smooth outlines in their 3-dimensional views.**

Confocal microscopy was performed on an endplate from an intact fiber. This fiber was from the same muscle which also had regenerated fibers. AChR was labeled by Alexa647-BTX and NT was labeled with CFP expression. In the picture, AChR appear in red and NT in green. Their overlaid maximum projection is on the upper left and X-Z section on the bottom, Y-Z section on the right. Btm or top refers to the position of the fiber. Top means above the fiber and btm the other direction. A representative section is shown here and where it was cut is indicated by lines. Both AChR and NT had long, smooth branches in their maximum projection. In both Z sections, NT was always on top of the AChR and the curve of their position outlined the crests of the junctional folds, which are approximately on the same level on the intact fibers. Bar: 10µm

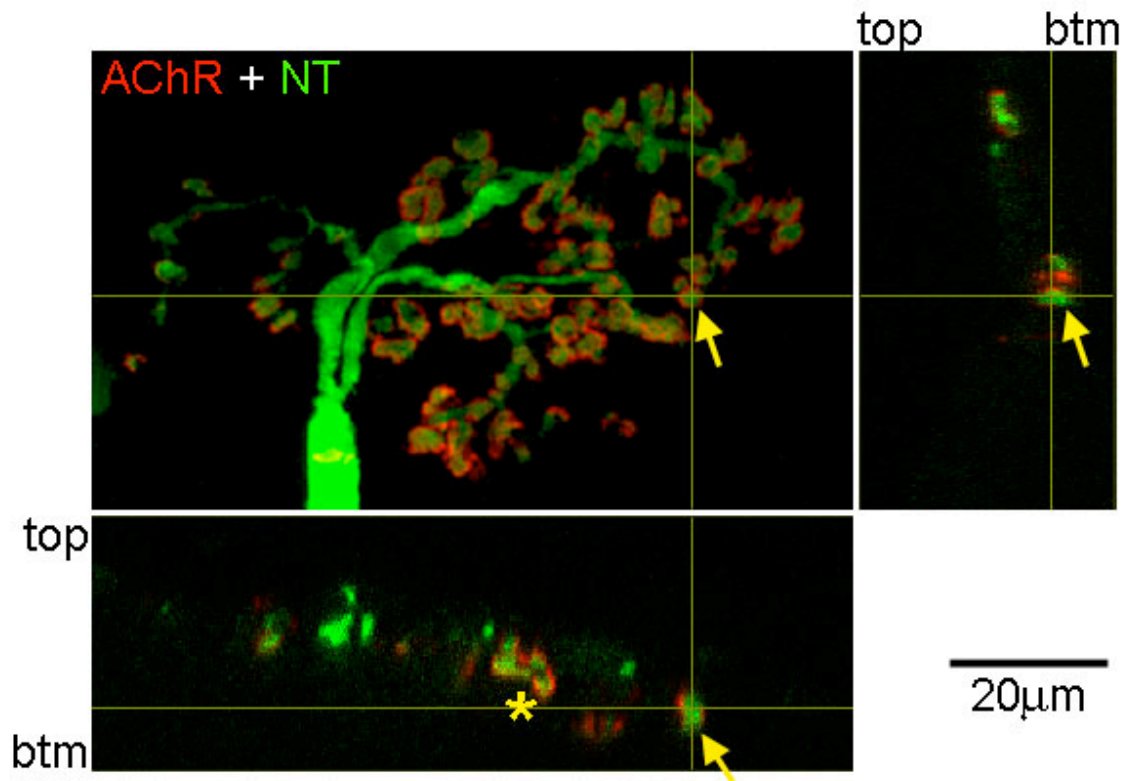


**Figure 4.7 The relative position of the AChR and NT is changed in 3-D space in the junctions on the regenerated fibers.**

Confocal microscopy was performed on an endplate from a regenerated fiber 80 days after laser ablation. AChR was labeled by Alexa647-BTX and NT was labeled with CFP expression. In the picture, AChR appear red and NT green. Their overlaid maximum projection is on the upper left and X-Z section on the bottom, Y-Z section on the right. Btm or top refers to the position of the fiber. Top means above the fiber and btm the other direction. The lines represent where the section was cut and here it is placed through a ring-shaped receptor cluster. The AChRs have lost their smooth outline and are not on the same plane any more on this regenerated fiber. At one place, the nerve terminal was enclosed inside the receptors (asterisk). Receptors were organized like a 'well' in 3-D too. The tip of the nerve terminal was not apposing AChRs, but the sides were (arrows). There were no receptor sites underneath the nerve terminal (arrows). Bar: 20μm

## **NMJs on the intact muscle fibers in the same muscle as the ablated fibers change little**

As described above, junctions on the regenerated fibers are highly dynamic. On the contrary, junctions on the intact fibers are quite stable in adult animals as previously showed by Lichtman et al. (Lichtman et al., 1987).

Five junctions on the intact fibers from two animals were followed by repetitive *in vivo* imaging along with the ones on the damaged fibers. Over the period of time when the junctions on the damaged fibers were changing, little change was detected at these junctions. There was no receptor loss or addition, or fragmentation. The branching pattern of TSC processes and nerve terminals remained the same. There was no swelling of the terminals and the number and position of TSC bodies stayed the same (Figure 4.8). Occasionally TSCs were seen to gain one cell body at the junction, which might be due to the growth of the animal.

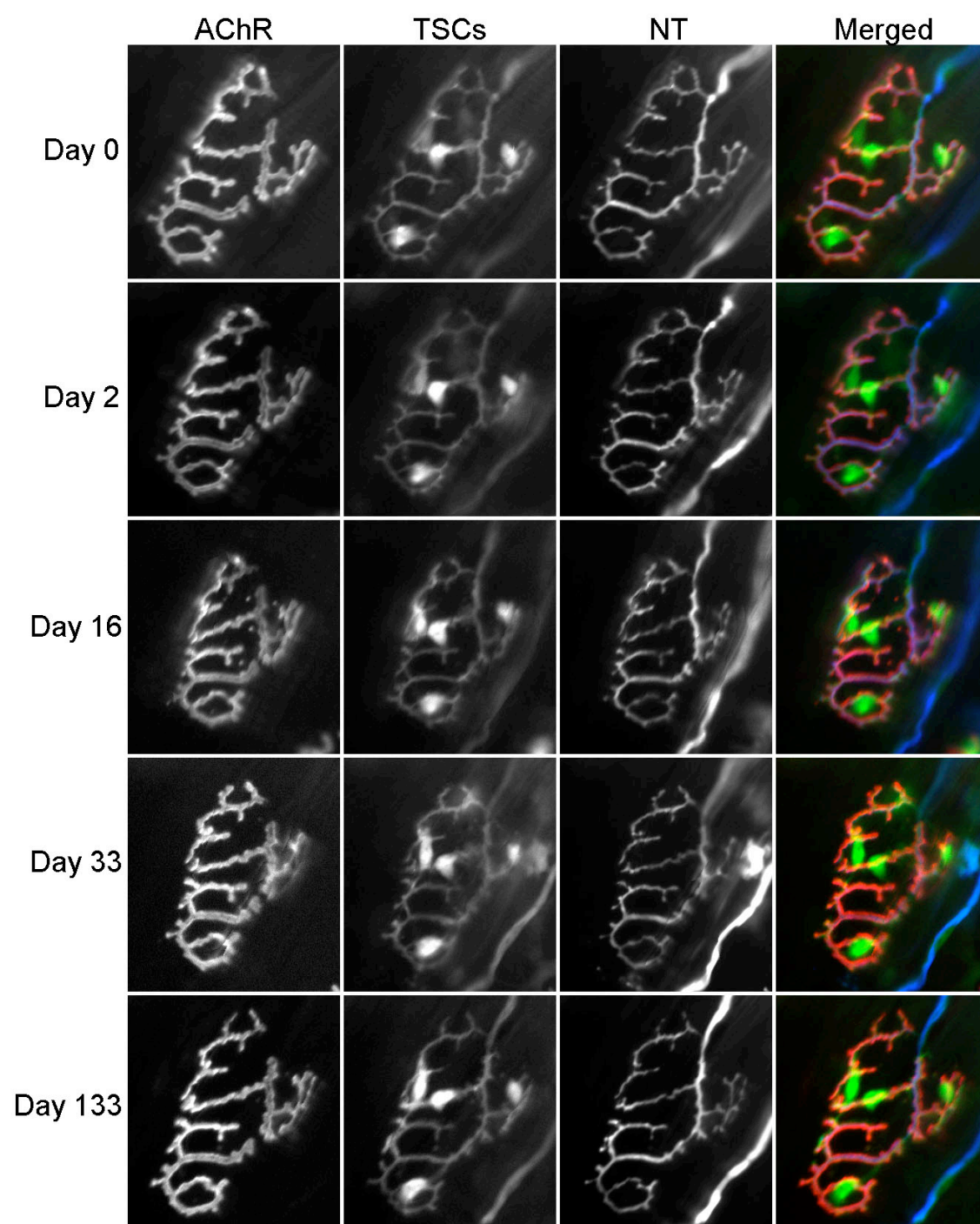


**Figure 4.8 NMJs on intact muscle fibers are usually stable for a long time.**

AChR, TSCs and nerve terminal (NT) of an endplate on an intact fiber were viewed repeatedly over the course of 133 days, together with 3 other junctions on the damaged fibers on the same muscle. The AChR was labeled with rho-BTX at day 0 and Alexa647-BTX on day 16, 33, and 133, respectively. In the merged images, AChR appear red, TSCs green and NT blue. Within the period of imaging, no changes were detected in AChR, TSCs or NT. AChR maintained the 'en plaque' pattern and the arborization of both TSCs and NT was smooth and unchanged in every image. The number and position of TSC bodies also stayed the same. Bar: 20 $\mu$ m

## DISCUSSION

Newly formed NMJs on the regenerated muscle fibers have a morphology and physiology that is similar to the ones on the intact fibers (Bader, 1981; Grubb et al., 1991). However, they can not maintain their early structure. When I followed these junctions for months by repetitive *in vivo* imaging, I found that they are quite dynamic and undergo remodeling slowly but continuously. AChRs seem to break into small clusters with a hollow ring appearance. TSCs and nerve terminals can retract a few original branches at some parts of the endplate and extend new branches at others. At the same time, AChR sites are either permanently lost underneath the previous nerve terminals or added underneath the new sprouts. In the end, nerve terminals will have an extensive arborization that matches the redistribution of the receptors. In addition, almost all the tips of the terminals become swollen, thus producing an ‘en grappe’ pattern at the endplate. The distribution of the AChR sites also seems changed on the 3-D space. This suggests that fiber regeneration has a big impact on the morphology of the new junction. Whether this will affect its physiology in the long run is still to be determined.

### **The dynamism of the newly formed NMJs on regenerated muscle fibers**

To watch the newly formed NMJs on the regenerated fibers undergoing continuous remodeling is most interesting. Considering the time point at which each change was detected, there are three things which are noteworthy. First, when the initial pattern of the new AChRs is completed around one week after fiber damage, although it looks similar to the original one in most of the cases; the contour of AChR distribution is very rugged which can be observed either by higher magnification (see Chapter 3) or Z

sections from the confocal stacks (data not shown). Second, when the growth of the regenerated fiber becomes prominent between one and two weeks, some of the AChRs start to become fragmented and the apposing nerve terminals begin to show bulbous endings. Third, addition or loss of the synaptic sites usually takes place at around one month and continues slowly for a long time. AChR fragmentation becomes more and more obvious as the regenerated fiber grows bigger with time. As a consequence, 3 to 4 months after fiber damage, the distribution of the AChRs on the regenerated fibers always looks very different in 3-D space. I think that such active transformation and structural abnormality may be explained partly by two mechanisms.

The first mechanism might be related to how the new junction is formed on the regenerated fiber. As discussed in Chapter 3, my results suggest that the expression of new receptor sites is induced by the persisting nerve terminals. Their position is related to whether the membrane of the regenerating fiber contacts the old basal lamina or not. Since the distance between the new fiber membrane and the old basal lamina sheath can be very unpredictable and occurs at different places within the endplate area, nerve terminals would have to induce new receptor sites on different levels. Since AChR molecules are normally concentrated on the crests of the junctional folds (Porter and Barnard, 1976), this also implies that junctional folds are not formed smoothly on the regenerated fibers in the first place. The irregularity of the junctional folds might destroy the stability within the new endplate. Therefore, synapse remodeling occurs.

Previous work from electron microscopic examination shows that terminal SC processes can invade into the cleft between the nerve terminal and the newly formed fiber membrane. The distance of the synaptic cleft is irregular. The number of junctional folds

is reduced on regenerated fibers as well (Duchen et al., 1974). The confocal images from my experiments also suggest that the regenerated fiber membrane seems to have a lot of furrows in which axon terminals are enclosed. Therefore, in this second mechanism, disrupted and uneven synaptic transmission which is caused by the abnormal junctional structure might be the reason for the remodeling on the regenerated fibers. It is still unknown why such synaptic abnormality happens to the junctions on the regenerated fibers.

### **The implications of ‘en grappe’ endplates on the regenerated muscle fibers**

Results from both previous studies and my experiments show that all the junctions on the regenerated fibers will take on an ‘en grappe’ appearance sooner or later. Such a unique morphology suggests that there are some inherent differences between the junctions on the regenerated muscle fibers and those on the intact fibers. However, this does not seem to affect the physiological properties and function of the regenerated fibers (Grubb et al., 1991). Therefore, what do all these tell us about the synaptic connections in the peripheral nervous system?

Interestingly, ‘en grappe’ junctions do exist in normal muscles from a widely different species in nature. For example, they are found in *M. brachialis* (a slow muscle which assists forearm flexion) in pigeon and fowl (Nene, 1977); slow muscles in garter snake (Hess, 1965); and extraocular muscles in mammals including human beings (Sadeh and Stern, 1984). It seems that all these ‘en grappe’ junctions share some common characteristics: they are the synapses on slow (tonic) muscle fibers; they are multiply innervated and they lack the regular junctional folds or have poorly developed ones.



Therefore, it has been suggested that the physiological reaction is correlated with the morphological appearance and innervation of the muscle fiber (Hess and Pilar, 1963). This might not always be true considering what happens to the regenerated fibers. These fibers are still singly innervated and can generate normal action potentials, yet they still acquire the 'en grappe' appearance.

Nonetheless, I think one of the reasons that might explain the situation in regenerated fibers is that muscle fibers have a big safety factor. They use this safety factor to ensure successful synaptic transmission, either by having a large amount of presynaptic transmitter release or having excessive postsynaptic receptors (Wood and Slater, 2001). In addition, these two can be further modulated in response to changing conditions. Because of this plasticity of the peripheral junctions, regenerated fibers can still function normally despite obtaining an abnormal endplate pattern.

## **CHAPTER 5**

### **CONCLUSION**

Muscle fibers are the only cells in the human body that can ‘repair’ themselves. Instead of the whole cell (one fiber) going through degeneration in response to any damage, only the injured segment becomes necrotic; the remainder of the fiber can regenerate at a later time. This specificity has intrigued many researchers. Here I’ve examined how the neuromuscular junction reacts to the damage of its underlying fiber. I have focused on the terminal Schwann cells at the cellular level. To my surprise and contrary to previous beliefs, I find a certain amount of AChRs present at the original synaptic sites persist for a long time after fiber degeneration. Moreover, I find that the whole arborization of both TSCs and nerve terminals is maintained at the endplate following fiber damage. A new fiber starts to form around 2-3 days after muscle injury and new receptors start to appear at day 4. Although new AChRs are expressed in the presence of the remaining old AChRs, they do not often intermix, but are commonly situated in separate layers. My studies show that the maintenance of the original nerve terminal at the junction seems to have an effect on the expression of the new receptor

plaque. This contradicts previous researchers who thought that only the basal lamina induces new receptor expression. In addition, terminal Schwann cells grow processes in response to fiber regeneration, both from damaged and the nearby intact fibers. However, nerve terminals follow these processes only on the damaged fibers, but not on the intact ones, to induce new AChR clusters. This suggests that the absence of the nerve might not be the stimulus that induces terminal Schwann cell processes (as shown in denervation experiments by Son and Thompson, 1995a,b). Rather it appears that the inactive muscle fibers in denervated muscle or regenerating fibers in my case can induce TSC processes.

Thus, evidence from my dissertation work provides new insights into the elements that are responsible for the signals that induce TSC processes in new NMJ formation. This information will be instructive for researchers conducting clinical trials in the future for the recovery of periphery nerve or muscle injuries.

### **The relationship between the muscle fiber and the maintenance of the neuromuscular junction**

Hints at mechanisms that maintain neuromuscular junctions come from the study of early development. The neuromuscular junctions of newborn mice are multiply innervated, but this multiple innervation disappears during the first 2 weeks after birth. The process of this conversion from multiple to single innervation is “synapse elimination”. When the events of synapse elimination were followed by repetitive imaging of individual junctions in living animals, it was found that not only are the eliminated axons withdrawing from the synaptic sites, but their underlying receptors are also disappearing. Observations suggest that postsynaptic receptors begin to disappear

before the removal of their apposing nerve terminals (Balice-Gordon and Lichtman, 1993). This finding suggests that events in the postsynaptic cell related to the maintenance of acetylcholine receptors may determine the removal of some motor axons while preserving at least one innervating axon at each junction. An understanding of the mechanism here is of importance for understanding the experiments I report here.

A variety of experiments suggest that synapse elimination may involve the relative activity levels of the competing axons. A direct test of this idea has been made at adult neuromuscular junctions. To create a disparity in the activity of different parts of singly innervated junctions, Balice-Gordon and Lichtman focally applied BTX to a portion of the receptors at several junctions and then followed with vital imaging the consequence of this blockade. They found that the portion of the nerve terminal over the blocked receptors was eliminated while the portion above unblocked receptors persisted. Since blockade of all the receptors at a junction produced no terminal loss, the elimination appeared to require the creation of disparity in the synaptic transmission effected from different portions of these nerve terminals. Moreover, their experiments suggested that, for the elimination to occur, a sufficient portion of the receptors had to remain unblocked so that the nerve terminal could bring the muscle fiber to threshold. If too large an area of the receptors was blocked, no elimination resulted. This suggested that if the remaining, active portion of the junction, transmitted effectively, it could cause the demise of the blocked portion of the synaptic site (Balice-Gordon and Lichtman, 1994). In a News and Views article accompanying this publication, Charles Jennings offered a model for these results (Figure 5.1). A “punishing” signal produced by the active portion of the synapse was viewed as promoting the removal of receptors; this

punishing signal was viewed as having a spatial spread that included the entire synaptic site. A “protective” signal produced by the active portion of the synapse that counteracted the punishing signal and promoted the retention of receptors was viewed as much more spatially restricted, confined to that portion of the junction that was active. Thus, blocked receptors in an active synapse would receive the punishing but not protective signal and be eliminated while unblocked receptors would receive both and be protected/maintained. Blocking all or the majority of the receptors would remove both the punishing and protective signals and result in maintenance of the nerve terminals (Jennings, 1994).

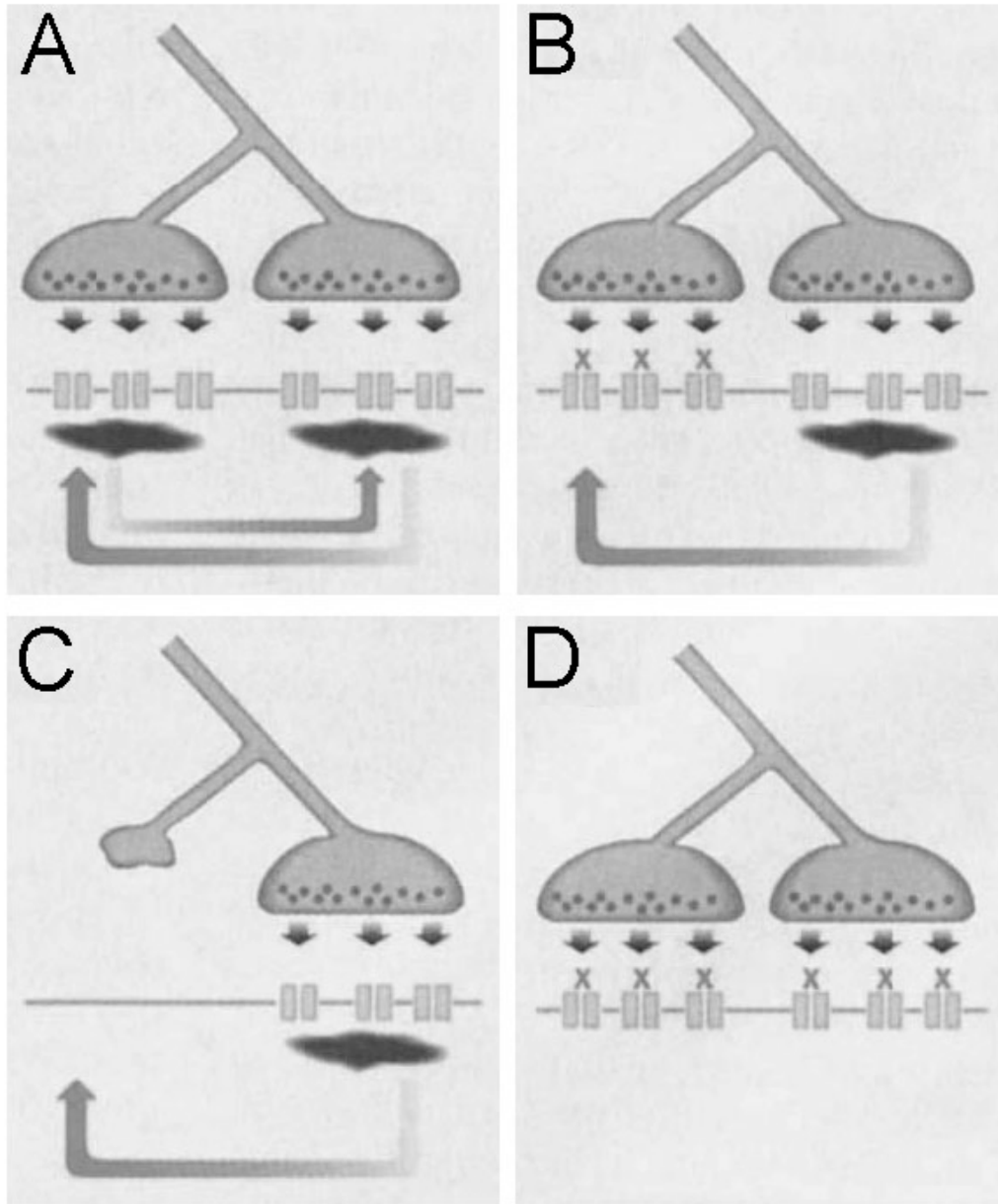


**Figure 5.1 Schematic illustration of the model for synaptic elimination in adult NMJs.**

A, In a normal adult neuromuscular junction, each terminal activates its underlying acetylcholine receptors (AChRs), thereby causing an elimination signal (arrows) and a local protective signal (oval dots). B, When AChRs under one terminal are blocked with toxin (crosses), they are no longer protected from elimination, and are unable to eliminate other terminals. C, The unprotected AChRs and their underlying terminal are eventually lost. D, If all AChRs are blocked, no elimination signal is produced, so no loss occurs. (adapted from Jennings, 1994)

My experiments show that ablation of the postsynaptic cell does not lead to loss of presynaptic components. In light of the above discussion, this result might appear unsurprising. Removing the postsynaptic cell would, after all, be expected to remove both punishing and protective signals, just like the blockade of all the receptors. However, Nguyen and Lichtman have reported that injection of a membrane-impermeable protein synthesis inhibitor into the postsynaptic muscle fiber at the site of the junction did not perturb synaptic transmission, the ability of the muscle to contract, nor the distribution of postsynaptic receptors. However, this manipulation resulted in the rapid loss (beginning within 24 hours) of nerve terminals (Santo Neto et al., 26<sup>th</sup> SFN meeting, 1996). These experiments imply that, in addition to any effects on synaptic maintenance operating through the distribution of acetylcholine receptors, there is some retrograde signal arising from the postsynaptic fiber required for the maintenance of the presynaptic nerve terminal. How is it possible that a protein synthesis inhibition within the muscle fiber results in a loss of nerve terminals, but the ablation of the postsynaptic cell seen in my experiments does not?

One explanation of this result is that there is also a retrograde punishing signal that acts, upon fiber activation, to punish the nerve terminal. Thus, in addition to signals that act on the postsynaptic muscle fiber and its acetylcholine receptors, there are both punishing and protective signals that act retrogradely on the nerve terminal. In this scenario, the punishing signal would arise from the postsynaptic cell in an activity dependent fashion, but its generation would not require protein synthesis. A postsynaptic protein synthesis inhibitor would block the protective signal but not the punishing signal; hence the nerve terminal would withdraw. Blockade of all receptors would prevent the

generation of both retrograde signals. Likewise, removal of the postsynaptic muscle fiber would also block both retrograde signals.

How do the muscle fibers exert these effects on the NMJs? They might do it through the basal lamina, which plays an important role in regulating the communications between the pre- and post-synaptic apparatus. It is possible that under normal conditions muscle fibers secrete some kind of inactive proteolytic enzymes to their membrane surface. The protein synthesis inhibitor somehow causes such proteases to become active and thus break down the matrix proteins that the nerve terminals cling to. As a consequence, the nerve terminal retracts. However, during muscle fiber degeneration, macrophages are going to clean up all the molecules within the damaged segment, including those inactive proteolytic enzymes. Therefore, the basal lamina is spared in this case and the nerve terminal is maintained.

### **The relationship between Schwann cell processes and muscle fibers**

Terminal SCs are a crucial component of the NMJ in mammals. The importance and function of those cells have intrigued researchers for decades. In the mid-90's, our lab found that TSCs grow processes in response to denervation, and these processes later guide axon terminals to reinnervate the denervated junctions. TSC processes are also responsible for reorganization of the reinnervated junctions. However, one more interesting question remains unanswered here—what send(s) out the signal(s) to induce TSC processes? Although the absence of the axon at the terminal seems to be the most natural conclusion, studies did show that the denervated muscle is more likely the cause (Brown and Holland, 1979). These researchers showed that direct muscle stimulation



inhibits terminal sprouting following partial denervation, yet direct nerve stimulation has no effect. Later, more evidence showed that regenerating muscle fibers can also induce sprouting from nearby intact fibers (van Mier and Lichtman, 1994). All these experiments suggest that the stimulus for nerve sprouting rises from inactivated muscle fibers. My experiments were intended to find out whether the sprouts in response to regenerating muscle fibers are again following TSC processes. In other words, are TSCs really the ones that answer the fiber's call to mediate the restoration of NMJ formation?

As I expected, TSCs do grow processes in response to fiber regeneration, but not in response to fiber degeneration. This is not surprising because once the damaged fiber degenerates, there is no living component at the junctional area to secrete any molecules to induce TSC processes. Macrophages may be able to secrete some cytokines when they are performing phagocytosis at the damaged area, but since no TSC processes have been detected until the fiber regenerates and no terminal sprouts are visible if fiber regeneration is prohibited (van Mier and Lichtman, 1994), it is unlikely that macrophages make a major contribution to these processes. However, it will be physiologically relevant that TSCs respond to the regenerating muscle fibers to help re-establish or make new synaptic connections. The signal will be dissipated to the nearby junctions as well, as my experiments suggest. This also might be important for how the new muscle fibers try to quickly restore their original strength. When necessary, the regenerating fiber can even induce TSC processes to extend across the original basal lamina to form a totally new receptor plaque. Again, this suggests that to regain a proper synaptic connection is the first priority of the NMJs after any injury.

This idea does not conflict with the conclusion from partial denervation. Since the

denervated junctions want to be reinnervated as soon as possible, inactivated, yet still functional muscle fibers will then send out signals to cause TSCs to extend processes which, in turn, will induce terminal sprouts to grow in from the nearby innervated junctions to reinnervate the denervated ones.

### **The abnormal morphology of the NMJs on the regenerated fibers and its implications in muscle disease and aging**

The development of the new NMJs on the regenerated fibers has never been studied *in vivo* before, although people have known for a long time that nerve terminals and the postsynaptic structure of the regenerated muscle appear in many respects to be different from those of the normal muscle (Duchen et al., 1974; Couteaux et al., 1988). My experiments suggest that nerve terminals still maintain relatively long and smooth branches during early fiber regeneration and new AChR plaque does not possess an obvious fragmented look. Usually around 2 weeks after fiber injury, new receptors seem to start to break into small islands and the nerve terminal extends fine and short twigs with bulbous looking endings. It is still to be determined whether new AChRs are added to the membrane in separated groups in the first place. Another possibility is that fiber growth later causes such abnormal appearance, or that new receptors that are continuous at first become fragmented. My results seem to favor the first explanation. More interestingly, the new NMJ appears to remodel itself slowly but consistently, suggesting that the synaptic activity can not reach a balanced state within such junctions--as is the case with normal junctions. This probably does not affect the overall strength of the regenerated fibers since their physiological properties are no different from the intact

fibers (Grubb et al., 1991). Nonetheless, the ‘en grappe’ pattern becomes the signature for the NMJs on the regenerated muscle fibers.

This has some important implications in human myogenic diseases, such as Duchenne muscular dystrophy (*mdx* mouse model). It was found that junctions in *mdx* mice showed strikingly abnormal morphologies. They have increased terminal arborizations with swelling boutons. Both AChR and AChE are redistributed in numerous small spots. The postsynaptic membrane is simplified with a reduction of secondary synaptic folds (Lyons and Slater, 1991; Torres and Duchen, 1987). However, the density of AChR on the surface and its area are not changed compared to the control fibers. The size of the individual nerve terminal bouton is normal. More importantly, the physiological properties of the NMJs from the *mdx* mouse are not significantly different from the control. Therefore, these researchers all suggest that the absence of dystrophin does not directly affect the junctional changes, but that degeneration and regeneration of the muscle fibers are the real cause for the abnormality. Deficiency of dystrophin only makes the fibers more fragile and more likely to break. What I observed in my experiments exactly confirms the previous conclusions.

Another interesting phenomenon resides in the NMJs from aging animals. Unlike young NMJs, aging NMJs have plenty of small discrete clusters of AChRs, nerve terminals with increased length and more short branches, and abnormal junctional folds (Oda, 1984; Courtney and Steinbach, 1981; Fahim et al., 1983; Oki et al., 1999). For decades, people have wondered what initiates these changes—muscle or nerve? Although a variety of studies have been conducted, it is still unknown whether the change is neurogenic or myogenic. My experiments strongly suggest that the causative mechanism

of such changes is in the postsynaptic muscle fibers, because these structural changes have a close similarity to what happens to the junctions on the regenerating muscle fibers after injury as well as in the dystrophic mice (Kitaoka et al., 1997). Additional evidence comes from the fact that there is no axonal degeneration obvious at the aging junction (Gutmann et al., 1971); synaptic transmission is unimpaired (Kelly and Robbins, 1983); yet activities of acetylcholinesterase which is mainly secreted by muscle fibers are changed in the aged mice (Washio et al., 1987). The proposal that denervation causes terminal sprouts to increase at the aging endplates (Rosenheimer, 1990) does not conflict with muscle being the reason for the morphology change, as such sprouts can be induced by inactivated fibers (discussed above). Knowing that change in muscle function is the primary consequence of aging is very important in that it can help people to find ways to delay aging process in human beings.

### **Concluding Remarks**

The first goal of this work was to determine how injured muscle fibers influence changes in TSCs. It turned out that more interesting results have emerged from the experiments than I had expected. In this dissertation, I have showed a few things that are contrary to conventional beliefs: 1) the original AChRs are not totally degraded following fiber damage. Those remaining can reside at the old endplate area for a long time. 2) nerve terminals do not retract from the original synaptic sites in response to degenerating fibers. 3) new AChRs on regenerated fibers usually do not occupy the original synaptic sites. However, the two are close to each other. 4) recruitment of new AChRs is more influenced by the existing nerve terminals than basal lamina (if it is involved at all in this

scenario). In addition, I also showed that TSC processes are induced by diffusible signals sent out by the regenerating muscle fibers. Terminal sprouts again follow the trails of SCs as they do during reinnervation. New NMJs on the regenerated fibers are very dynamic and undergo remodeling constantly. Although this work may raise more questions than it actually has solved, it does demonstrate that postsynaptic cells (muscle fibers) are the key factor in restoring the function of the NMJs. In addition, its implications in human diseases and aging might have clinical applications in the future.

## BIBLIOGRAPHY

- Akkaboune M, Culican SM, Turney SG, Lichtman JW. 1999. Rapid and reversible effects of activity on acetylcholine receptor density at the neuromuscular junction in vivo. *Science*. 286(5439):503-7.
- Akaaboune M, Grady RM, Turney S, Sanes JR, Lichtman JW. 2002. Neurotransmitter receptor dynamics studied in vivo by reversible photo-unbinding of fluorescent ligands. *Neuron*. 34(6):865-76.
- Allen RE, Boxhorn LK. 1989. Regulation of skeletal muscle satellite cell proliferation and differentiation by transforming growth factor-beta, insulin-like growth factor I, and fibroblast growth factor. *J Cell Physiol*. 138(2):311-5.
- Anderson JE. 1998. Murray L. Barr Award Lecture. Studies of the dynamics of skeletal muscle regeneration: the mouse came back! *Biochem Cell Biol*. 76(1):13-26.
- Anglistter L. 1991. Acetylcholinesterase from the motor nerve terminal accumulates on the synaptic basal lamina of the myofiber. *J Cell Biol*. 115(3):755-64.
- Anton ES, Weskamp G, Reichardt LF, Matthew WD. 1994. Nerve growth factor and its low-affinity receptor promote Schwann cell migration. *Proc Natl Acad Sci U S A*. 91(7):2795-9.
- Austin L, Burgess AW. 1991. Stimulation of myoblast proliferation in culture by leukaemia inhibitory factor and other cytokines. *J Neurol Sci*. 101(2):193-7.
- Bader D. 1981. Density and distribution of alpha-bungarotoxin-binding sites in postsynaptic structures of regenerated rat skeletal muscle. *J Cell Biol*. 88(2):338-45.
- Balice-Gordon RJ, Lichtman JW. 1993. In vivo observations of pre- and postsynaptic changes during the transition from multiple to single innervation at developing neuromuscular junctions. *J Neurosci*. 13(2):834-55.

- Balice-Gordon RJ, Lichtman JW. 1994. Long-term synapse loss induced by focal blockade of postsynaptic receptors. *Nature*. 372(6506):519-24.
- Balon TW, Nadler JL. 1994. Nitric oxide release is present from incubated skeletal muscle preparations. *J Appl Physiol*. 77(6):2519-21.
- Barres BA. 1991. New roles for glia. *J Neurosci*. 11(12):3685-94.
- Borg TK, Caulfield JB. 1980. Morphology of connective tissue in skeletal muscle. *Tissue Cell*. 12(1):197-207.
- Brenner HR, Herczeg A, Slater CR. 1992. Synapse-specific expression of acetylcholine receptor genes and their products at original synaptic sites in rat soleus muscle fibres regenerating in the absence of innervation. *Development*. 116(1):41-53.
- Brown MC, Holland RL. 1979. A central role for denervated tissues in causing nerve sprouting. *Nature*. 282(5740):724-6.
- Burden SJ, Sargent PB, McMahan UJ. 1979. Acetylcholine receptors in regenerating muscle accumulate at original synaptic sites in the absence of the nerve. *J Cell Biol*. 82(2):412-25.
- Caroni P, Grandes P. 1990. Nerve sprouting in innervated adult skeletal muscle induced by exposure to elevated levels of insulin-like growth factors. *J Cell Biol*. 110(4):1307-17.
- Carpenter S. 1990. Regeneration of skeletal muscle fibers after necrosis. *Adv Exp Med Biol*. 280:13-5.
- Carpenter S, Karpati G. 1989. Segmental necrosis and its demarcation in experimental micropuncture injury of skeletal muscle fibers. *J Neuropathol Exp Neurol*. 48(2):154-70.
- Chiu SY, Kriegler S. 1994. Neurotransmitter-mediated signaling between axons and glial cells. *Glia*. 11(2):191-200.
- Cohen I, Rimer M, Lomo T, McMahan UJ. 1997. Agrin-induced postsynaptic-like apparatus in skeletal muscle fibers in vivo. *Mol Cell Neurosci*. 9(4):237-53.
- Courtney J, Steinbach JH. 1981. Age changes in neuromuscular junction morphology and acetylcholine receptor distribution on rat skeletal muscle fibres. *J Physiol*. 320:435-47.
- Couteaux R, Mira JC, d'Albis A. 1988. Regeneration of muscles after cardiotoxin injury. I. Cytological aspects. *Biol Cell*. 62(2):171-82.

- Dahm LM, Landmesser LT. 1991. The regulation of synaptogenesis during normal development and following activity blockade. *J Neurosci.* 11(1):238-55.
- d'Albis A, Couteaux R, Janmot C, Mira JC. 1989. Myosin isoform transitions in regeneration of fast and slow muscles during postnatal development of the rat. *Dev Biol.* 135(2):320-5.
- Dememes D, Lleixa A, Dechesne CJ. 1995. Cellular and subcellular localization of AMPA-selective glutamate receptors in the mammalian peripheral vestibular system. *Brain Res.* 671(1):83-94.
- Dong Z, Brennan A, Liu N, Yarden Y, Lefkowitz G, Mirsky R, Jessen KR. 1995. Neu differentiation factor is a neuron-glia signal and regulates survival, proliferation, and maturation of rat Schwann cell precursors. *Neuron.* 15(3):585-96.
- Duchen LW, Excell BJ, Patel R, Smith B. 1974. Changes in motor end-plates resulting from muscle fibre necrosis and regeneration. A light and electron microscopic study of the effects of the depolarizing fraction (cardiotoxin) of *Dendroaspis jamesoni* venom. *J Neurol Sci.* 21(4):391-417.
- Dunaevsky A, Connor EA. 1998. Stability of frog motor nerve terminals in the absence of target muscle fibers. *Dev Biol.* 194(1):61-71.
- Fahim MA, Holley JA, Robbins N. 1983. Scanning and light microscopic study of age changes at a neuromuscular junction in the mouse. *J Neurocytol.* 12(1):13-25.
- Feng G, Mellor RH, Bernstein M, Keller-Peck C, Nguyen QT, Wallace M, Nerbonne JM, Lichtman JW, Sanes JR. 2000. Imaging neuronal subsets in transgenic mice expressing multiple spectral variants of GFP. *Neuron.* 28(1):41-51.
- Fertuck HC, Salpeter MM. 1976. Quantitation of junctional and extrajunctional acetylcholine receptors by electron microscope autoradiography after <sup>125</sup>I-alpha-bungarotoxin binding at mouse neuromuscular junctions. *J Cell Biol.* 69(1):144-58.
- Fry RW, Morton AR, Keast D. 1991. Overtraining in athletes. An update. *Sports Med.* 12(1):32-65.
- Gautam M, Noakes PG, Moscoso L, Rupp F, Scheller RH, Merlie JP, Sanes JR. 1996. Defective neuromuscular synaptogenesis in agrin-deficient mutant mice. *Cell.* 85(4):525-35.
- Georgiou J, Robitaille R, Trimble WS, Charlton MP. 1994. Synaptic regulation of glial protein expression in vivo. *Neuron.* 12(2):443-55.



- Grinnell AD. 1995. Dynamics of nerve-muscle interaction in developing and mature neuromuscular junctions. *Physiol Rev.* 75(4):789-834.
- Grubb BD, Harris JB, Schofield IS. 1991. Neuromuscular transmission at newly formed neuromuscular junctions in the regenerating soleus muscle of the rat. *J Physiol.* 441:405-21.
- Gunning P, Hardeman E. 1991. Multiple mechanisms regulate muscle fiber diversity. *FASEB J.* 5(15):3064-70.
- Gutmann E, Hanzlikova V, Vysokocil F. 1971. Age changes in cross striated muscle of the rat. *J Physiol.* 216(2):331-43.
- Hansen-Smith FM. 1986. Formation of acetylcholine receptor clusters in mammalian sternohyoid muscle regenerating in the absence of nerves. *Dev Biol.* 118(1):129-40.
- Helveston EM, Grossman RD. 1976. Extraocular muscle lacerations. *Am J Ophthalmol.* 81(6):754-60.
- Henderson CE, Phillips HS, Pollock RA, Davies AM, Lemeulle C, Armanini M, Simmons L, Moffet B, Vandlen RA, Simpson LC. 1994. GDNF: a potent survival factor for motoneurons present in peripheral nerve and muscle. *Science.* 266(5187):1062-4.
- Hess A. 1965. The sarcoplasmic reticulum, the T system, and the motor terminals of slow and twitch muscle fibers in the garter snake. *J Cell Biol.* 26(2):467-76.
- Hess A, Pilar G. 1963. Slow fibers in the extraocular muscles of the cat. *J Physiol.* 169:780-98.
- Jennings C. 1994. Developmental neurobiology. Death of a synapse. *Nature.* 372(6506):498-9.
- Kelly SS, Robbins N. 1983. Progression of age changes in synaptic transmission at mouse neuromuscular junctions. *J Physiol.* 343:375-83.
- Kitaoka K, Matsuda Y, Desaki J, Oki S, Nagano Y, Shibata T. 1997. Topographic comparison of subneural apparatuses at neuromuscular junctions in normal and dystrophic (mdx) mice: a scanning electron microscope study. *J Electron Microsc.* (Tokyo). 46(2):193-7.
- Kuffler SW, Nicholls JG. 1966. The physiology of neuroglial cells. *Ergeb Physiol.* 57:1-90.

- Lake DA. 1992. Neuromuscular electrical stimulation. An overview and its application in the treatment of sports injuries. *Sports Med.* 13(5):320-36.
- Laurie GW, Leblond CP. 1983. What is known of the production of basement membrane components. *J Histochem Cytochem.* 31(1A Suppl):159-63.
- Lichtman JW, Magrassi L, Purves D. 1987. Visualization of neuromuscular junctions over periods of several months in living mice. *J Neurosci.* 7(4):1215-22.
- Lingle CJ, Steinbach JH. 1988. Neuromuscular blocking agents. *Int Anesthesiol Clin.* 26(4):288-301.
- Loeb JA. 2003. Neuregulin: an activity-dependent synaptic modulator at the neuromuscular junction. *J Neurocytol.* 32(5-8):649-64.
- Loring RH, Salpeter MM. 1980. Denervation increases turnover rate of junctional acetylcholine receptors. *Proc Natl Acad Sci U S A.* 77(4):2293-7.
- Love FM, Son YJ, Thompson WJ. 2003. Activity alters muscle reinnervation and terminal sprouting by reducing the number of Schwann cell pathways that grow to link synaptic sites. *J Neurobiol.* 54(4):566-76.
- Love FM, Thompson WJ. 1999. Glial cells promote muscle reinnervation by responding to activity-dependent postsynaptic signals. *J Neurosci.* 19(23):10390-6.
- Lyons PR, Slater CR. 1991. Structure and function of the neuromuscular junction in young adult mdx mice. *J Neurocytol.* 20(12):969-81.
- Magnaghi V, Ballabio M, Consoli A, Lambert JJ, Roglio I, Melcangi RC. 2006. GABA receptor-mediated effects in the peripheral nervous system: A cross-interaction with neuroactive steroids. *J Mol Neurosci.* 28(1):89-102.
- Marchionni MA, Grinspan JB, Canoll PD, Mahanthappa NK, Salzer JL, Scherer SS. 1997. Neuregulins as potential neuroprotective agents. *Ann N Y Acad Sci.* 825:348-65.
- Marques MJ, Conchello JA, Lichtman JW. 2000. From plaque to pretzel: fold formation and acetylcholine receptor loss at the developing neuromuscular junction. *J Neurosci.* 20(10):3663-75.
- Martin LJ, Price AC, Kaiser A, Shaikh AY, Liu Z. 2000. Mechanisms for neuronal degeneration in amyotrophic lateral sclerosis and in models of motor neuron death (Review). *Int J Mol Med.* 5(1):3-13.
- Mauro A. 1961. Satellite cells of skeletal muscle fibres. *J Biophys Biochem Cytol* 9: 493-95.

- McMahan UJ, Sanes JR, Marshall LM. 1978. Cholinesterase is associated with the basal lamina at the neuromuscular junction. *Nature*. 271(5641):172-4.
- McMahan UJ, Slater CR. 1984. The influence of basal lamina on the accumulation of acetylcholine receptors at synaptic sites in regenerating muscle. *J Cell Biol*. 98(4):1453-73.
- Minatel E, Santo Neto H, Marques MJ. 2001. Acetylcholine receptors and neuronal nitric oxide synthase distribution at the neuromuscular junction of regenerated muscle fibers. *Muscle Nerve*. 24(3):410-6.
- Morgan JE. 2005. Stem cells to treat muscular dystrophies. *Acta Myol*. 24(3):181-3.
- Nene RV. 1977. A histochemical study of cholinesterases in arm and forearm muscles of the pigeon and fowl. *J Anat*. 123(Pt 3):745-9.
- Newman EA. 1984. Regional specialization of retinal glial cell membrane. *Nature*. 309(5964):155-7.
- Nishimune H, Sanes JR, Carlson SS. 2004. A synaptic laminin-calcium channel interaction organizes active zones in motor nerve terminals. *Nature*. 432(7017):580-7.
- Oda K. 1984. Age changes of motor innervation and acetylcholine receptor distribution on human skeletal muscle fibres. *J Neurol Sci*. 66(2-3):327-38.
- Oki S, Desaki J, Ezaki T, Matsuda Y. 1999. Aged neuromuscular junctions in the extensor digitorum longus muscle of the rat as revealed by scanning electron microscopy. *J Electron Microsc (Tokyo)*. 48(3):297-300.
- O'Malley JP, Waran MT, Balice-Gordon RJ. 1999. In vivo observations of terminal Schwann cells at normal, denervated, and reinnervated mouse neuromuscular junctions. *J Neurobiol*. 38(2):270-86.
- Papadimitriou JM, Robertson TA, Mitchell CA, Grounds MD. 1990. The process of new plasmalemma formation in focally injured skeletal muscle fibers. *J Struct Biol*. 103(2):124-34.
- Patton BL. 2003. Basal lamina and the organization of neuromuscular synapses. *J Neurocytol*. 32(5-8):883-903.
- Porter CW, Barnard EA. 1976. Ultrastructural studies on the acetylcholine receptor at motor end plates of normal and pathologic muscles. *Ann N Y Acad Sci*. 274:85-107.

- Reist NE, Werle MJ, McMahan UJ. 1992. Agrin released by motor neurons induces the aggregation of acetylcholine receptors at neuromuscular junctions. *Neuron*. 8(5):865-8.
- Reynolds ML, Woolf CJ. 1992. Terminal Schwann cells elaborate extensive processes following denervation of the motor endplate. *J Neurocytol*. 21(1):50-66.
- Rich MM, Lichtman JW. 1989a. In vivo visualization of pre- and postsynaptic changes during synapse elimination in reinnervated mouse muscle. *J Neurosci*. 9(5):1781-805.
- Rich M, Lichtman JW. 1989b. Motor nerve terminal loss from degenerating muscle fibers. *Neuron*. 3(6):677-88.
- Robitaille R. 1995. Purinergic receptors and their activation by endogenous purines at perisynaptic glial cells of the frog neuromuscular junction. *J Neurosci*. 15(11):7121-31.
- Robitaille R. 1998. Modulation of synaptic efficacy and synaptic depression by glial cells at the frog neuromuscular junction. *Neuron*. 21(4):847-55.
- Robitaille R, Jahromi BS, Charlton MP. 1997. Muscarinic Ca<sup>2+</sup> responses resistant to muscarinic antagonists at perisynaptic Schwann cells of the frog neuromuscular junction. *J Physiol*. 504 (Pt 2):337-47.
- Rosenheimer JL. 1990. Factors affecting denervation-like changes at the neuromuscular junction during aging. *Int J Dev Neurosci*. 8(6):643-54.
- Sadeh M, Stern LZ. 1984. Observations on the innervation of human extraocular muscles. *J Neurol Sci*. 66(2-3):295-305.
- Sadeh M, Stern LZ, Czyzewski K. 1985. Changes in end-plate cholinesterase and axons during muscle degeneration and regeneration. *J Anat*. 140 ( Pt 1):165-76.
- Sanes JR. 1982. Laminin, fibronectin, and collagen in synaptic and extrasynaptic portions of muscle fiber basement membrane. *J Cell Biol*. 93(2):442-51.
- Sanes JR, Marshall LM, McMahan UJ. 1978. Reinnervation of muscle fiber basal lamina after removal of myofibers. Differentiation of regenerating axons at original synaptic sites. *J Cell Biol*. 78(1):176-98.
- Santo Neto H, Nguyen QT, Lichtman JW. 1996. Protein synthesis inhibition in postsynaptic cells is followed within several days by elimination of nerve terminals. 26<sup>th</sup> society for neuroscience meeting. Abstract: 665.9

- Schultz E. 1989. Satellite cell behavior during skeletal muscle growth and regeneration. *Med Sci Sports Exerc.* 21(5 Suppl):S181-6.
- Schultz E, Jaryszak DL, Valliere CR. 1985. Response of satellite cells to focal skeletal muscle injury. *Muscle Nerve.* 8(3):217-22.
- Schultz E, McCormick KM. 1994. Skeletal muscle satellite cells. *Rev. Physiol. Biochem. Pharmacol.* 123: 213-57.
- Slater CR, Allen EG. 1985. Acetylcholine receptor distribution on regenerating mammalian muscle fibers at sites of mature and developing nerve-muscle junctions. *J Physiol (Paris).* 80(4):238-46.
- Son YJ, Thompson WJ. 1995a. Schwann cell processes guide regeneration of peripheral axons. *Neuron.* 14(1):125-32.
- Son YJ, Thompson WJ. 1995b. Nerve sprouting in muscle is induced and guided by processes extended by Schwann cells. *Neuron.* 14(1):133-41.
- Son YJ, Trachtenberg JT, Thompson WJ. 1996. Schwann cells induce and guide sprouting and reinnervation of neuromuscular junctions. *Trends Neurosci.* 19(7):280-5.
- Takala TE, Virtanen P. 2000. Biochemical composition of muscle extracellular matrix: the effect of loading. *Scand J Med Sci Sports.* 10(6):321-5.
- Torres LF, Duchon LW. 1987. The mutant mdx: inherited myopathy in the mouse. morphological studies of nerves, muscles and end-plates. *Brain.* 110 (Pt 2):269-99.
- Trachtenberg JT, Thompson WJ. 1996. Schwann cell apoptosis at developing neuromuscular junctions is regulated by glial growth factor. *Nature.* 379(6561):174-7.
- van Mier P, Lichtman JW. 1994. Regenerating muscle fibers induce directional sprouting from nearby nerve terminals: studies in living mice. *J Neurosci.* 14(9):5672-86.
- Verdi JM, Groves AK, Farinas I, Jones K, Marchionni MA, Reichardt LF, Anderson DJ. 1996. A reciprocal cell-cell interaction mediated by NT-3 and neuregulins controls the early survival and development of sympathetic neuroblasts. *Neuron.* 16(3):515-27.
- Washio H, Imazato-Tanaka C, Kanda K, Nomoto S. 1987. Choline acetyltransferase and acetylcholinesterase activities in muscles of aged mice. *Brain Res.* 416(1):69-74.

- Whalen RG, Harris JB, Butler-Browne GS, Sesodia S. 1990. Expression of myosin isoforms during notexin-induced regeneration of rat soleus muscles. *Dev Biol.* 141(1):24-40.
- Wood SJ, Slater CR. 2001. Safety factor at the neuromuscular junction. *Prog Neurobiol.* 64(4):393-429.
- Zuo Y, Lubischer JL, Kang H, Tian L, Mikesh M, Marks A, Scofield VL, Maika S, Newman C, Krieg P, Thompson WJ. 2004. Fluorescent proteins expressed in mouse transgenic lines mark subsets of glia, neurons, macrophages, and dendritic cells for vital examination. *J Neurosci.* 24(49):10999-1009.

## **VITA**

Yue Li was born in Nantong, Jiangsu Province in China on August 17<sup>th</sup>, 1977. She is the daughter of Wenlong Li and Jiying Gu. In China, she attended University of Science & Technology of China and earned a Bachelor of Science degree in Neurobiology & Biophysics in 2000. In September 2000, she entered graduate school of Institute of Cellular & Molecular Biology at the University of Texas at Austin. Her graduate studies were supported by fellowships, research assistantships and teaching assistantships.

Permanent Address: 1501 Willow Crest Dr., Richardson, Texas 75081

This dissertation was typed by the author.